ABSTRACT

ABUBEKER, SITRA U. B.Sc. GEORGIA STATE UNIVERSITY, 1997

A NEW CLASS OF MESOPOROUS MATERIALS FOR APPLICATIONS IN PETROLEUM REFINING

Advisor: Dr. Conrad W. INGRAM

Thesis dated May, 2002

Lamellar and hexagonal mesostructured aluminophosphates with pore diameters > 2 nm were synthesized as potential high surface area petroleum refining or oxidation catalysts. Phosphoric acid and three different aluminum sources, aluminum hydroxide, aluminum isopropoxide and psuedobohemite alumina, were used as the inorganic precursors. Cetyltrimethylammonium chloride surfactant was used as charge compensating cation and structure directing agent. Synthesis were conducted from reaction mixtures within the following molar composition range:

$xAl_2O_3:P_2O_5:yC_{16}TMACl:zTMAOH:wH_2O$, where x= 0.29-2.34, y = 0.24-0.98, z=0.34-1.95, w= 86-700.

The Lamellar phase was favored by extremely low Al/P ratios (<0.33), low TMAOH content, high $C_{16}TACl$ concentrations and high synthesis temperature (110°C). The hexagonal phase was favored by higher Al/P ratios and TMAOH content, pH range between 8-10, low $C_{16}TACl$ concentration and ambient temperature. With $Al(OH)_3$ as the hydroxide source, the hexagonal phase demonstrated the highest lattice ordering at Al/P ratios 0.47-1.25, above which increasingly disordered products were observed.

Aluminum and phosphorus were present in tetrahedral coordination in the lamellar phase, while both tetrahedral and octahedral coordination was present in the hexagonal phase. No mesostructured products were observed under TMAOH-free conditions. The influence of synthesis variables are investigated.

A NEW CLASS OF MESOPOROUS MATERIALS FOR APPLICATIONS IN PETROLEUM REFINING

A THESIS

SUBMITTED TO THE FACULTY OF CLARK ATLANTA UNIVERSITY

IN PARTIAL FULFILLMENT OF THE REQUIREMENTS FOR

THE DEGREE OF MASTER OF SCIENCE

BY

SITRA ABUBEKER

DEPARTMENT OF CHEMISTRY

ATLANTA, GEORGIA

MAY 2002

ACKNOWLEDGEMENTS

My sincere thanks go to my advisor, Dr. C. W. Ingram. I thank him for his patience, valuable advice and friendship as well as mentorship. Thanks to my thesis committee members, Dr. M. B. Mitchell and Dr. I. Harruna for their patience and help in reviewing this manuscript. I would like to thank Dr. Emmanuel Karikari, Paul Abraham, Enid Gatimu, and Dr.Johannes Leisen, for their assistance in X-ray analysis, ICP/MS, DRIFTS, and MAS NMR studies. Thanks to Dr. M. B. Mitchell for his assistance in the calculation of the BJH pore size distributions. Thanks to my family and Abdull Ibrahim for their guidance and endless support. I am grateful to the U.S. Department of Energy for financial support of this project through grant number DE FG 26-00NT 40833.

TABLE OF CONTENTS

LIST OF FIGURES

LIST OF TABLES

LIST OF SCHEMES

LIST OF ABBREVIATIONS

MCM-41	Mobil Composite Material-41
SBA-15	Santa Barbara-15
TMAOH	Tetramethylammonium hydroxide
CTACl	Cetyltrimethylammonium chloride
XRD	X-ray Diffraction Spectrometry
TGA	Thermogravemetric Analysis
DTA	Differential Thermogravemetric Analysis
ICP-MS	Inductively Coupled Plasma-Mass Spectrometry
MAS-NMR	Magic Angle Spining Nuclear Magnetic Resonance
BET	Braunauer, Emmett and Teller
BJH	Barrett, Joyner and Halenda

CHAPTER 1

INTRODUCTION AND STATEMENT OF THE PROBLEM

1.1 Introduction

Increasing demand for processing heavy petroleum feedstocks has heightened the importance of developing new catalyst systems. Many conventional crude oils from around the world contain 10-30% residue (which is the fraction of crude oil with boiling point greater than 525 °C). As conventional crude oils have become more expensive, interest in processing heavier feeds has increased. These heavier feeds have residue contents of 40% or more, and require further processing in order to find a market. The current motivations for conversion technologies are multifold. The market for heavier fuels is decreasing while that for middle distillate is increasing at a rapid rate.[1]

In many parts of the world, light oil production is declining and heavy oil conversion, therefore, becomes increasingly important to maintain economic viability of these regions. Further tightening of environmental regulations in Europe and North America has provided incentives to refiners to further reduce sulfur and aromatic levels of the finished products. Additional stringent requirements on the disposal of refinery residues such as coke or residua encourage "minimum-waste" refinery strategies.

To process heavy feedstocks, the catalyst of use must possess high surface area, Bronsted acidic properties, as well as thermal stability. Zeolites and other catalysts have

been encountering a growing interest due to their critical applications in petroleum refining. Therefore, there are currently massive efforts in trying to synthesize new kinds of zeolite-type materials. Zeolites possess high acidity, high surface area and a rigid three-dimensional framework structure. These properties make them useful for petroleum processing. Zeolites, however, often suffer from diffusion limitation and their uses are therefore limited to petroleum fractions containing small substrates with kinetic diameters less than 7Å. Because of these limitations, a myriad of synthetic efforts are being conducted to design catalysts with enlarged pore sizes.[2]

According to IUPAC definition, porous materials are divided into three classes; microporous (<2 nm diameter pores), mesoporous (2-50 nm diameter pores) and macroporous (50 nm diameter pores).[2] The initial discovery of synthetic aluminosilicate zeolites in the late 1940s and early 1950s by Breck *et al.*,[3] in the Union Carbide Laboratory, served as the beginning of today's large microporous catalyst industry. During the 1950s more siliceous zeolite framework such as zeolite Y were developed. This was followed by the high silica zeolites, such as the zeolites Beta and ZSM-5, in the late 1960s and 1970s by researchers Wadlineger *et al.*, and Argauer *et al.*,[4] In the early 1980s, Union Carbide Laboratories reported a new generation of zeolite-like microporous materials, the aluminophosphates. The aluminophosphates ($AlPO_4$) with open network structure were synthesized using similar template molecules as in zeolite synthesis.[4,5] This represented a significant advancement in the field of porous materials as these materials contained similar framework topologies as those found in zeolites but differed in chemical composition. Their applications as catalysts were restricted, since the neutral framework was lacking in acidic characteristic. These porous aluminophosphate

molecular sieves are known to exist in a wide range of structural and compositional diversity, and are generally prepared from gels containing aluminum, phosphorous and an amine acting as a structure-directing agent. The addition of silicon and other metals to the framework resulted in the silicoaluminophosphate (SAPO) and metal substituted aluminophosphates (MeAPO).[4,6] The substitution of divalent metal ions in the framework of an aluminophosphate molecular sieve imparts acidity, redox characteristics, ion-exchange capacity and enhanced hydrophilicity with greater stability, structural and chemical diversity.[7] In the quest for high surface area catalysts with greater stability, structural and chemical diversity, large pore size materials in the mesoporous range denoted as M41S aluminosilicate were invented by Mobil researchers in 1992.[8,9] MCM-41, a member of this series, possesses a regular array of uniform and one-dimensional mesopores that can be tuned to the desired pore diameter in the range of 15Å to 100Å.[6] The use of surfactants plays an extremely important role in the synthesis of these solids due to a self-assembly process, known as the liquid crystal templating mechanism (LCT), to form the mesoporous materials.

1.2 Objective

Following the successful synthesis of MCM-41, it is instructive that the synthesis of the mesoporous aluminophosphate counterparts be investigated. Mesoporous aluminophosphates are expected to retain the physiochemical characteristics of their microporous counterparts, but with significant increase in pore size, pore volume and surface area. This study is focused on the synthesis of mesoporous aluminophosphates using the liquid crystal templating mechanism. Factors affecting the synthesis are investigated.

CHAPTER 2

SURVEY OF RELEVANT LITERATURE

2.1 Structure of aluminophosphates

Aluminophosphate inorganic framework composed of Al^{3+}or P^{5+} is based on the assemblage of aluminate and phosphate species as indicated in Scheme 1. A notable feature of the microporous $AlPO_4$ composition is the invariant Al_2O_3/ P_2O_5 ratio, which is in direct contrast with the variable compositions of SiO_2/ Al_2O_3 ratio found in the aluminosilicate zeolite counterparts. Whereas zeolites contain Al^{3+} and Si^{4+} in the tetrahedral coordination and exhibit a net negative framework charge, the $AlPO_4$ materials may contain aluminum in coordination other than tetrahedral and a framework that is neutral, as well as Brønsted acid sites caused by the presence of terminal -OH bonds on the external surface of the crystal.

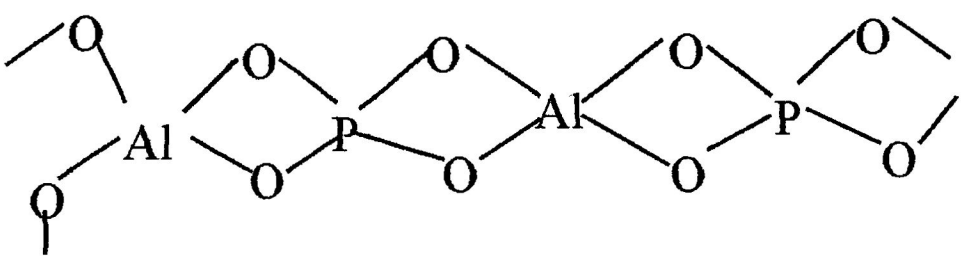

Scheme 1: Representation of the arrangement of $AlPO_4$ structural framework

The overall composition of the $AlPO_4$ molecular sieves is written as: $xR: Al_2O_3: P_2O_5: yH_2O$, where R is an organic amine or quaternary ammonium ion. The quantities x and y represent the amount of organic or water that fills the pores of the crystal. Just as the zeolites obey Lowenstien's rule for the avoidance of tetrahedral Al-O-Al groupings within the structure, the $AlPO_4$ structures avoid forming tetrahedral Al-O-Al bonds as well as P-O-P bonds.[12]

2.2 Synthesis

Phosphate-based molecular seives, for example, $AlPO_4$-42 which have been shown to overcome the 12-membered ring (12MR) pore-opening barrier found in most zeolites, are normally synthesized from initially acidic gels containing organic additives in an aqueous medium.[12] It is well known that the choice of aluminum source plays a crucial role in the synthesis and phase purity of $AlPO_4$ molecular seives.[13] Moreover, parameters such as temperature, duration of crystallization and agitation will also affect the crystallization of the molecular seives. The synthesis of aluminophosphate therefore normally takes place by the following steps: neutralization of the Al source suspended in water with a nearly equimolar amount of dilute phosphoric acid to obtain the reactive $AlPO_4$ gel, aging of the reactive gel, addition of a particular organic additive to the reactive gel referred to as the precursor gel, and aging of the precursor gel.[12] Aluminum species can exist in solution in a number of forms:

1) hydrated octahedral Al^{3+}
2) polymeric octahedral AlO_6
3) mixed AlO_4/AlO_6 species

4) polymeric AlO_4

5) isolated $Al(OH)_4^-$ and various deprotonated forms

2.2.1 Mechanistic considerations

The formation of aluminophosphate materials is suggested by a precipitate obtained by the condensation of aluminophosphate oligomers formed through a sol gel process and the use of an organic moiety as structure directing agent.

2.2.1.1 Sol gel process

Sol gel processing is a wet chemical route to synthesizing of a colloidal suspension of a solid particle in a liquid (sol) and subsequently to the formation of a dual phase material of a solid skeleton filled with a solvent (wet gel) through sol-gel transition (gelation). When the solvent is removed, the wet gel converts to a xerogel through ambient pressure drying or an aerogel through supercritical drying. The structures and properties of gels depend on the initial stages of the polymerization in the conventional hydrolytic sol-gel transformation.[10]

Two reactions occur during the sol-gel transition: hydrolysis and condensation. The process uses inorganic or metal organic precursors. In aqueous or organic solvents, the precursors are hydrolyzed and condensed to form inorganic polymers composed of M-O-M bonds. Aluminum gels are most often synthesized by hydrolyzing monomeric alkoxide precursors using an acid or base as a catalyst. The following reactions are generally used to describe the sol-gel process:

$$-\text{Al-OR} + H_2O = \text{Al-OH} + \text{ROH} \quad (1)$$

$$-\text{Al-OR} + \text{HO-Al-} = \text{Al-O-Al} + \text{ROH} \quad (2)$$

$$-\text{Al-OH} + \text{HO-Al-} = \text{Al-O-Al} + H_2O \quad (3)$$

where R is an alkyl group.

Equation 1 shows the hydrolysis reaction, where alkoxide groups (OR) are replaced by hydroxyl groups (OH). Equations 2 and 3 represent condensation, which often commences before and after hydrolysis is complete.

Gel formation depends on the type of catalyst used. Acid catalyzed hydrolysis alkoxides form gels with linear branched polymeric chains. The entangling of these polymer chains forms a gel.[11] The gel structure, however, is different when base catalyzed. Base catalyzed hydrolysis alkoxides forms gels with chains that become highly branched prior to entanglement, and thus begin to take on a particulate nature. In this case, gelation occurs by these chains linking together. Acid addition has little effect on surface area, porosity or oxide conversion of the gels, while the base addition has a large effect. Addition of base gives a more condensed polymer at the gelation point. [11] Increasing the base content thereby decreases surface area and porosity, and oxide conversion is never complete. The mechanism for the acid-catalyzed hydrolysis and condensation is indicated in schemes 2 and 3.

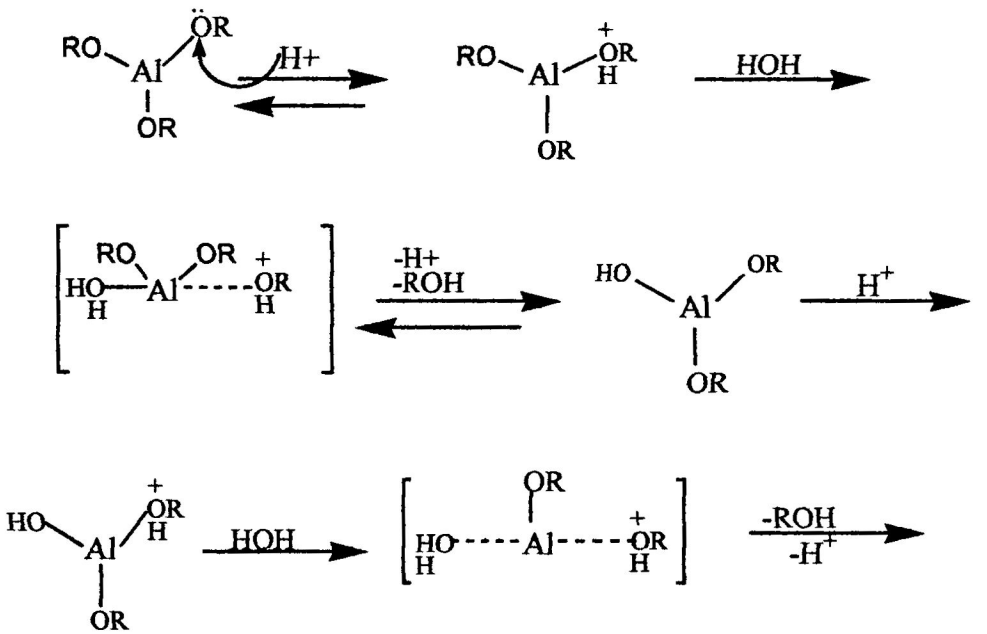

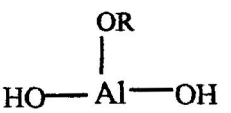

where R = C_3H_7

Scheme 2: Mechanism of acid catalyzed hydrolysis of aluminum isopropoxide.

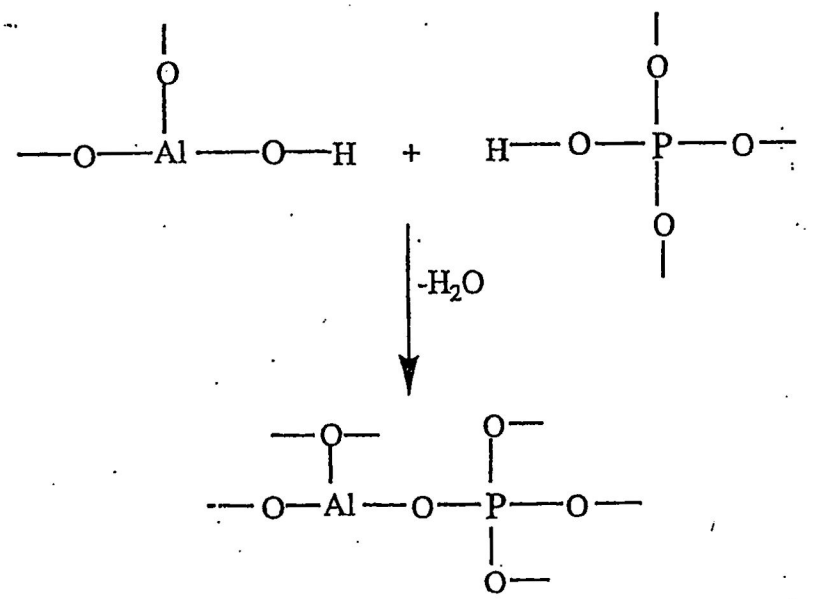

Scheme 3: Plausible condensation for Al and P inorganic precursors

The form in which aluminum is present in solution octahedral vs. tetrahedral, polymer vs monomer, is also strongly dependent on the hydroxide content of the solution. Under very acidic conditions, aluminum ions exist mainly as hydrated Al^{3+} species but as the hydroxide concentration increases, deprotonation of the amphoteric aluminum occurs.[12] In addition to this deprotonation, polymeric species begin to appear in solution. These aluminum-containing aggregates form slowly in solution but appear to maintain equilibrium with the monomeric forms. In aqueous solutions $Al(H_2O)_6^{3+}$ ions are considered to be the major species. However, the aluminum in alkaline solutions is tetrahedral which is in agreement with incorporation into the zeolite framework.[12]

The pH was found to play an important role in deciding the outcome of crystallization, as pH between 3.5 and 6 appeared to produce less dense phases compared to products formed at pH 9.[12] NMR analysis has been used to examine the crystallization of $AlPO_4$ molecular seives. The analysis indicates the formation of tetrahedral aluminum

with the phosphate addition to the coordination sphere. The initiation of formation of the gel or crystals is thought to occur via the following sets of reactions[12]:

$$Al(H_2O)_6^{3+} + H_3PO_4 \rightarrow [Al(H_2O)_5(H_3PO_4)]^{3+} + H_2O \quad (4)$$

$$Al(H_2O)_6^{3+} + H_2PO_4^- \rightarrow [Al(H_2O)_5(H_2PO_4)]^{2+} + H_2O \quad (5)$$

$$2Al(H_20)_6^{3+} + H_2PO_4^- \rightarrow \{(OH)_2 P[OAl(H_2O)_5]_2\}^{5+} + 2H_2O \quad (6)$$

2.2.1.2 Role of organic additive

The synthesis of the $AlPO_4$ analogues of the zeolites and the structurally novel aluminophosphates have required the addition of organic cationic or neutral amines to the reaction mixtures. The organic additive appears to promote crystallization of a specific aluminophosphate structure, though it is unclear if it promotes crystallization of a specific structure the same way as in the synthesis of the aluminosilicates. The TMA cation promotes the crystallization of the structure in the aluminophosphate systems as it does in the aluminosilicate system.[12] The organic additives used include quaternary ammonium cations, primary, secondary and ternary neutral amines, diamines, cyclic amines and alkanolamines. Compared to the aluminosilicate system, a wide range of neutral organic amines have been found to aid in the crystallization of the aluminophosphate structures. This, however, may be a result of the initially acidic environment of the aluminophosphate gel, which would encourage the formation of a protonated amine, thus generating the cationic form in situ.[12] It is also found that one organic amine can promote crystallization of differing structures depending on the temperature of

crystallization. The synthesis of mesoporous aluminophosphates employs the use of surfactants. The nature of surfactants is therefore explored below.

2.2.2 Definition and classification of surfactants

Surfactants are surface active agents that, when present at low concentration in a system, have the property of adsorbing onto the surfaces or interfaces of the system. They have a characteristic amphipathic molecular structure consisting of a structural group (hydrophobic) that has very little attraction for the solvent together with a hydrophilic group that has strong attraction for the solvent. The hydrophobic group is usually a long–chain hydrocarbon and the hydrophilic group is an ionic or highly polar-group.[14] Surfactants are classified as follows:

(1) anionic: where the hydrophilic portion of the molecule bears a negative charge.

(2) cationic: where the surface active portion bears a positive charge.

(3) zwitterionic: where both positive and negative charges may be present in surface active portion.

4) nonionic: where the surface active portion bears no apparent ionic charge.

2.2.2.1 Micelle assembly

The self-assembly process of surfactants (amphiphilic molecules) in water or any suitable solvent, "is a widely studied area" which results in the formation of a wide range of interesting liquid and liquid crystalline phases. The amphiphilic molecule, as mentioned above, possesses a hydrophilic head group and a hydrophobic chain. Above a certain amphiphile concentration (critical micellar concentration, CMC) molecular

rearrangement drives the formation of aggregates of individual amphiphiles (micelles). These aggregates possess well-defined hydrophobic parts in which the chains are sequestered into the core of the aggregates, while the hydrophobic head group remains in contact with the solvent on the outer surface of the aggregate. The size and shape of these micelles, at low amphiphite concentration, is controlled by a balance of the need to keep water from contact with the core of the micelles and by the packing of the head groups around the surface of the aggregates. The aggregates in the liquid phase can be spheres, discs, rods or lamellae. The surfactant parameter can be used as an indication of which type of aggregate forms can be expected in solution for a given surfactant. These type of structures that micelles form are then determined by the packing parameter. As the concentration of the surfactant increases, intermicellar interactions become significant and take on local ordering to form hexagonal, cubic, lamellar or intermediate phases as a precursor to the formation of the liquid crystalline phases.[14]

2.2.2.2 Packing characteristics

Aggregate structures have a lower energy than non-aggregated molecules in solution. However, molecular geometry constraints determine the actual shape of the aggregate.[15] Molecular packing characteristics are determined with the use of the dimensionless packing parameter, P, where,

$$P = V_c/a_o\, l_c.$$

V_c = chain volume (this is the volume of the hydrocarbon tail)

a_o = optimal head group area

l_c = critical chain length (this is the largest effective length that the chain can be extended in the fluid)

The packing parameter can be thought of as a measure of the curvature of the molecular aggregate. It is the ratio of the tail volume to the volume projected by the optimal head group area. A small packing parameter indicates a small tail attached to a large head, and a large packing parameter indicates a large tail connected to a smaller head. Therefore, small packing parameter leads to highly curved aggregates, for example, spheres while a larger packing parameter leads to aggregates with less curvature, for example, bilayers.[15]

For cylindrical micelles composed of N number of molecules, the total micelle volume V and surface area S are given by :

$$V = NV_c = L\pi r^2 \quad (7)$$

$$S = 2\pi rL \quad (8)$$

$$aa = 2\pi rL/N \quad (9)$$

$$aa = 2V_c/r \quad (10)$$

$$aa/a_o = 2V_c/ra_o \quad (11)$$

$$aa/a_o = (2l_c/r)(V_c/a_o l_c) \quad (12)$$

$$r_{cyl} = 2l_c(V_o/a_o l_c) \quad (13)$$

L = length of cylindrical micelle

aa = actual area per head group

r = the radius of the micelle

Since it is not geometrically possible to form micelle with $r > l_c$, the packing parameter $(V_c/a_o l_c)$ less than 1/2 will, therefore, form cylindrical micelles.

In general, if P $\leq$1/3 the micelles are spherical; if P is between 1/3 and 1/2, the micelles are rod shaped; for 1/2 $\leq$P $\leq$1 lamellar structures are formed, and when the P >1 the structures are inverted.[15]

2.2.3 Mesoporous materials

In 1992, scientists at Mobil Oil Corporation discovered the M41S family of silicate/aluminosilicate mesoporous materials with high surface areas and large pore diameters in the range of 20-100Å.[16] The M41S family contains several members, such as the hexagonal phase referred to MCM-41, and a cubic structure MCM-48, both employing cetyltrimethylammonium chloride as surfactant. An interesting feature of these materials is the ability to adjust the pore sizes allowing different types of compounds to access their internal surface areas.

2.2.3.1 Synthesis of M41S materials

The first synthesis mechanism of MCM-41 was proposed by Beck and co-workers[16] who suggested that the liquid crystal templating mechanism in which the surfactant liquid crystal structures serve as organic templates.[17] Two pathways were proposed for the formation of MCM-41.

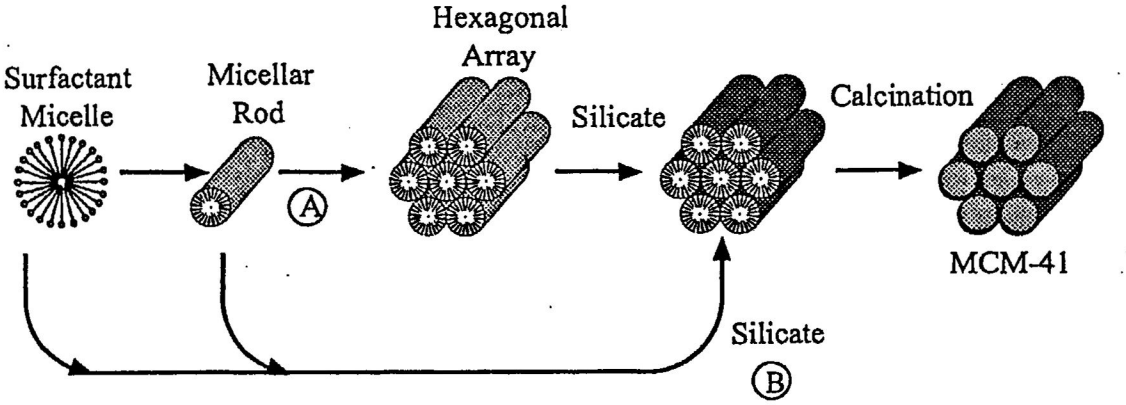

Scheme 4: Possible mechanistic pathway for the formation of MCM-41.[17]

The first route (A) is based on the presence of the liquid crystal phase before inorganic precursors are added. The second route (B) is based on the formation of the surfactant liquid crystals through the addition of silicate species which occupy the space between cylinders, thus influencing the ordering of the micelles.[17] In both cases, the mesostructure is formed via a cooperative mechanism in which the electrostatic interaction between the inorganic species and the charged surfactant ion determine the mesostructure.[16]

After the successful synthesis of the hexagonal and cubic members of the ordered mesoporous materials, massive research efforts led to a wide range of other structures, such as the well ordered hexagonal mesoporous silica structures (SBA-15) with uniform pore sizes up to approximately 300Å. Prior to the discovery of these materials, the mesoporous silicas were limited to 100Å and had wall thicknesses around 10Å.[18] The use of triblock copolymer surfactants, for example, poly(alkylene)oxide ($EO_5PO_7EO_5$) expands the wall thickness up to 60Å and gives substantially higher pore sizes up to 300Å.[19]

Based on the catalytic success of zeolites and the great catalytic potential of microstructured aluminophosphates and the mesostructured M41S family, numerous attempts have been made to prepare mesostructured aluminophosphates but with inconsistent results.

Reddy *et al.*, reported the use of dodecylamine surfactant as a structure-directing agent to synthesize mesoporous aluminophosphates at 100 °C and 24 hours reaction conditions, which resulted in a lamellar phase.[20] Calcination of the lamellar material at 400 °C under flowing nitrogen followed by a flow of air resulted in a collapse of the lamellar structure. The organic moiety, in addition, could not be removed by solvent extraction.[20] A lamellar aluminophosphate phase was also reported by Klinowki *et al.*, using a cationic surfactant templating agent. Reaction temperatures employed ranged from 80-150 °C for 24-96 hours. Upon calcinations at 250 °C, an amorphous product was similarly obtained.[28] Yue *et al.*, also reported the synthesis of lamellar aluminophosphates using a mixture of ethylene glycol and an unbranched primary alchol as the medium and hexylamine as the template. The mixtures were kept at 180 °C for 8

days.[21] Using dodecylphosphate as a template Tiemann *et al.*, also reported the synthesis of lamellar aluminophosphates. The mixture was kept at 120 °C for 24 hours without agitation. [22] Ozin *et al.*, also reported the synthesis of lamellar aluminophosphate under solvothermal conditions using primary alkyl amines in tetraethylene glycol.[23] On the other hand, Stucky and coworkers prepared the hexagonal phase by adding phosphoric acid and hydrofluoric acid to aluminum isopropoxide in ethanol, followed by cetyltrimethylammonium bromide (CTAB) at room temperature. Placing the gel in an oven at 70 °C for a few days led to a partial conversion of a lamellar to hexagonal phase. Attempts to calcine the products into a mesoporous structure resulted in structural collapse.[24]

Kevan *et al.*, reported the room temperature synthesis of a partially stable hexagonal aluminophosphate using CTACl as templating agent and aluminum hydroxide as the aluminum source.[25] Kuroda *et al.*, reported that synthesis conducted at 130 °C for 5 days resulted in a lamellar mesostructure. A hexagonal phase was, however, obtained only when the liquid mixture was dispersed in distilled water.[26] Thermally stable microporous/mesoporous aluminophosphates with continuously adjustable pore sizes prepared at 160 °C and cooled to 120 °C using $Al(OBut)_3$ and triethanolamine through the surfactant (CTAB) assisted procedure was reported.[27] In addition, silicoaluminophosphate synthesis based on a self assembly process using CTACl, tetraorthosilicate (TEOS) and aluminum hydroxide at room temperature was also reported.[25]

As indicated above, several synthetic methods have been applied to the successful synthesis of various mesoporous metal oxides. A wide variety of surfactants with different head groups and inorganic precursors often lead to the same product. Because of the differences in the synthesis procedures and products obtained, it is not clear as to what factors affect their crystallization. It is, therefore, of interest to conduct a comprehensive investigation on the synthesis of mesoporous aluminophosphates and the effect of reaction parameters such as the amount of TMAOH, Al/P ratio and water content as well as reaction temperature and time.

CHAPTER 3

MATERIALS AND METHODS

3.1 Materials

Hexadecyltrimethylammonium chloride [C_{16} H_{33} $(CH_3)_3N^+Cl^-$, C_{16}TMACl, 25 wt % in water, Aldrich Chemical Co], tetramethylammonium hydroxide [$(CH_3)_4NOH$, TMAOH, 25 wt % in water, Aldrich Chemical Co.], aluminum isopropoxide [$(CH_3)_2CHO)_3Al$, 98% Aldrich Chemical Co.], aluminum hydroxide hydrate [Al $(OH)_3xH_2O$, Aldrich Chemical Co.], psuedobohemite alumina [AlOOH, Vista Chemical Co.], O-Phosphoric acid,85% H_3PO_4, Fischer Scientific].

3.2. Synthesis

3.2.1 Synthesis of aluminophosphates using aluminum hydroxide

Aluminum hydroxide has previously been used for the synthesis of microporororous aluminophosphates. This research, therefore, utilized aluminum hydroxide as the initial source of aluminum. Several parameters that affect the synthesis were investigated. In a typical synthesis, 3.53 g aluminum hydroxide was slowly added to a solution of 4.2 g phosphoric acid in 15 ml water under vigorous stirring. The mixture was added to a solution of 11.6 g CTACl in 100 ml water with vigorous stirring. After 0.5 hour, 17.3 g of TMAOH were slowly added dropwise and a wet gel was obtained. The final mixture was then divided into two aliquots. One

aliquot was stirred for 24 hour at 25 °C. The second was heated at 110 °C under static conditions.

3.2.1.1 Effect of the Al/P ratio

Six synthesis mixtures were prepared as in Section 3.2, each with different amounts of aluminum hydroxide as follows: 0.83, 0.95, 1.33, 1.66, 3.59 and 6.66 g. The molar compositions of the reaction mixtures were as follows: $xAl_2O_3:P_2O_5:0.50C_{16}TACl:2.60TMAOH:350H_2O$ where x = 0.29-2.34. The reaction mixtures were allowed to react for 72 hour and were otherwise treated as in Section 3.2.

3.2.1.2 Effect of TMAOH concentration

Reaction mixtures with three different Al/P ratios (0.58, 1.17 and 1.77) were used for this experiment. For each Al/P ratio, five synthesis mixtures, each with different amounts of TMAOH, were prepared as follows: (1) 7.40, 9.87, 14.64, 22.96 and 24.39 g of TMAOH for Al/P ratio equal to 0.58; (2) 5.32, 8.78, 15.73, 19.97 and 22.39 g of TMAOH for Al/P ratio equal to 1.17, and 4.54, 7.60, 15.44, 20.77 and 26.00 g of TMAOH for Al/P ratio equal to 1.77. The molar composition of the reaction mixtures were as follows:

$0.58Al_2O_3:P_2O_5:0.50C_{16}TMACl:xTMAOH:347H_2O$, where x = 0.53-1.82

$1.17Al_2O_3:P_2O_5:0.50C_{16}TMACl:yTMAOH:344H_2O$, where y = 0.39-1.68

$1.77Al_2O_3:P_2O_5:0.50C_{16}TMACl:zTMAOH:350H_2O$, where z = 0.34-1.40

The reaction mixtures were otherwise treated as in Section 3.2.

3.2.1.3 Effect of CTACl concentration

Since a highly crystalline hexagonal phase was obtained at A/P ratio of 0.58, this ratio was therefore used for this experiment. Four synthesis mixtures were prepared with the following CTACl weights: 5.82, 8.00, 17.00 and 23.23 g. The molar composition of the reaction mixtures were as follows: $0.58Al_2O_3:P_2O_5:yC_{16}TACl:3.44TMAOH:348H_2O$, where y=0.24-0.98. The reaction mixtures were otherwise treated as in Section 3.2.

3.2.1.4 Effect of synthesis time

Six identical reaction mixtures with molar composition of $0.58Al_2O_3:P_2O_5:0.50C_{16}TACl:3.22TMAOH:350H_2O$ were prepared as per section 3.2. The mixtures were allowed to react and one sample was analyzed after each of the following synthesis times: 5, 10, 24, 48, 72 and 96 hours.

3.2.1.5 Effect of mixing time of aluminum and phosphorous precursors

This experiment was done to investigate the effect of mixing time of aluminum and phosphorous precursors on the product obtained. Reaction mixtures with two Al/P ratios (0.58 and 1.17) were used with molar composition of the starting mixtures as follows:

$0.58\ Al_2O_3:P_2O_5:0.50\ C_{16}TACl:3.02\ TMAOH:349\ H_2O$

$1.17\ Al_2O_3:P_2O_5:0.50\ C_{16}TMACl\ :2.68\ TMAOH:349\ H_2O$

Aluminum and phosphorous precursors were mixed for 0.5, 2, 4, and 6 hour prior to the addition of TMAOH. The synthesis time was at 72 hour at 25 °C. The reaction mixtures were otherwise treated as in Section 3.2.

3.2.2. Synthesis of aluminophosphates using aluminum isopropoxide

The synthesis procedure was as per Section 3.2.1 except that aluminum isopropoxide was used as the aluminum source.

3.2.2.1 Effect of the Al/P ratio and mixing time

Four synthesis mixtures, differing only in the amounts of aluminum isopropoxide, were prepared. Aluminum isopropoxide weights were as follows: 4.36, 5.82, 8.74 and 17.54 g. The molar composition of the synthesis mixture were as follows: xAl_2O_3:P_2O_5:0.50 C_{16}TACl: 1.5TMAOH:349H_2O, were varied from 0.58 to 2.33. The aluminum and phosphorous species were mixed for 6 hour before the addition of TMAOH. The synthesis mixtures were otherwise treated as in Section 3.2.

3.2.2.2 Effect of TMAOH concentration

A study of the effect of TMAOH variation on each of two reaction mixtures of different Al/P ratios (0.59 and 1.17) was conducted. For the 0.59 Al/P ratio mixture, 2.88, 3.46 and 7.22 g of TMAOH were added, while for the 1.17 Al/P ratio mixture, 0.0, 2.18 and 20.39 g of TMAOH were added. The molar compositions of the mixtures obtained were as follows:

$0.58Al_2O_3$:P_2O_5:0.50C_{16}TACl:xTMAOH:347 H_20, where x = 0.53-1.82

$1.17Al_2O_3:P_2O_5:0.50\ C_{16}TACl:xTMAOH:349\ H_20$, where x = 0.34 -1.95.

In addition to synthesis at 25 °C, separate aliquots of the mixtures were also subjected to a higher temperature (110 °C). The mixtures were otherwise treated in the same manner as in Section 3.2.

3.2.2.3 Effect of CTACl concentration

Three CTACl variations of each of two reaction mixtures with different Al/P ratios (0.58 and 1.16) were prepared. For mixtures with Al/P ratio equal to 0.58, the CTACl weights were 5.80, 7.74 and 17.4 g, while for mixtures with Al/P ratio equal to 1.16, the weights were 5.80, 7.75 and 17.4 g. The molar compositions obtained from these mixtures were as follows:

$0.58Al_2O_3:P_2O_5:xC_{16}TACl:3.44\ TMAOH:348\ H_2O$, where x = 0.24-0.74

$1.16Al_2O_3:P_2O5:xC_{16}TACl:1.80\ TMAOH:346\ H_20$, where x = 0.24-0.74.

The synthesis mixtures were conducted at 25 and 110 °C but otherwise were treated in the same manner as in Section 3.2.

3.2.2.4 Effect of water concentration

Three different water concentrations in each of the two reaction mixtures with different Al/P ratios (0.58 and 1.15) were evaluated. For mixtures with Al/P ratio equal to 0.58, the water weights were 28.75, 57.47 and 230 g, while for mixtures with Al/P ratio equal to 1.15, the weights used were 28.70, 57.47 and 230 g. The syntheses were conducted at 25 and 110 °C for 72 hours with the following molar compositions:

0.58Al_2O_3:P_2O_5:0.50 C_{16}TACl:2.30 TMAOH:w H_2O, where w = 86.0-689

1.15 Al_2O_3:P_2O_5:0.48 C_{16}TACl:1.48 TMAOH:w H_2O, where w = 86.0-687.

The mixtures were otherwise treated as in Section 3.2.

3.2.3 Synthesis of aluminophosphates using psuedobohemite alumina

Psuedobohemite alumina was another choice of aluminum source that is widely used in the synthesis of microporous and mesoporous materials. The products obtained using this aluminum source were investigated.

3.2.3.1 Effect of Al/P ratio

Four different synthesis mixtures were prepared, each containing 2.57, 3.42, 5.14 and 10.28 g of pseudobohemite alumina, giving the following molar composition; xAl_2O_3:P_2O_5:0.50CTACl:2.98 TMAOH:350.0H_2O, where x = 0.59-2.34. The mixtures were otherwise treated as in Section 3.2.1.

3.2.3.2 Effect of water concentration

Using synthesis mixtures at two Al/P ratios (0.58 and 1.17) various amounts of water were added. The water weights at both ratios were 28.75, 57.47 and 230 g. The molar composition for these synthesis mixtures were as follows:

0.86 Al_2O_3:P_2O_5:0.50 C_{16}TACl:3.22 TMAOH:x H_2O, where x = 87-700

0.43 Al_2O_3:P_2O_5:0.50 C_{16}TACl:3.26 TMAOH:xH_2O, where x = 87-700.

The synthesis mixtures were otherwise treated as in Section 3.2.1.

3.3 Calcination

The as-synthesized, dried samples were calcined in a Thermolyne tube furnace to remove the organic template. The samples were placed in a quartz boat, placed in the tube furnace, and slowly heated to various temperatures up to 500°C in the presence of flowing nitrogen, followed by oxygen at 70ml/min.

3.4 Characterization

3.4.1 X-ray powder diffraction

A typical x-ray diffractometer consists of an x-ray source with a fixed wavelength, a mount for a single crystal or fine powder of the compound being investigated, and an x-ray detector. The positions of the detector and the crystal are controlled by a computer. For certain orientations of the crystal relative to the x-ray beam, the crystal diffracts the x-rays at a fixed angle and the intensity is measured when the detector is placed in the direction of this diffracted beam. A powder x-ray diffractogram gives a plot of the intensity of scattered radiations as a function of the angular positions at which the x-ray was scattered.[29] The Bragg equation[30] is the mathematical relation connecting the wavelength λ of the reflected x-radiation, the spacing, d, of the reflecting planes within a sample (substrate), and the angle of reflection, θ, and is written as :

$$n\lambda = 2d \sin \theta.$$

The crystallinity of the materials was characterized by the x-ray powder diffraction method using a Philips X'PERT diffractometer with Cu-Kα radiation and nickel filters. The samples were first ground into fine powders and then packed into aluminum sample holders. The sample holder was mounted in the path of the x-ray beam and the instrument started by turning on the x-ray source through the computer interface. The x-ray source was a Cu-Kα anode, and the voltage and current were maintained at 40 KV and 50mA, respectively. The diffractometer was programmed to scan diffraction angles (2θ) from 1 to 25 at a step size of 0.02 (2θ) and a step time of 10 second.

3.4.2 Surface area and pore size distribution analysis

The gas volume adsorbed by a substrate at each pressure increment at constant temperature defines an adsorption isotherm, from which the quantity of gas required to form a monolayer over the external surface of the solid and its pores is determined. From the known area covered by each adsorbed gas molecule, the surface area can be calculated. The three isotherm equations that are most frequently used are those due to Langmuir, Freundlich and Braunauer, Emmett and Teller (BET). For each point designated for surface area calculation, a BET surface area (m^2/g) can be performed with the following equation.[31]

$$SA_{BET} = (CSA)(6.023 \times 10^{23})/(22414\ cm^3\ STP)\ (10^{18}\ nm^2/m^2)\ (S+Y_{INT})$$

CSA = analysis gas molecular cross-sectional area (nm^2)

S=Slope (S g/cm^3 STP)

Y_{INT}= Y intercept (g/cm^3 STP)

In the BET analysis, physical adsorption is not limited to a monomolecular layer, but can continue until a multimolecular layer of liquid covers the adsorbent surface. The theory of BET is an extension of the Langmuir treatment to allow for multilayer adsorption on non-porous solid surfaces.[31]

Multiple-point BET surface area and pore size analyses were done on the calcined products using a Micromeretics Gemini 2360 Surface Area Analyzer. To determine surface area and pore size measurements, a preweighed portion of each sample was placed in a tube and degassed for 2 hour at 200 °C to remove adsorbed contaminants acquired from atmospheric exposure. The sample was placed in the BET analyzer and adsorption was performed at 77 K using nitrogen as an adsorbate. Relative pressure range (P/Po) of 0.1-0.3 and 0.1-1.0 was used for surface area and pore size analysis, respectively. The Barret, Joyner and Halenda (BJH)[31] model was used to calculate the pore size distribution from the relative pressure and volume obtained from BET data.

3.4.3 Thermogravimetric analysis

In thermogravimetric analysis, the mass of a sample in a controlled atmosphere is recorded continuously as a function of temperature. A plot of mass or mass percent as a function of temperature yields a thermogram.[29]

The changes in physiochemical states of solids subjected to temperature variation are accompanied by heat transfer. The exothermic and endothermic effects can be measured quantitatively by differential thermal analysis (DTA). In this technique the

difference in temperature between a substance and a reference material is measured as a function of temperature, while the substance and reference material are subjected to a controlled temperature program. The DTA is performed simultaneously with the TGA analysis, by using an empty ceramic pan as the reference.

TGA analysis was performed on a SDT 2960 from TA Instruments, Inc. Milligram quantities of sample were placed in a ceramic crucible. The sample was heated from ambient to 700 °C at a heating rate of 10 °/min in flowing air.

3.4.4 Magic Angle Spinning NMR analysis

When the nuclei of certain elements are subjected to a strong magnetic field, additional quantized energy levels can be observed as a consequence of the magnetic properties of the elementary particles. Absorption by nuclei or by electrons in a magnetic field can thereby be studied by nuclear magnetic resonance (NMR). This technique is mainly used to study compounds in solution. However, solids can be investigated by the technique of Magic Angle Spinning (MAS). Magic angle spinning involves rotating the solid samples rapidly at a frequency greater than 2KHz in a special sample holder that is maintained at an angle of 57.4° with respect to the applied field. In effect, the solid then acts like a liquid being rotated in the field.[35] NMR is also used to differentiate nuclei, e.g., ^{27}Al, in different chemical environments.

^{27}Al MAS NMR measurement was performed on a DSX-400 spectrometer at a resonance frequency of 104.18 MHz, spinning rate of 7.5 KHz with a 45° pulse length of 4.5 μsec. For each spectrum, 128 scans were acquired with a 5 sec repetition between scan. Aluminum nitrate was used as an external reference. ^{31}P MAS NMR

spectra were measured at a resonance frequency of 161.86 MHz with 60°pulse length of 5.0 μsec at a spinning rate of 9.9 KHz, 32 scans and a 30 second repetition between scans. ^{31}P chemical shifts were quoted with respect to an external standard of 85% phosphoric acid.

3.4.5 Chemical analysis by Inductivley Coupled Plasma Mass Spectroscopy

In the ICP-MS spectrometry an ICP torch serves as an atomizer and ionizer. The torch is usually operating at temperatures as high as 10,000 K at which stage all components of a compound are converted to elemental form. Sample introduction occurs by a conventional or an ultrasonic nebulizer. In these instruments, positive metal ions produced in a conventional ICP torch are sampled through a differentially pumped interface linked to a quadrupole mass spectrometer.[29]

A mass spectrometer separates ions on the basis of their mass-to-charge ratios, m/z. The principal components include an inlet system where a micro amount of sample is introduced into the ion source and the components are converted into gaseous ions by bombardment with electrons, photons, other ions or molecules. Alternatively, ionization is brought about by thermal or electrical energy. The output of the ion source is a stream of positive or negative gaseous ions that are then accelerated into the mass analyzer. A transducer then converts the beam of ions to an electrical signal that can then be processed, stored in the memory of a computer and displayed or recorded.[29] The spectra obtained consists of a simple series of isotope peaks for each element present. These spectra are used for quantitative determination of elements based upon calibration curves in which the ratio of the ion count for the analyte to the count for an internal standard is plotted as a function of concentration.

The aluminum and phosphorus compositions of samples were determined by ICP-MS using the Perkin Elmer Elan 5000 instrument. The samples were prepared by mixing accurately weighed aliquots (0.006 g) of sample with 0.025 g of sodium borate ($Na_2B_4O_7{\cdot}10H_2O$). The mixtures were fused (melted) in a platinum crucible at 700 °C in a Fisher Scientific Isotemp muffle furnace. After 2 hours the melt was allowed to cool slowly. The solid mass was then dissolved in 5 ml of hot concentrated HNO_3, placed in a 100 ml volumetric flask and made up to the mark with deionized water. The solution was then diluted by a 100-fold with deionized water and ICP-MS analysis was performed.

3.4.5.1 Preparation of standards: The standard solution for analysis of Al and P was prepared by taking appropriate amounts of certified stock standard (10 μg/ml of P and 100 μg/ml of Al, Accustandard Co.) into a 100 ml volumetric flask and filled to the mark with 1% HNO_3 acid. From this solution the following working standards were prepared: 10, 50, 100, 500 and 1000 ppb.

3.4.6. Infrared Spectrometry

Infrared absorption, emission and reflection spectra for molecular species arise by transitions of molecules from one vibrational or rotational energy state to another. The infrared region encompasses radiation with wave numbers ranging from about 12,800 to 10 cm^{-1}. The infrared spectrum is divided into near-, mid-, and far-infrared radiations. Typical spectroscopic instruments contain five components, including a stable source of energy, a transparent container for holding the sample, a device that isolates a restricted region of the spectrum for measurement, a radiation detector to convert radiant energy to

a usable signal (usually electrical) and a signal processor and readout, which displays the transduced signal.[31]

Infrared spectroscopy analysis was performed with a Harrick high–vacuum temperature-controlled stainless steel reaction chamber (HVC) diffuse reflectance accessory fitted to a Nicolet 750 Magna IR. Samples were prepared by mixing, 0.002 g quantities of finely ground sample with approximately 0.005 g of the KBr powder. This was then placed in the cell and the infrared spectrum measured.

CHAPTER 4

RESULTS AND DISCUSSION

4.1 Synthesis of aluminophosphate with aluminum hydroxide

The composition of the starting mixtures for various Al/P ratios was as follows: $xAl_2O_3:P_2O_5:0.5CTACl:2.6TMAOH:351H_2O$, where x was varied from 0.3 to 2.3. Depending on the Al/P ratios of the synthesis mixtures, x-ray diffraction patterns in Figure 1 indicate that a lamellar and/or hexagonal phase was obtained. For samples with an Al/P ratio 0.33-1.25, the XRD patterns show a prominent peak at 2θ of 2.1°, corresponding to hkl (100) reflections with a d-spacing of 4.1 nm; and a much weaker peak at 2θ of 3.8° corresponding to hkl (110) reflections. This combination of peaks is reported to correspond to a hexagonal lattice.[25] For a sample with an Al/P ratio equal to 0.29, the XRD pattern shows a main peak at 2θ of 2.1° corresponding to d-spacing of 3.1 nm, and a second peak at 2θ of 5.1° corresponding to d-spacing of 3.51 nm. Several peaks in the 2θ region higher than 15° were observed. This combination of peaks is characteristic of a lamellar phase.[26]

The ^{27}Al and ^{31}P MAS NMR spectra of the lamellar and hexagonal phases prepared from reaction mixture with Al/P ratio equal to 0.58 conducted at 110 and 25 °C are shown in Figure 2 correspondingly. The ^{27}Al NMR spectrum of the lamellar phase showed a sharp signal at 42.5 ppm indicating the presence of four-coordinated Al, which

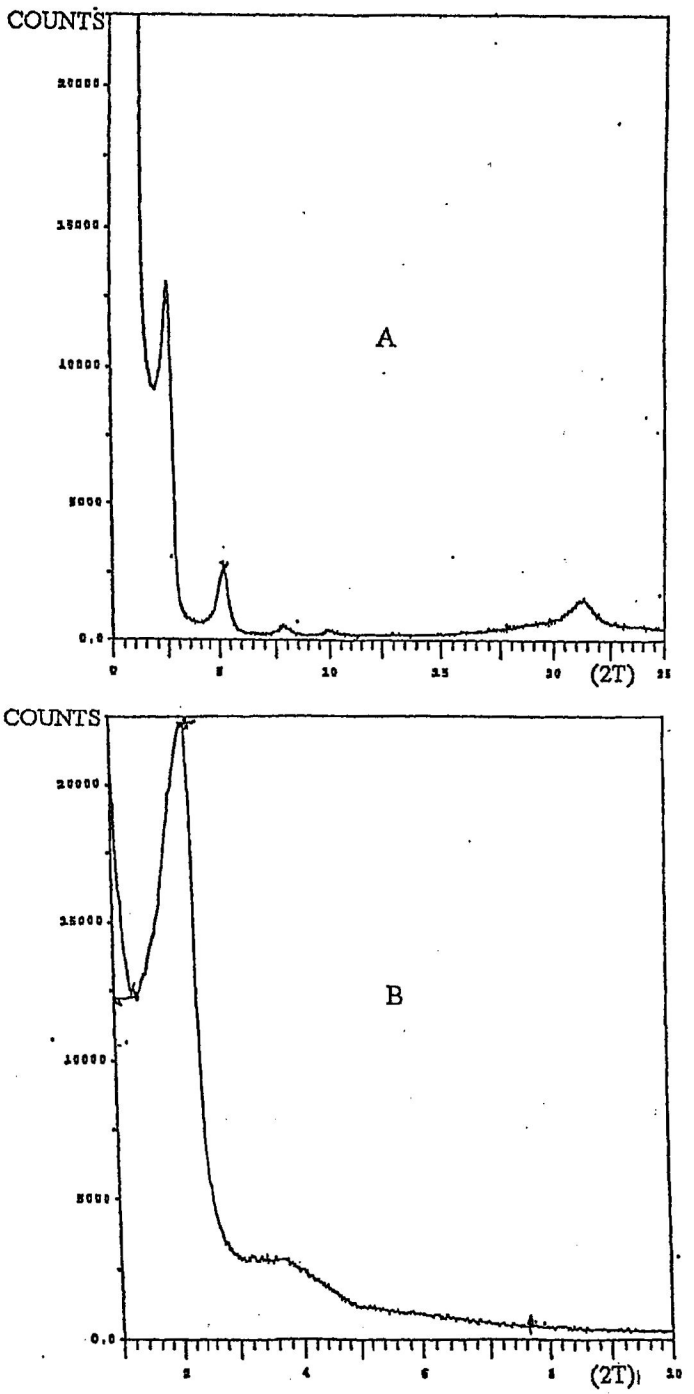

Figure 1: XRD patterns of a) Lamellar and b) Hexagonal phases

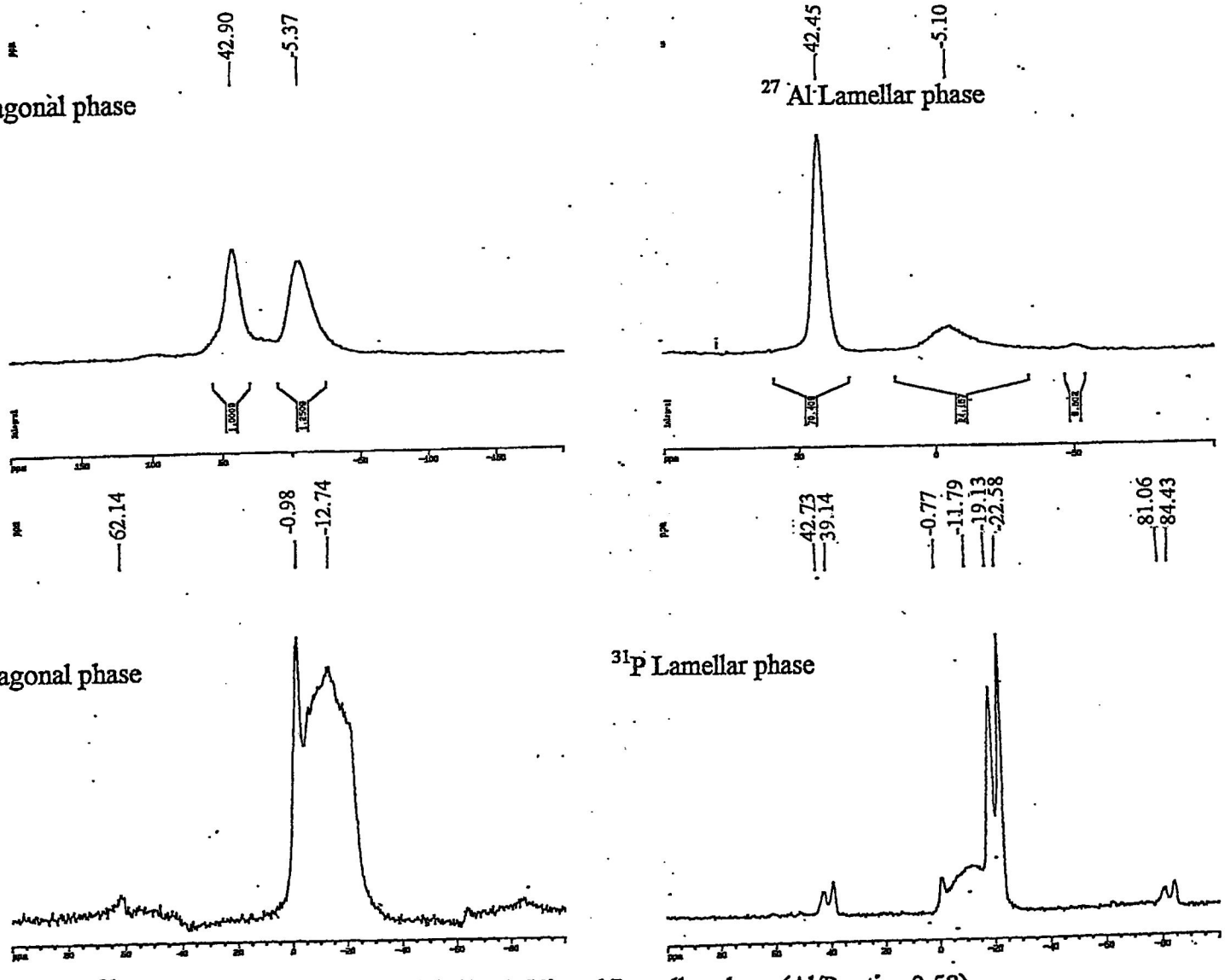

Figure 2: ^{27}Al and ^{31}P MAS NMR of Hexagonal (Al/P=0.58) and Lamellar phase (Al/P ratio=0.58)

can be assigned to $Al(OP)_4$ units.[20] A small peak observed at -5.1 ppm is assigned to small amounts of six-coordinated Al.[20] The ^{31}P MAS NMR spectrum for the lamellar phase shows two peaks at -19.1 and -22.6 ppm, both of which are assignable to $OP(OAl)_3$ units.[20]

The ^{27}Al MAS NMR spectrum for the hexagonal phase indicates two different chemical shifts. The signal at 42.9 ppm is assigned to four-coordinated Al bonded to phosphorus atoms via oxygen bridges, represented as $AlPO_4$ and or $Al(OP)_{4-x}(OH)_x$. The peak at –5.4 ppm is attributed to the framework octahedral aluminum, coordinated possibly with both water and PO_4 groups.[20] The ^{31}P MAS NMR spectrum for hexagonal phase shows several peaks ranging from 0 to –20 ppm. Two peaks at -12.7, -0.98 ppm were observed. Mortlock *et al.*, reported that the P atoms in Al $(H_2O)_5$ (H_3PO_4), Al $(H_2O)_4$ $(H_3PO_4)_2$ and Al $(H_2O)_4$ $-(H_3PO_4)$ (H_2PO_4) are observed at –12.6 ppm and $P(OAl)_4$ units are observed at –0.98.[32] Phosphorous present in hexagonal phase in Figure 2 may therefore be attributed to tetrahedral phosphorus bonded to aluminum tetrahedra and hydroxyl groups or water. The reported chemical shifts of ^{31}P in microporous $AlPO_4$ type materials generally fall in the range –19 to –30 ppm.[20] The shift of the ^{31}P NMR signal to lower fields can be caused by several factors: monovalent cations, acid protons, and coordinated water can all cause downward shifts in the spectra of phosphates.[20] The PO_4 units are therefore bonded to one or two Al atoms, suggesting some octahedral coordination. Therefore, the hexagonal phase has a less condensed framework.[26]

The IR spectra of the lamellar and hexagonal phases described above are shown in Figure 3. The lamellar phase shows several peak in the region of 1668-739 cm^{-1}. The region of 1225-1056 cm^{-1}, 739 cm^{-1} are due to the asymmetric stretching of

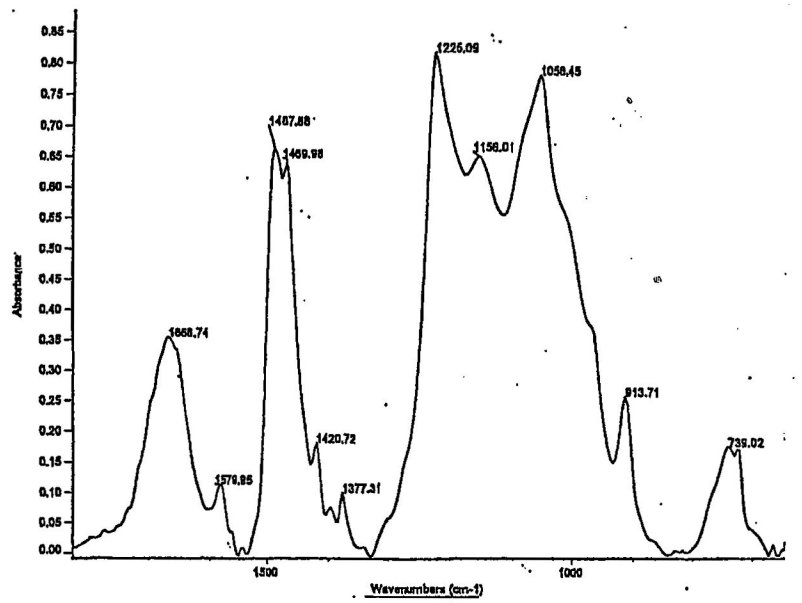

Lamellar phase

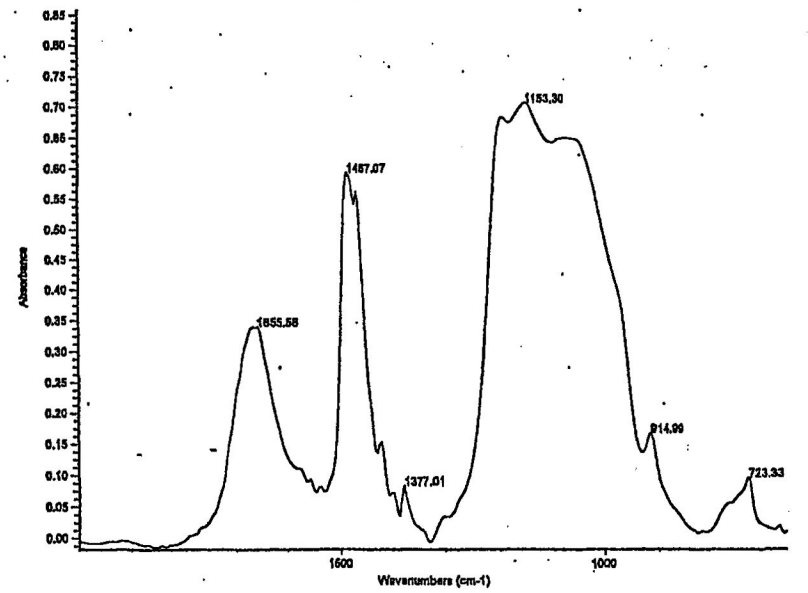

Hexagonal phase

Figure 3: IR Spectrum of a) Lamellar b) Hexagonal Phase

Al-O-P and the symmetric stretching of Al-O-P, respectively.[26] The hexagonal phase shows several peaks in the 1655 to 723 cm^{-1} region. The peak at 1487cm^{-1} and a broad peak at 1153 cm^{-1} correspond to the asymmetric stretching of Al-O-P and the peak located at 723 cm^{-1} is due to the symmetric stretching of Al-O-P.[26] IR analysis, therefore, provided further evidence for the presence of Al-O-P bonding in the products but did not provide further information differentiating the lamellar and hexagonal phases obtained.

Figure 4 shows the thermograms obtained from the thermogravimetric analysis of the lamellar phase from samples synthesized with Al/P equal to 0.29 in mixture, and hexagonal phase from samples with Al/P equal to 0.58. A total weight loss of 67.3% for lamellar phase and 60.03% for hexagonal phase is exhibited in three stages. For both lamellar and hexagonal phases the weight loss events at 80 °C, 121 °C, and 353 °C correspond to water desorption, decomposition of CTACl, and decomposition of TMAOH, respectively.[25] For samples with Al/P ratio equal to 0.29, a 52% weight loss corresponding to the loss of the CTACl was obtained while a Al/P ratio equal to 0.58 a 41% weight loss was determined. TGA analysis also established that calcination of the samples could be conducted at less than 400 °C to remove the organics.

4.1.1 Effect of Al/P ratio

For sample synthesized with Al/P ratio less than 0.33 in mixture, a lamellar phase was observed in the diffractogram with the major peak at 2θ of 2.7°corresponding to d (100) spacing of 3.5 nm shown in Figure 5. As the Al/P ratio increased to the range 0.33-1.25 the hexagonal phase was obtained, with a main peak at 2θ of 2.1° corresponding to a

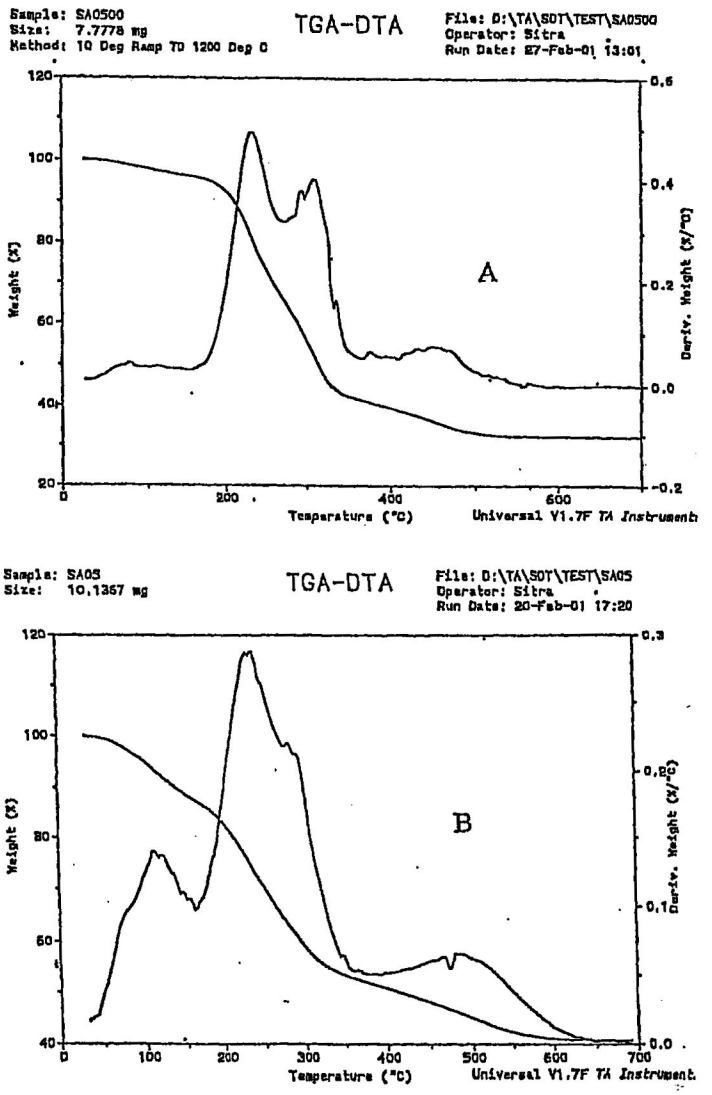

Figure 4: TGA/DTA data of a) Lamellar and b) Hexagonal phase

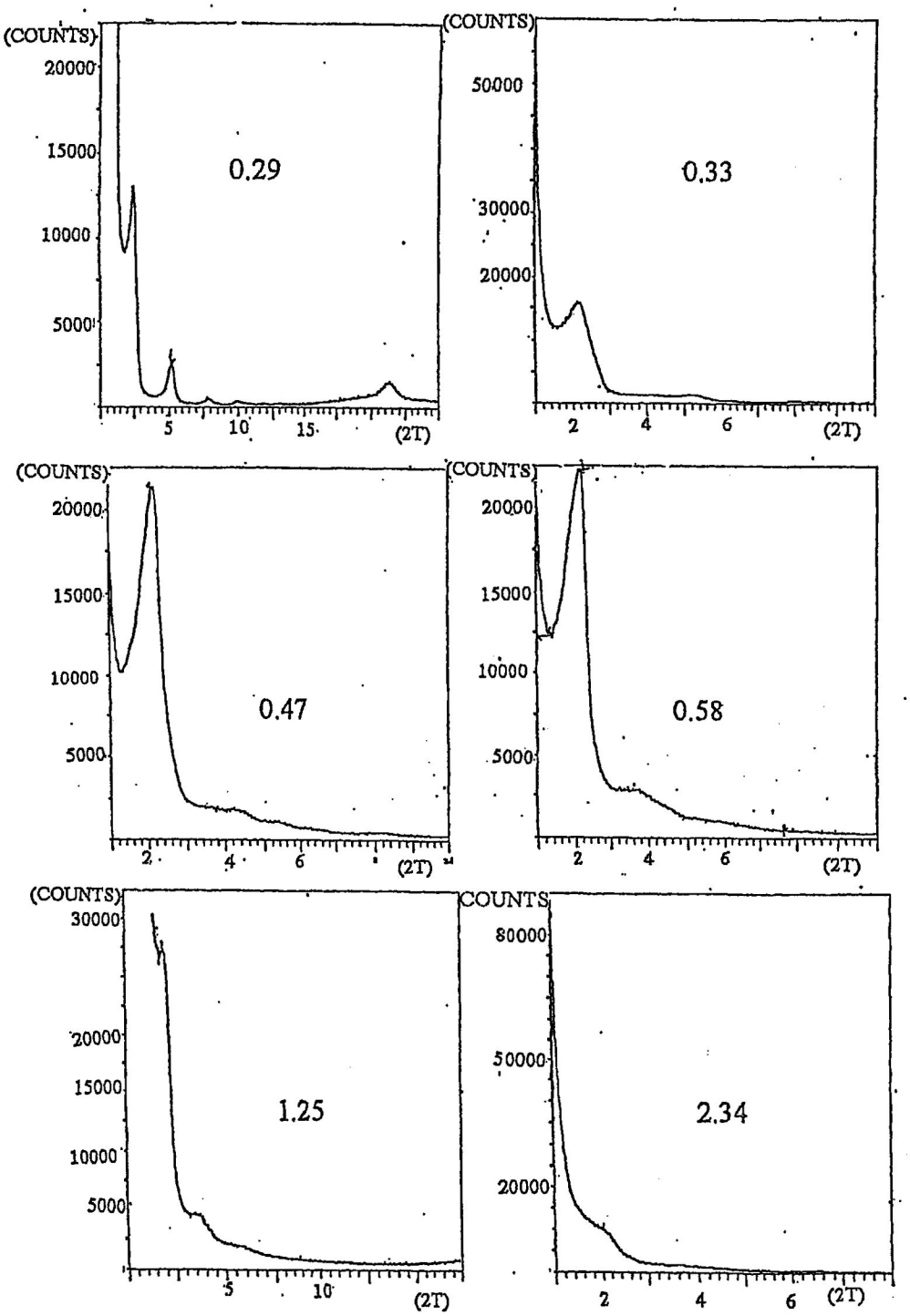

Figure 5: XRD patterns of samples synthesized at various Al/P ratios in mixture (Al/P as indicated on graph)

d (100) spacing of 4.1 nm and a smaller peak at 2θ of 3.9° with a d (110) spacing of 1.4 nm. For the hexagonal phase, peaks were most defined within Al/P ratios of 0.47-1.25. The highest lattice ordering was, therefore, obtained in this range. At higher Al/P ratio (>1.25), a broad, low intensity peak was observed due to a disordered hexagonal array. Aluminophosphates can form over a range of Al/P mole ratios (0.29-2.34) in the gel, which is different from a fixed Al/P ratio required for synthesis of microporous aluminophosphates.

The Al/P ratio in the product as indicated in Table 1 increases with increasing Al/P ratios in the gel. The Al/P ratio less than 1.25 in the mixture shows better resolved XRD patterns. This is because the Al/P ratios in the products range from 1.64-0.92 which correspond to the ideal $Al(PO)_4$ coordination. This was also observed by Kimura *et al.*, who reported that the Al/P ratios of the products increased with increase in Al/P ratio and TMAOH/P in the synthesis mixture.[26] They also reported that from their synthesis mixture of Al/P ratio 1, an increase in Al/P ratio to 2.23 was obtained in the products.

Table1: Effect of Al/P composition of starting mixtures on Al/P ratio in products

Al/P ratio in synthesis mixtures	pH of mixture	Al/P ratio of products obtained *RPD 8.3%
0.29	7.31	0.92
0.33	7.37	1.01
0.47	8.01	1.53
0.58	8.46	1.64
1.25	9.42	2.45
2.34	9.5	5.31

* RPD = Relative percent difference from 2 determinations 2 (A-B)/(A+B).

In order to determine the thermal stability of the as-synthesized materials, calcination at 500°C for 1 hour in nitrogen followed by air was conducted to remove the occluded organic template. Amorphous products were obtained for all Al/P ratios except for Al/P 1.25 (Figure 6). At this ratio, x-ray patterns indicated a partial loss in intensity of the main peak at 2θ of 2.1°, from 28000 counts in the as-synthesized material to 15000 counts in the calcined form. A peak broadening was also observed. This observation is likely due to the loss of crystallinity of the hexagonal array when subjected to calcinations determined by the decrease in intensity of XRD patterns. Surface area of the corresponding calcined product was 446 m^2/g. In order to examine the temperature at which the mesoporous materials of Al/P ratios 0.29, 0.33, 0.47, 0.58 and 2.34 lost stability, calcinations as low as 300 °C under flowing N_2 for 1 hour was conducted. This also resulted in a structural collapse, as evidenced by loss of peaks in x-ray diffraction patterns. An alternative organic extraction to remove the template using sodium acetate/ethanol mixture also resulted in similar structural collapse.

Since the mesoporous materials formed above indicated low thermal stability, it was considered that an increase in pore wall thickness might result in a stabilized framework upon calcination. Therefore, the effects of several reaction parameters on the synthesis and thermal stability of mesoporous aluminophosphates were investigated. The parameters included TMAOH and surfactant concentration, the aluminum source as well as reaction temperature, and time.

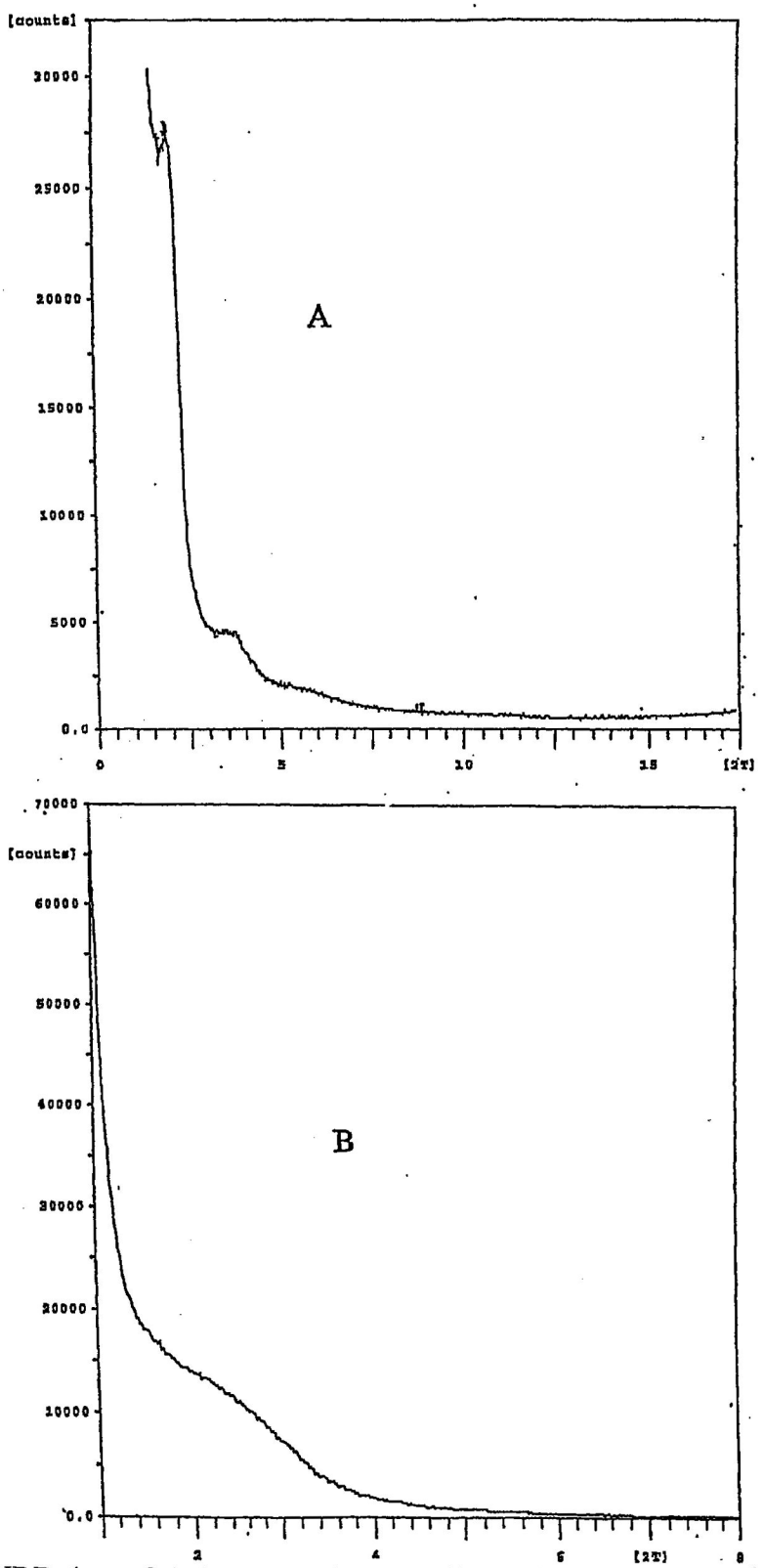

Figure 6: XRD data of a) As-synthesized and b) Calcined sample synthesized at Al/P ratio=1.25

4.1.2 Effect of TMAOH concentration

The TMAOH content of the starting mixtures were changed for three different Al/P ratio as follows:

$0.58Al_2O_3:P_2O_5:0.50CTACl:xTMAOH:347H_2O$, where x = 1.06-3.64

$1.17Al_2O_3:P_2O_5:0.50CTACl:yTMAOH:344H_2O$, y = 0.78-3.36

$1.77Al_2O_3:P_2O_5:0.50CTACl:zTMAOH:350H_2O$, where z = 0.68-2.80.

The XRD patterns of the products synthesized at room temperature are shown in Figure 7 with molar compositions $0.58Al_2O_3:P_2O_5:0.50CTACl:xTMAOH:347H_2O$, where x = 1.06-3.64 is shown in Figure 7. In the absence of TMAOH or with TMA/P_2O_5 ratio up to 1.06 (pH 5.2) amorphous products was observed. With further increase in the amount of TMAOH, the structure of the products changed from lamellar to hexagonal. At TMA/P_2O_5 of 1.48 (pH 6.51) a combination of hexagonal and lamellar type products with major peaks at 2θ values of 2.6 and d spacing of 3.33 nm were observed. An increase in the TMA/P_2O_5 ratio from 2.2 to 3.64 (pH 8.0 to 10.4) resulted in the hexagonal phase as the only ordered phase. Conducting the synthesis at 110 °C (Figure 8) gave lamellar phase for TMA/P_2O_5 ratio as high as 2.2 (pH 7.95). At this temperature, the hexagonal phase was formed at much higher TMA/P_2O_5 ratios of 3.44 and 3.64. A combination of low Al/P ratio and high TMAOH therefore favors the formation of the hexagonal phase at room temperature and the lamellar phase at high temperature. The formation of the mesoporous aluminophosphate materials is postulated to occur by a modified S^+I^- ion-pair process.[25] It is reported that the inorganic precursors (I^-) are non-ideal aluminophosphate species of low polymerization degree with some hydroxyl groups.

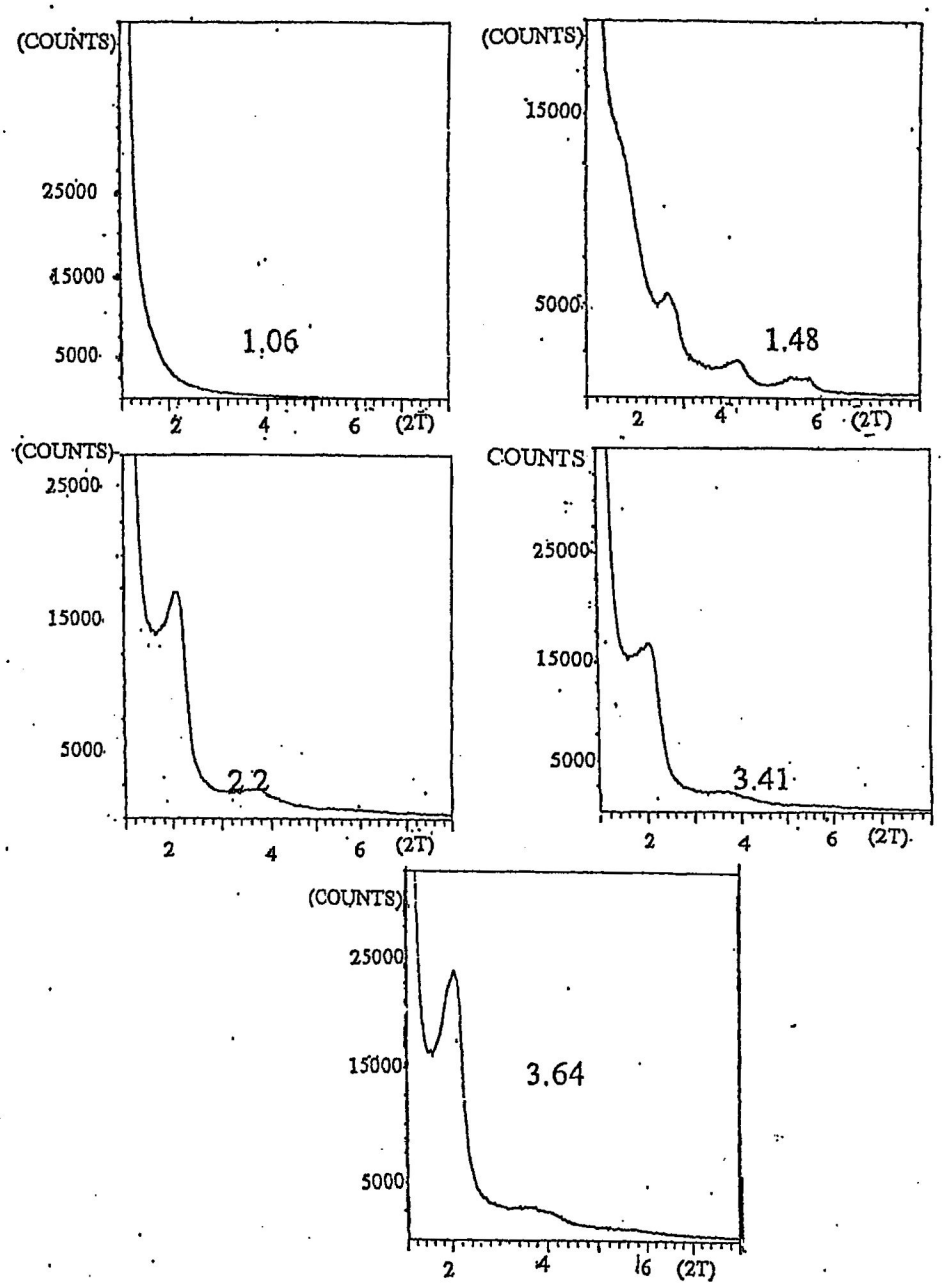

Figure 7: XRD patterns of products obtained from synthesis mixtures of various TMA/P_2O_5 ratios and fixed Al/P of 0.58 (synthesis conducted at 25°C). (TMA/P_2O_5 ratio as indicated on graph)

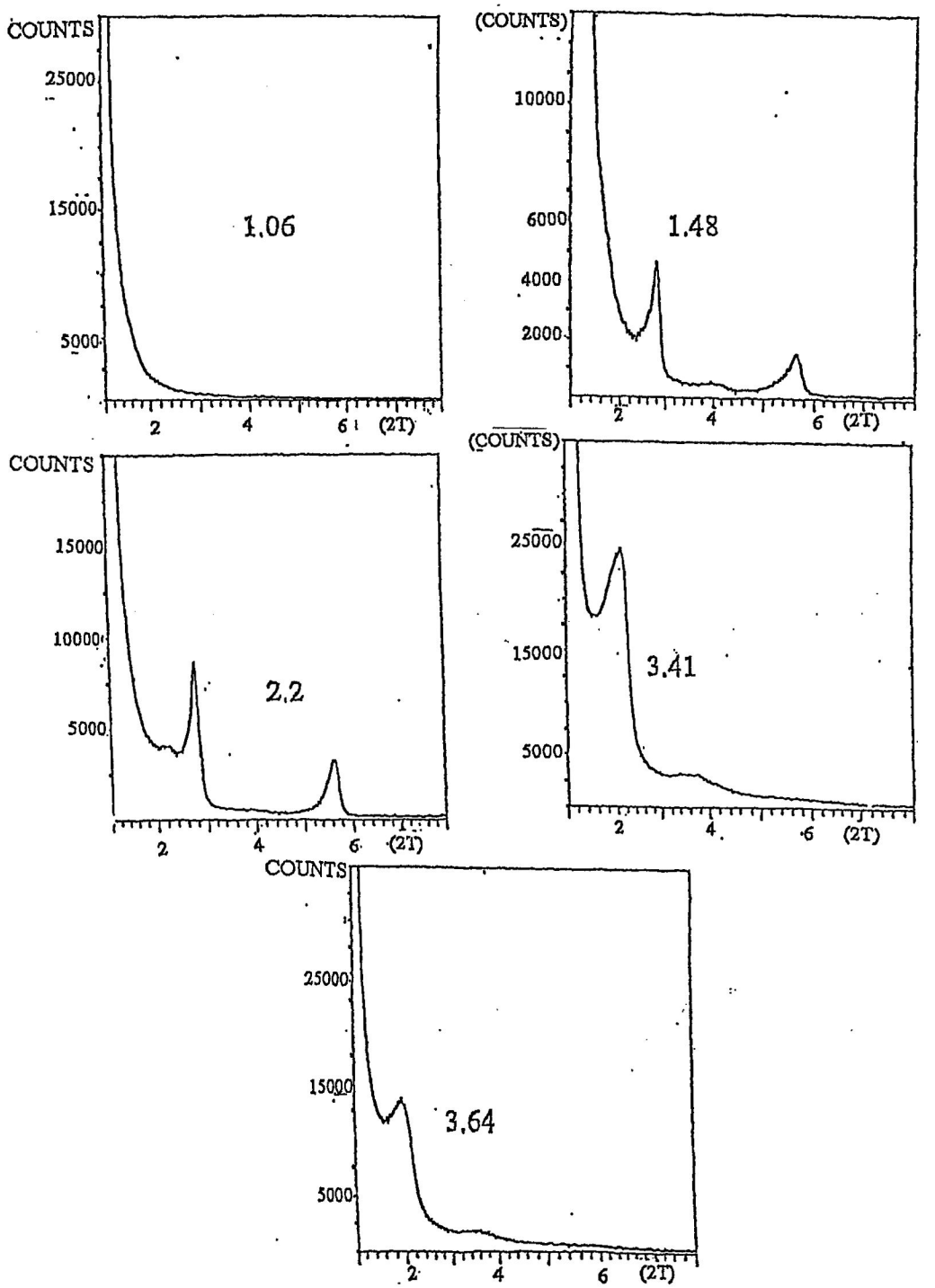

Figure 8: XRD patterns of products obtained from synthesis mixtures of various TMA/P_2O_5 ratios and fixed Al/P of 0.58 (synthesis conducted at 110°C). (TMA/P_2O_5 ratio as indicated on graph)

When TMAOH is added, it reacts with the hydroxyl groups of these aluminophosphate species to produce a weak ion pair ($I^-....TMA^+$) since the TMA^+ cation has a large ionic radius. These ion-pair species diffuse to the surfactant (S^+) assembly (micelle) interface and interact strongly with the cationic surfactant headgroups. The interaction of the aluminophosphate species with the cationic surfactant headgroups is stronger than that with TMA^+ cation. The micellar structure then organizes the condensation and polymerization of adjacent aluminophosphate species to form an ordered hexagonal mesostructure.[25]

The function of the organic ammonium cation from TMAOH, therefore, seems to be to modify the strength of the electrostatic interaction between the aluminophosphate species and the cationic surfactant micelle assembly to form the $S^+ I^-... TMA^+$ ion pair. It is reported that if NaOH is used instead, the Na^+ cation has a smaller ionic radius than TMA^+ cation, therefore, the Na^+ cation possesses a stronger ion-pair interaction with the aluminophosphate species and, therefore prevents sufficient interaction with the cationic surfactant assembly. Thus, the assembly of mesostructural aluminophosphate fails.[25]

In addition, TMA^+ also affects the phase change as indicated in Figure 4. High TMA^+ concentration suppresses the polymerization of the aluminophosphate oligomers, resulting in incomplete condensation occurring in the hexagonal phase as observed earlier by NMR data.[26] On the other hand, the lamellar phase has mainly tetrahedral coordination which affords a relatively condensed framework. Furthermore, the hydroxide species from TMAOH facilitates the hydrolysis of the inorganic precursors, so an increase in TMAOH concentration also resulted in more species that are hydrolyzed.

With an increase in the synthesis temperature to 110 °C, the progress of the condensation of inorganic species led to the formation of lamellar phase.

XRD patterns from the synthesis mixture at Al/P ratio equal to 1.17 are shown in Figures 9 and 10 for syntheses conducted at 25 and 110 °C, respectively. A similar trend is observed as was found in Figure **7,** except that a less ordered hexagonal phase was obtained at high TMA/P_2O_5 ratio of 3.64 (pH 10.03). Mokaya *et al.*,[33] reported that Al buried deep within the pore walls is known to reduce the structural ordering of aluminosilicate MCM-41, and may have a negative effect on stabilization of the framework. The position occupied by the directly incorporated Al may therefore be an important factor with respect to framework stabilization. Low Al content may favor the presence of Al predominantly on or near the surface, while in higher Al content materials the Al may occupy positions deeper within the pore walls.[33] With the higher Al/P ratio synthesis (1.77) (Figure 11), the hexagonal product formed at the TMA/P_2O_5 ratio of 2.32 and at room temperature decreased in quality relative to products synthesized at Al/P ratio 0.58 and 1.17. This may be due to the presence of high aluminum concentration that result in poor condensation. At higher temperature and Al/P ratio 1.77 (Figure 12), a hexagonal phase was found at the lower TMA/P_2O_5 ratio of 2.32. As indicated above, high temperature, low TMA concentration and low Al/P ratio favors the lamellar phase, but an increase in aluminum content may assist the formation of the hexagonal phase at low TMA content.

The extent of the condensation of inorganic species is important for the formation of both phases. Thus, it is necessary for the synthesis temperature to be low

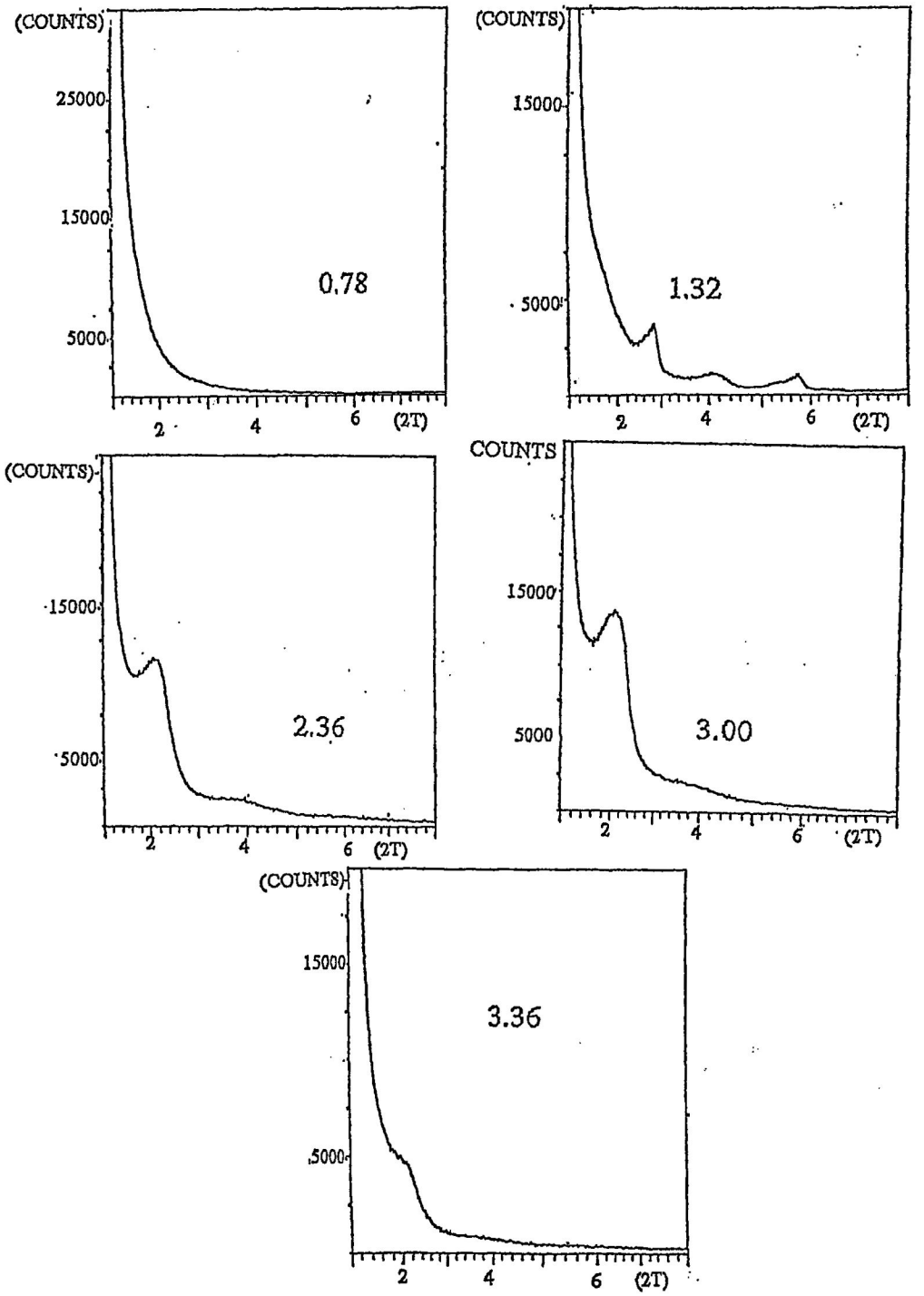

Figure 9: XRD patterns of products obtained from synthesis mixtures of various TMA/P2O5 ratios and fixed Al/P of 1.17 (synthesis conducted at 25°C) · (TMA/P2O5 ratios indicated on graph)

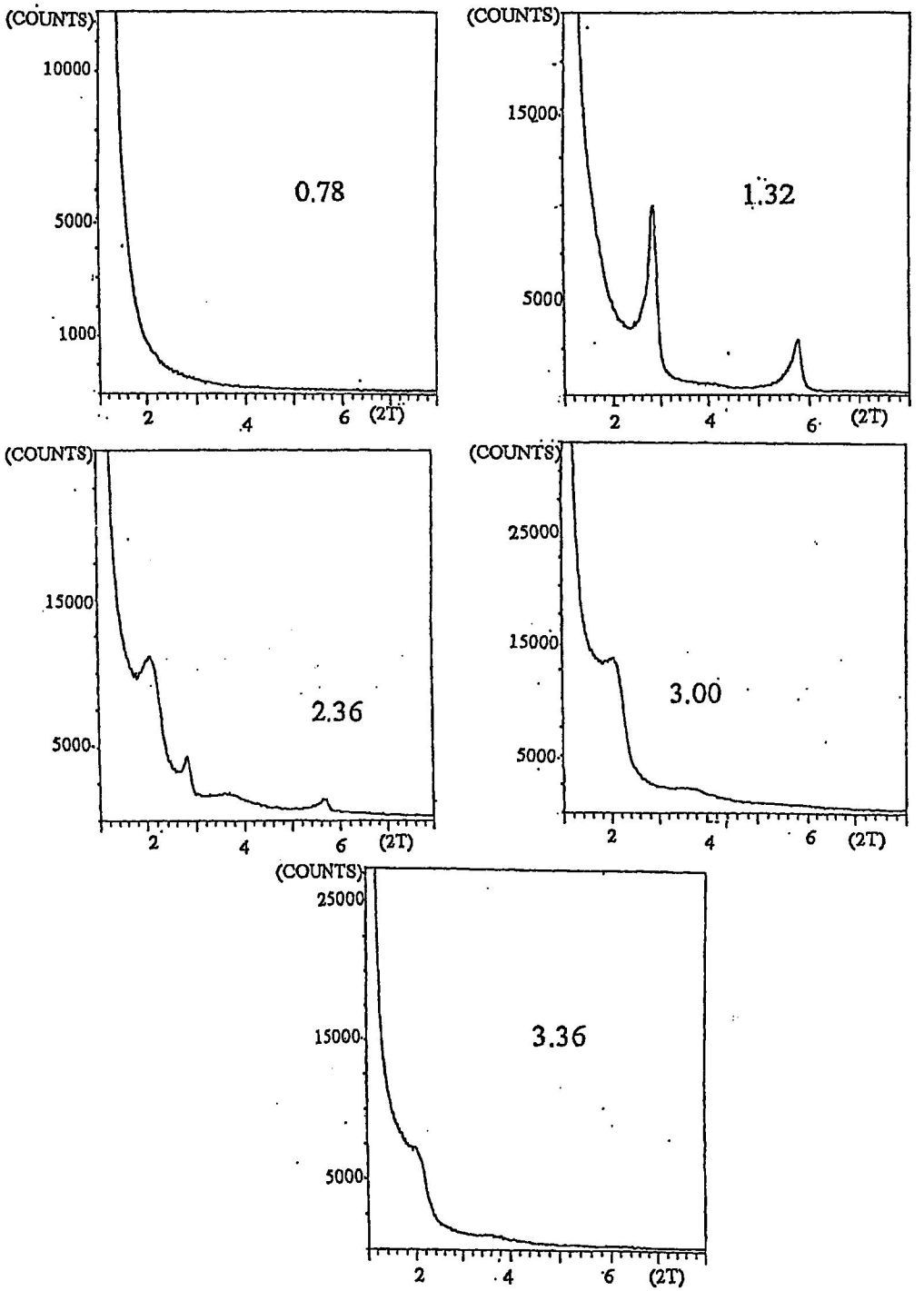

Figure 10: XRD patterns of products obtained from synthesis mixtures of various TMA/P_2O_5 ratios and fixed Al/P of 1.17 (synthesis conducted at 110°C). (TMA/P_2O_5 ratios indicated on graph)

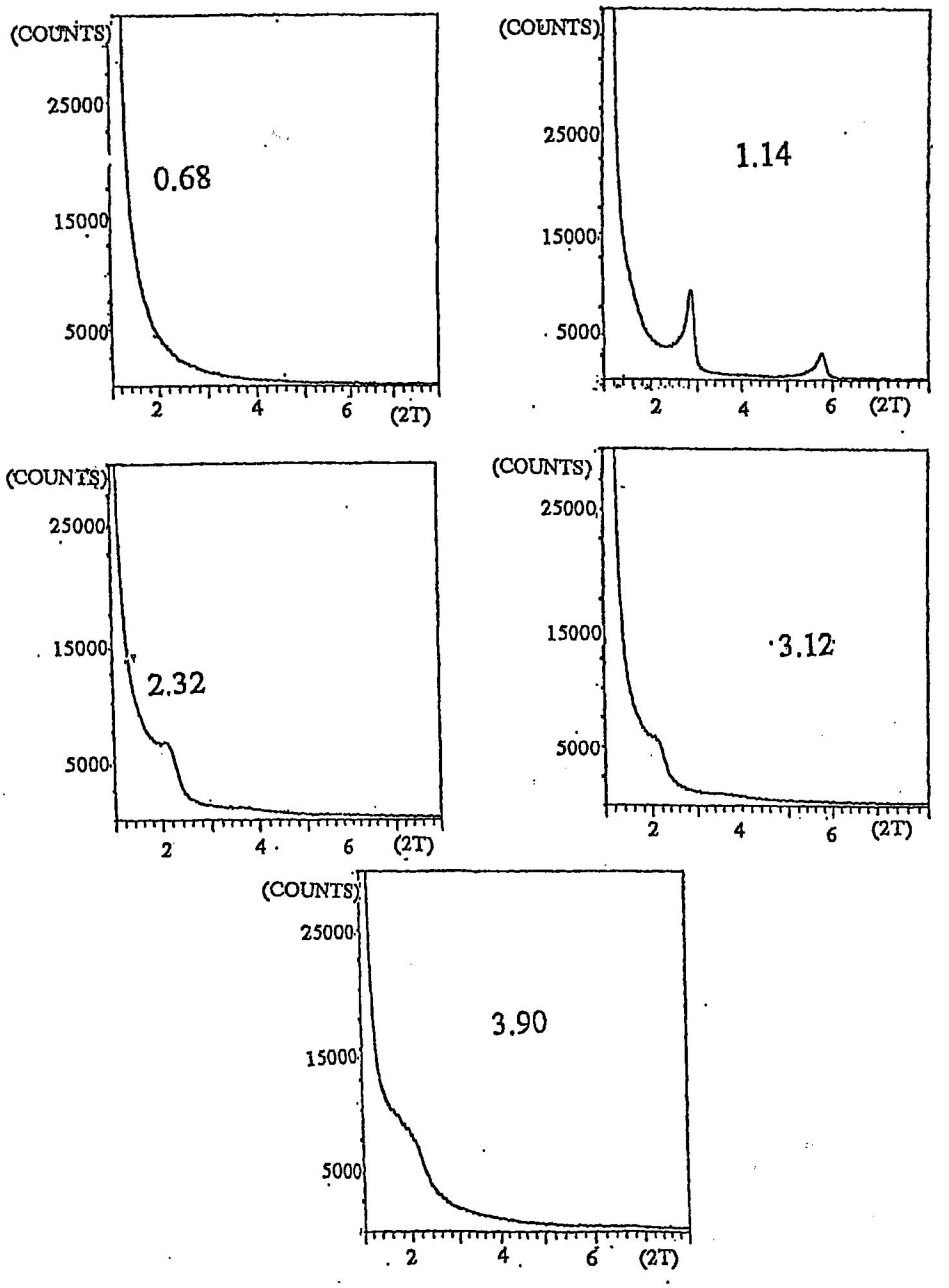

Figure 11: XRD patterns of products obtained from synthesis mixtures of various TMA/P_2O_5 ratios and fixed Al/P of 1.77 (synthesis conducted at 25°C) (TMA/P_2O_5 ratios indicated on graph)

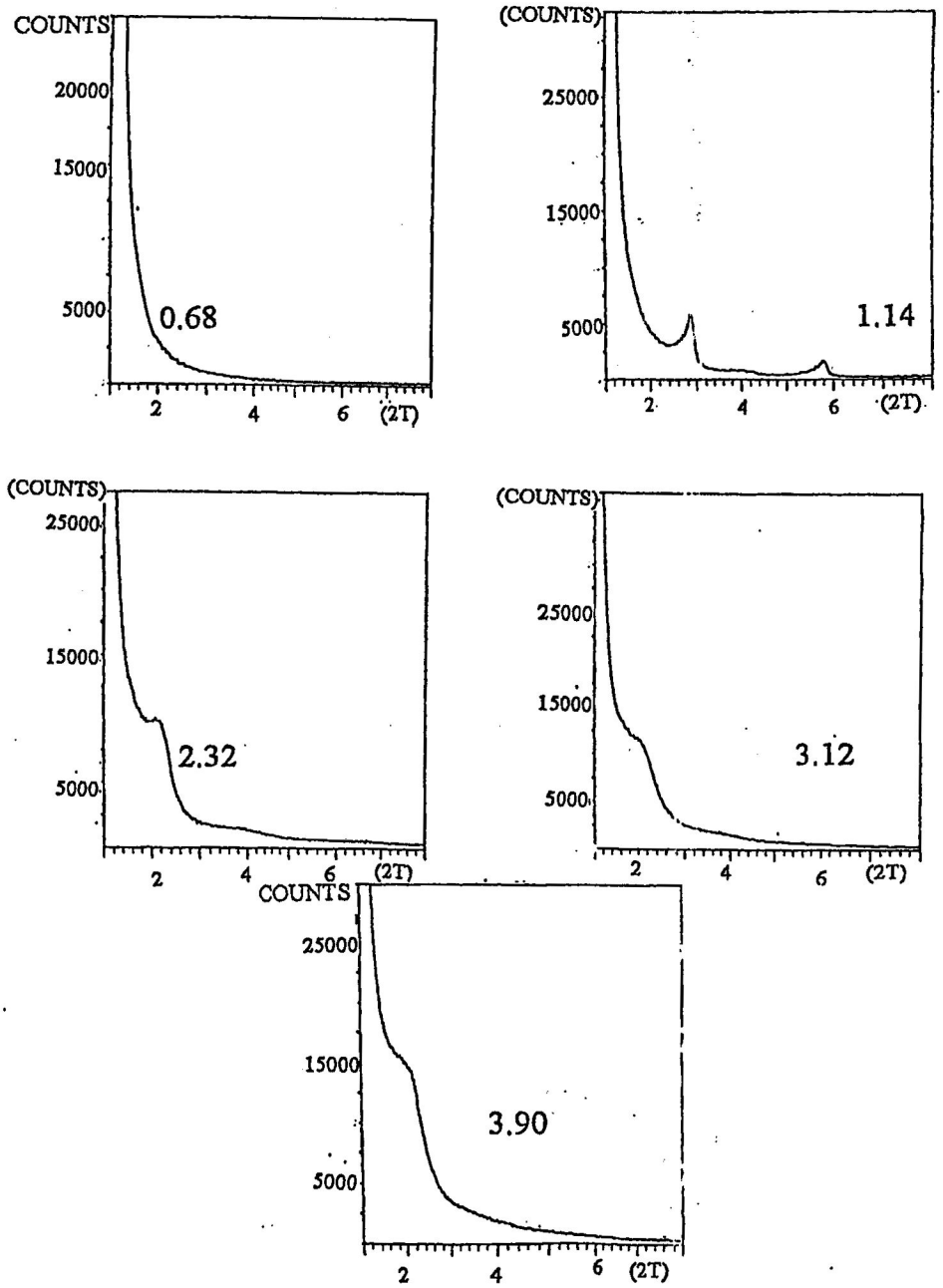

Figure 12: XRD patterns of products obtained from synthesis mixtures of various TMA/P_2O_5 ratios and fixed Al/P of 1.77 (synthesis conducted at 110°C) (TMA/P_2O_5 ratios indicated on graph)

in the preparation of the hexagonal phase in order to suppress the rate of condensation of inorganic species.[26]

4.1.3 Effect of surfactant concentration

Using the following molar composition, $0.58Al_2O_3:P_2O_5:yC_{16}TACl:3.44TMAOH:348H_2O$, a series of samples was prepared where y = 0.24-0.98. The critical micellar concentration of CTACl in the aqueous medium is $1.30x10^{-3}$ M,[28] the lowest CTACl concentration used in this experiment was 0.4617 M. Thus, the surfactant is in the micellar form. X-ray diffraction patterns in Figures 13 and 14 show that a significant increase in crystallinity was observed as $CTACl/P_2O_5$ was increased from 0.24 to 0.98. At $CTACl/P_2O_5$ ratio of 0.98 a lamellar phase was observed at 25 and 110 °C, whereas a crystalline hexagonal type structure was obtained for the $CTACl/P_2O_5$ ratio between 0.24 to 0.72. The fact that aluminophosphates can be synthesized from solutions containing only CTACl/OH micelles,[28] suggests that the inorganic precursors form an electrostatic bond with surfactant cations. Once the inorganic precursor and the micelles are in place, the interfacial charge redistributes leading to the formation of mesophase with lower curvature. It can also be suggested that high CTACl facilitates more condensation, resulting in a lamellar phase.

4.1.4 Effect of synthesis time

A reaction mixture with molar composition $0.58Al_2O_3: P_2O_5: 0.50\ C_{16}TACl: 3.22$ TMAOH: 350 H_2O was used to study the formation of mesoporous materials at

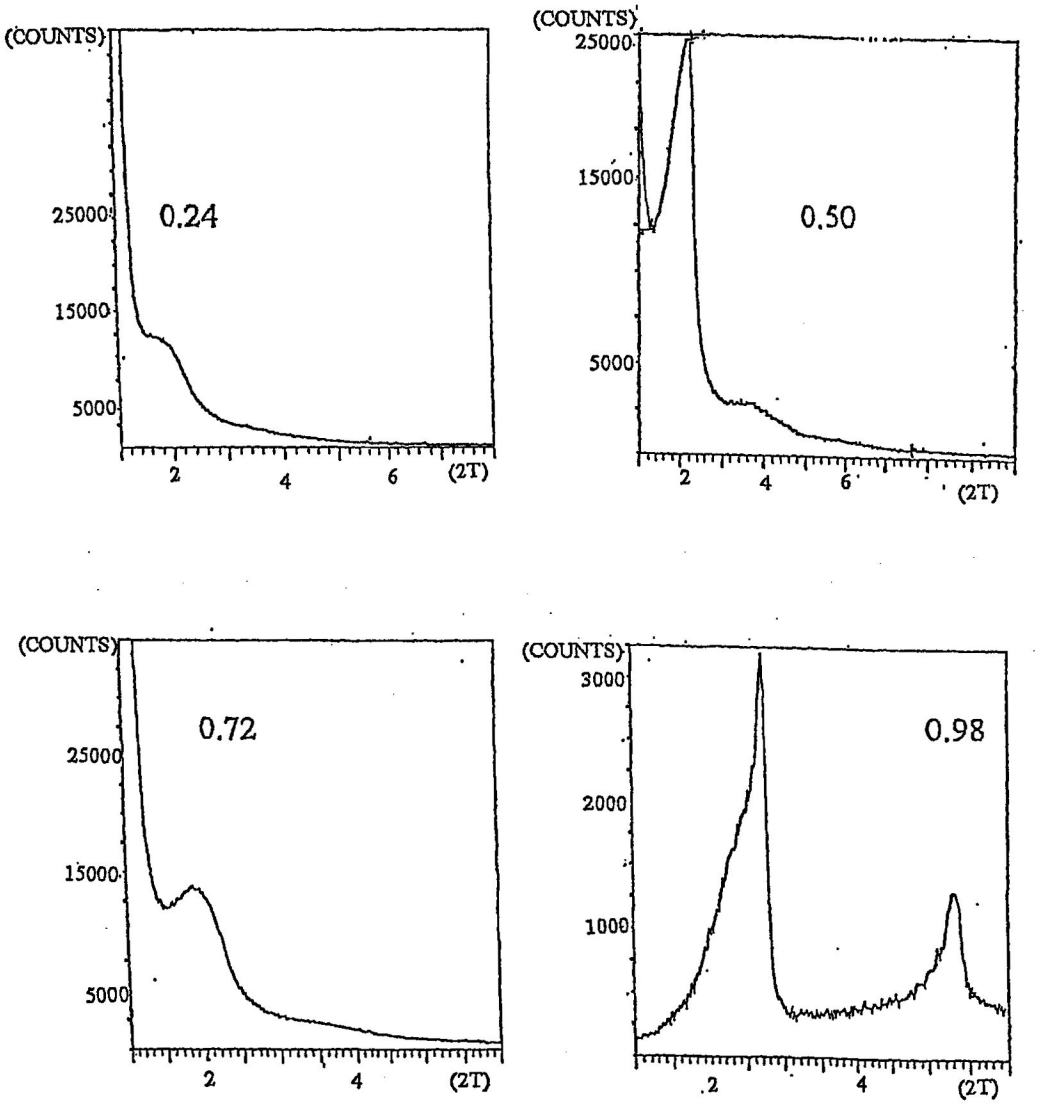

Figure 13: XRD patterns of products obtained from synthesis mixtures of various $CTACl/P_2O_5$ ratios and fixed Al/P of 0.58 (synthesis conducted at 25°C) ($CTACl/P_2O_5$ ratios indicated on graph)

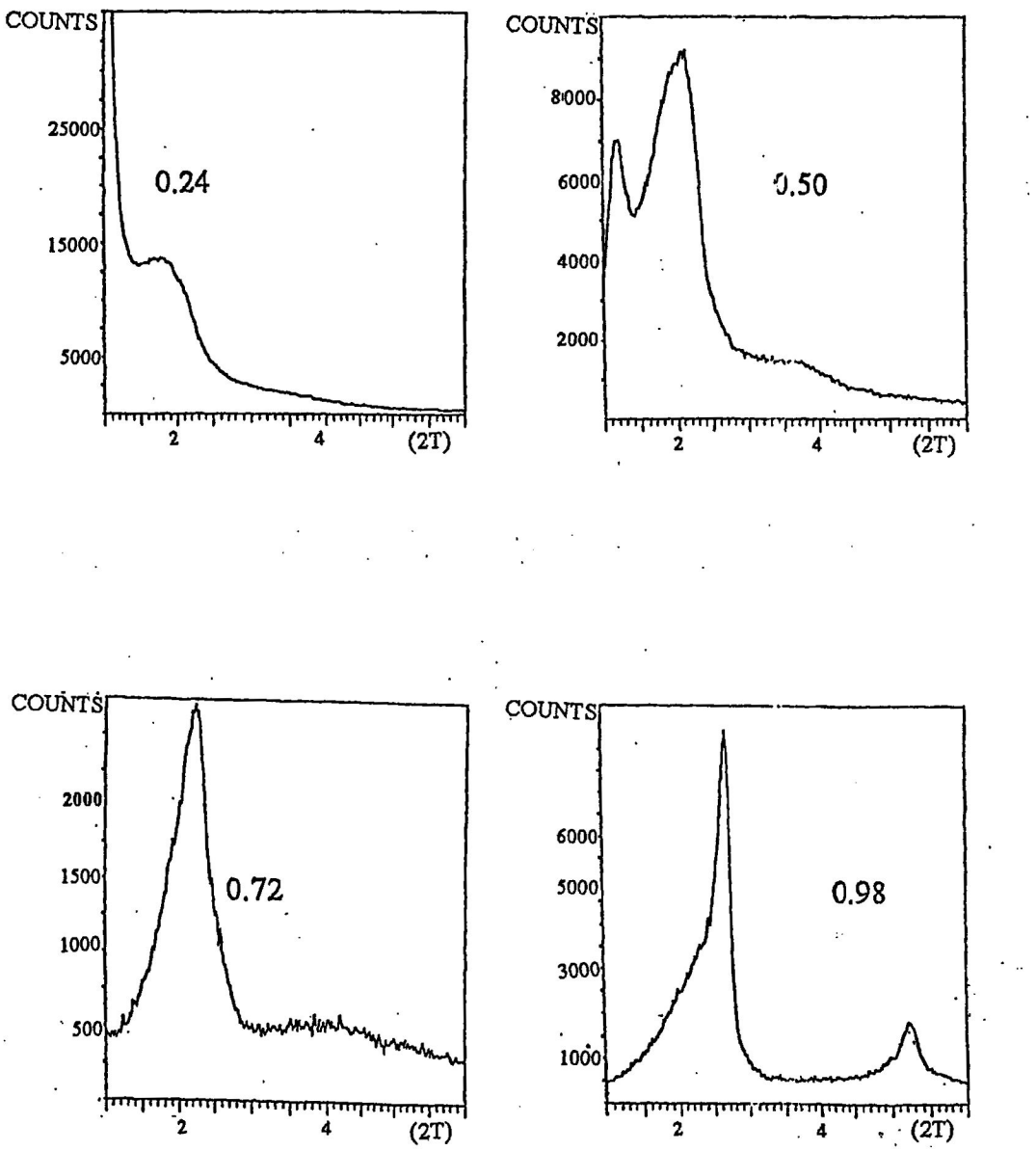

Figure 14: XRD patterns of products obtained from synthesis mixtures of various CTACl/P_2O_5 ratios and fixed Al/P of 0.58 (synthesis conducted at 110°C) (CTACl/P_2O_5 ratios indicated on graph)

reaction times 5, 10, 24, 48 and 72 hour. Intermediate solid products collected in the course of the reaction were investigated. The relative degree of their crystallinity, represented by the intensity of (100) XRD reflections, increases during the course of the reaction. A 0.5 and 2 hour mixing of aluminum and phosphorous prior to the addition of TMAOH was also carried out during the synthesis. For samples obtained from 0.5 hour mixing before TMAOH addition, x-ray diffraction (Figure 15) indicates hexagonal phase for all reaction times investigated and a solid product were obtained even at 5 hour synthesis time. However, with 2 hour mixing before TMAOH addition x-ray diffraction data in (Figure 16) indicated a highly disordered phase at 5 hour synthesis time. The degree of crystallinity for 2 hour mixing time, represented as the intensity of X-ray diffraction reflections, increases from 10 to 72 hour during the course of the reaction.

4.1.5 Effect of mixing time

The lack of hydrothermal stability is a considerable drawback in making the mesoporous aluminophosphates. Improvement in thermal stability may be achieved via an increase in pore wall thickness, which is related to extent of condensation within the pore walls. This experiment, therefore, examines the effect of mixing time of the aluminum and phosphorous precursors on the extent of hydrolysis and condensation. The reaction mixtures of the following molar compositions were used:

$1.17Al_2O_3:P_2O_5:0.50C_{16}TMACl:2.68TMAOH:348H_2O$

$0.58Al_2O_3:P_2O_5:0.50C_{16}TACl:3.02TMAOH:348H_2O$.

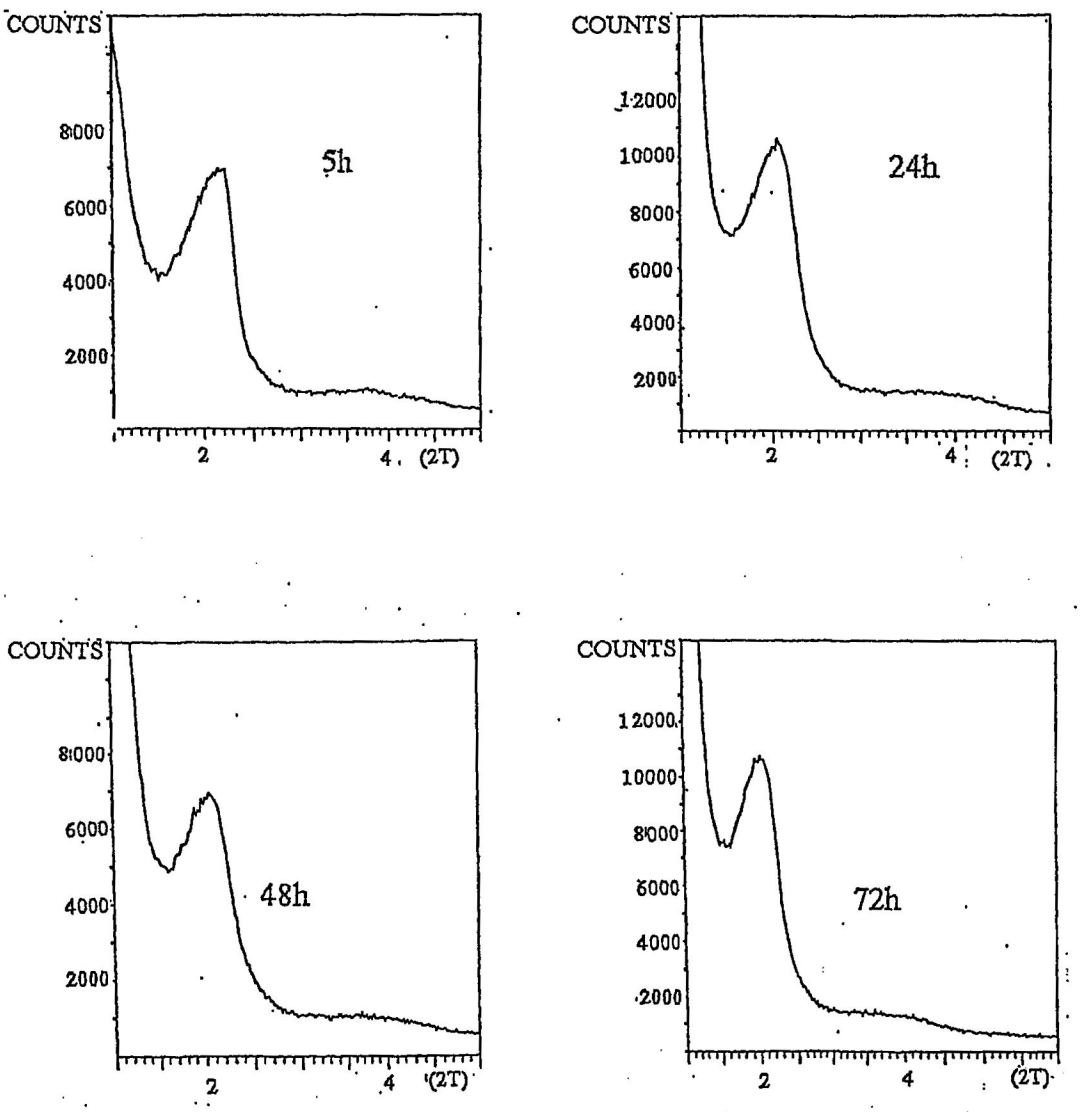

Figure 15: XRD patterns obtained at various reaction mixture times and fixed Al/P of 0.58 (0.5hrs mixing before TMAOH addition)

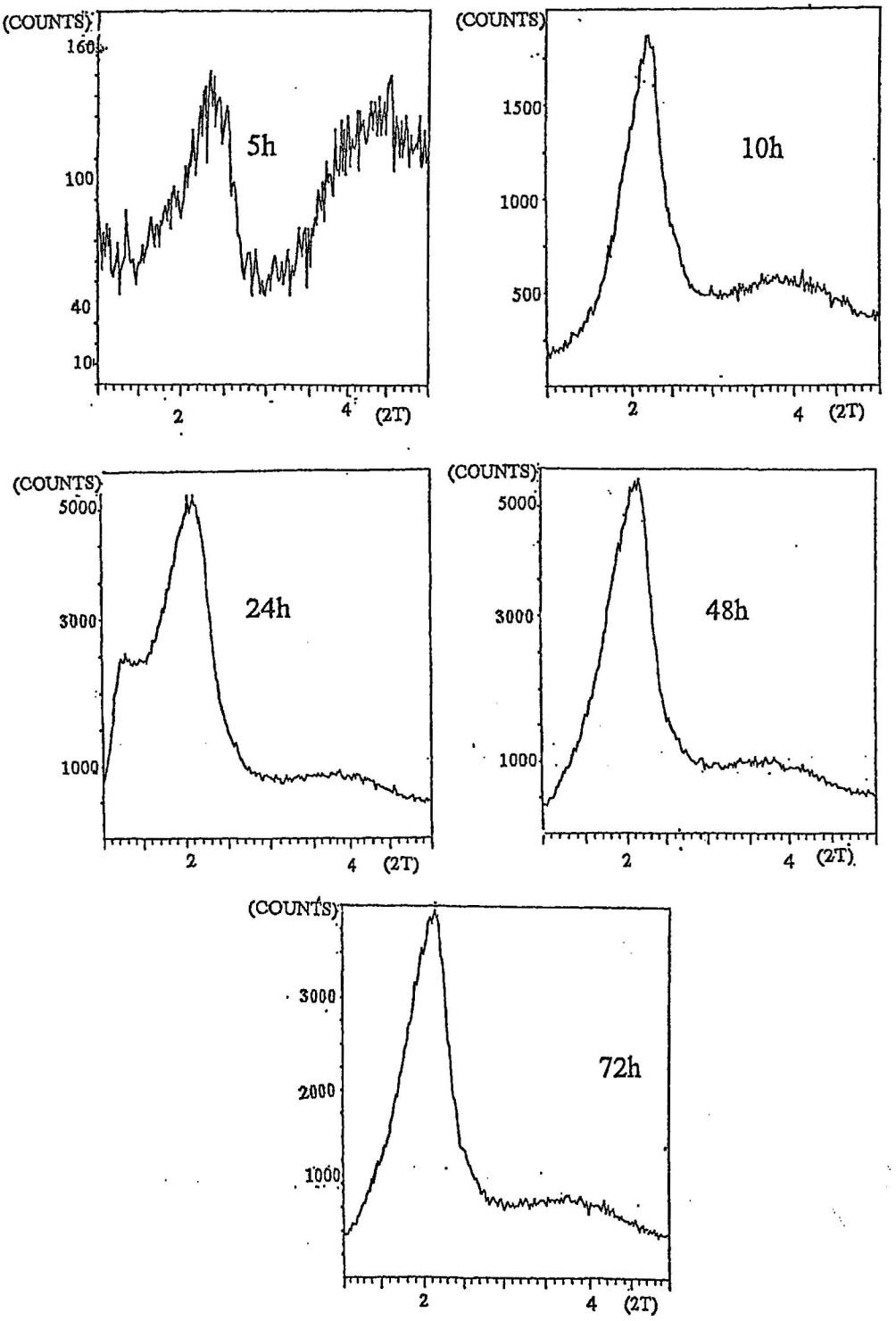

Figure 16: XRD patterns obtained at various reaction mixture times and fixed Al/P of 0.58 (2hrs mixing before TMAOH addition)

XRD patterns from both ratios are shown in Figure 17. For samples with Al/P ratio equal to 0.58, a hexagonal phase was observed at 2 and 4 hour mixing time, while a highly ordered hexagonal phase is obtained at 6 hour mixing time. Calcinations at 400 $^{\circ}C$ under 1 hour N_2 for the 2 hour mixing-time sample, resulted in an amorphous product, while for the 4 and 6 hours mixing-time samples, a broad low intensity peak was observed. The nitrogen isotherm and pore size distribution for Al/P equal to 0.58 is shown in Figure 18. A microporous (Type I) isotherm was exhibited for 4 and 6 hour mix time samples, while an isotherm was unattainable for 2 hour mix-time samples. The pore size distributions were, however, poorly defined for 4 and 6 hour mix-time samples, possibly due to a highly disordered of framework upon calcination. For samples with Al/P ratio equal to 1.17, X-ray diffraction data indicated a similar hexagonal phase at 2, 4 and 6 hour mixing-time. The nitrogen isotherms and pore size distributions are shown in Figure 19. The isotherms for samples at 2, 4 and 6 hours indicate a microporous (Type I) isotherm as well with no significant improvement in pore volume with increased mixing time. The corresponding pore size diameter indicate similar distributions for 2, 4 and 6 hour mix-time samples with a pore size of 12.6Å.

Longer mixing time, therefore, resulted in an increase in pore volume. At higher Al/P ratio (1.17) the pore size distribution indicates larger surface area and pore volume. At Al/P equal to 0.58 a highly disordered pore size distribution is noted at 6 and 4 hour mixing time, while at 2 hour mix time a pore size could not be determined.

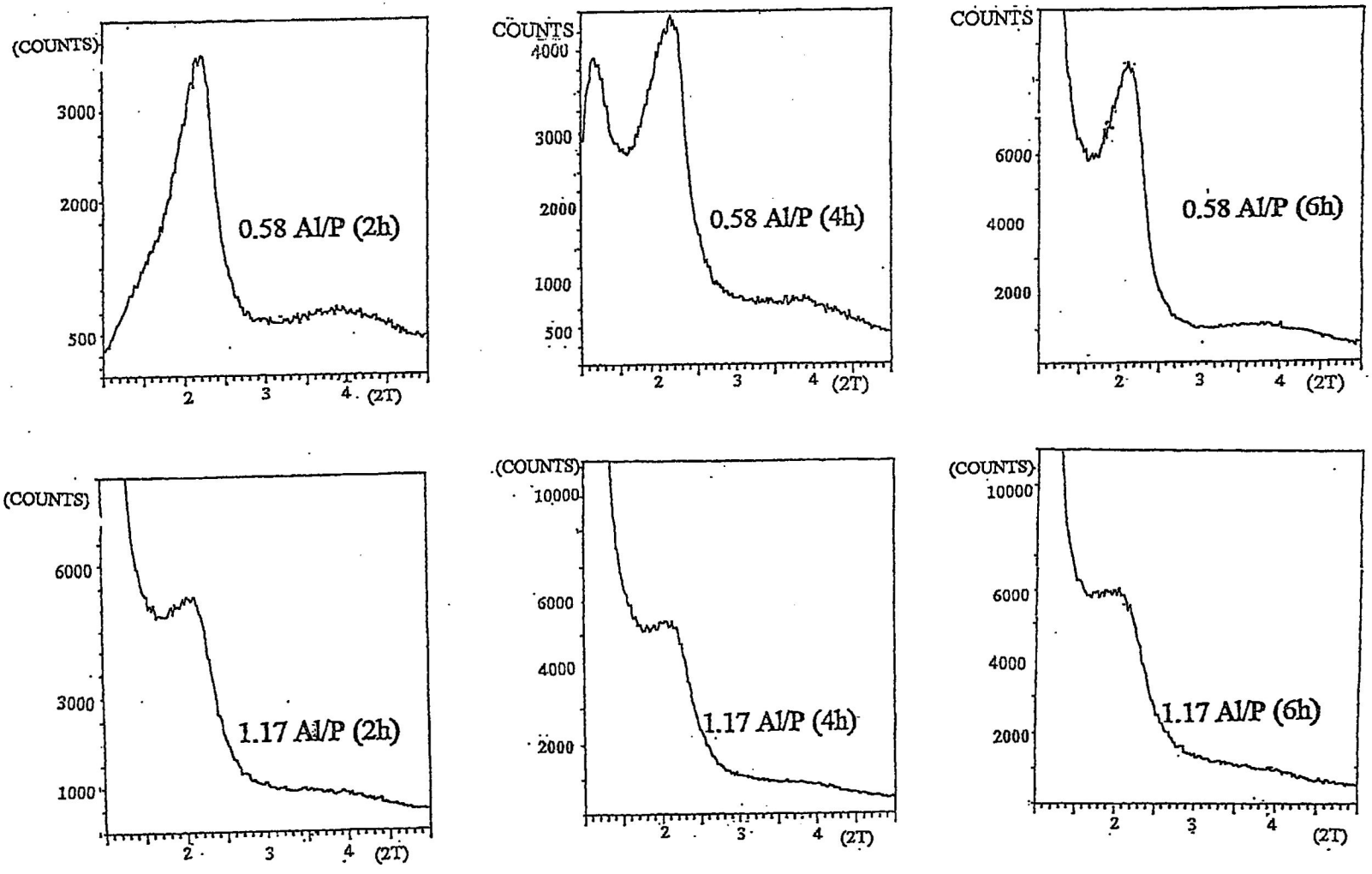

Figure 17: XRD patterns of the effect of mixing time before TMAOH addition at a fixed Al/P of 0.58 and 1.17 (synthesis conducted at 25°C)

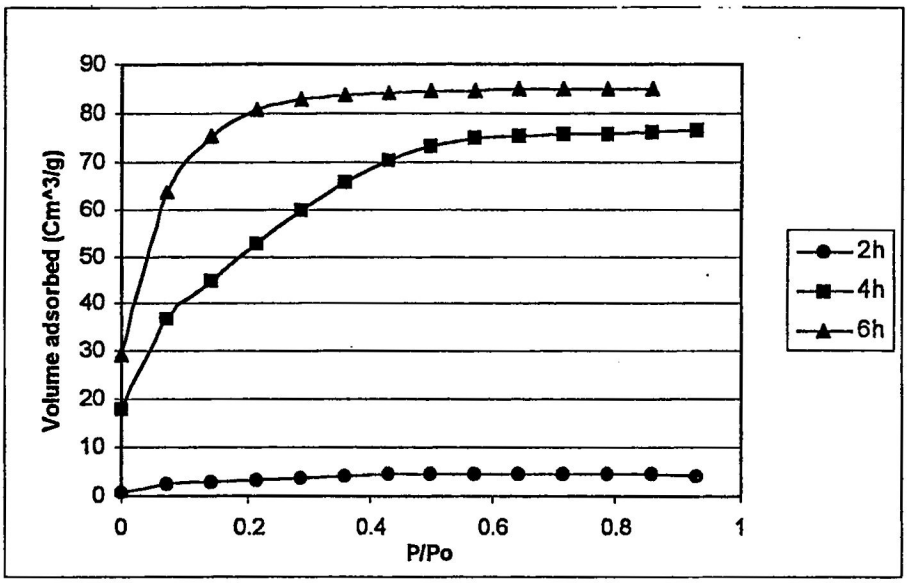

a) Adsorption isotherm at 2,4 and 6h mix time

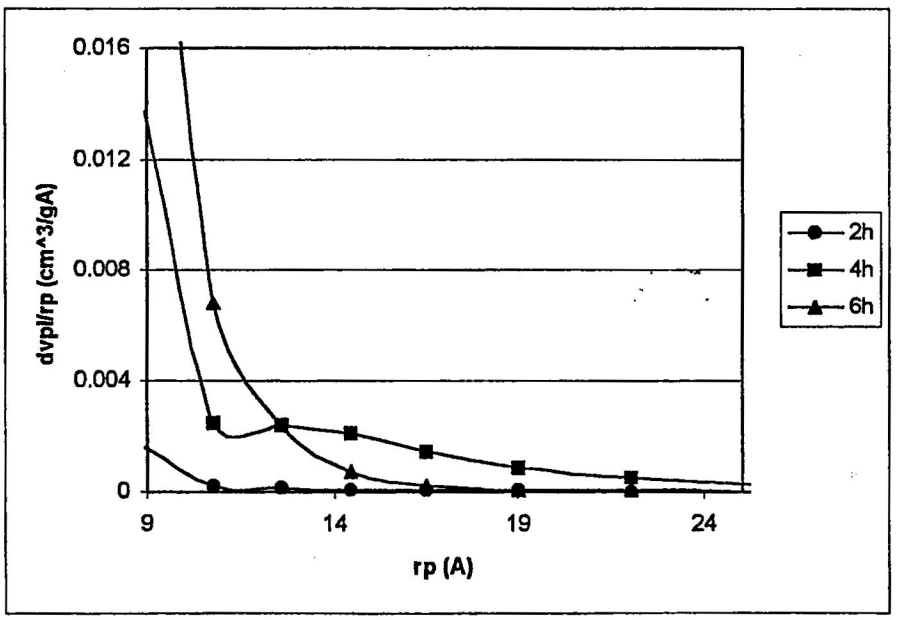

b) Pore size distribution at 2, 4 and 6h mix time

Figure 18: a) Adsorption isotherm b) pore size distribution of calcined samples from various mix time at a fixed Al/p of 0.58

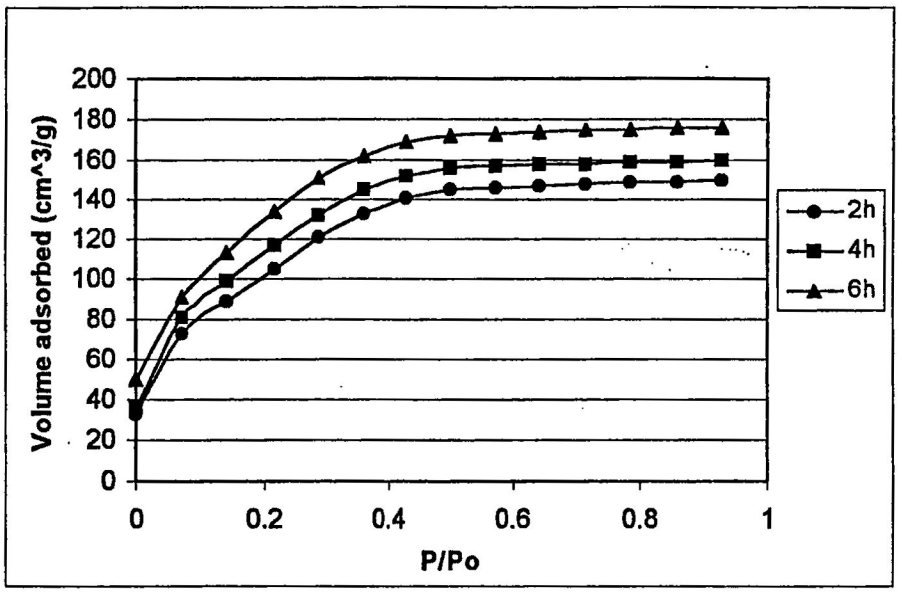

a) Adsorption isotherm at 2,4 and 6h mix time

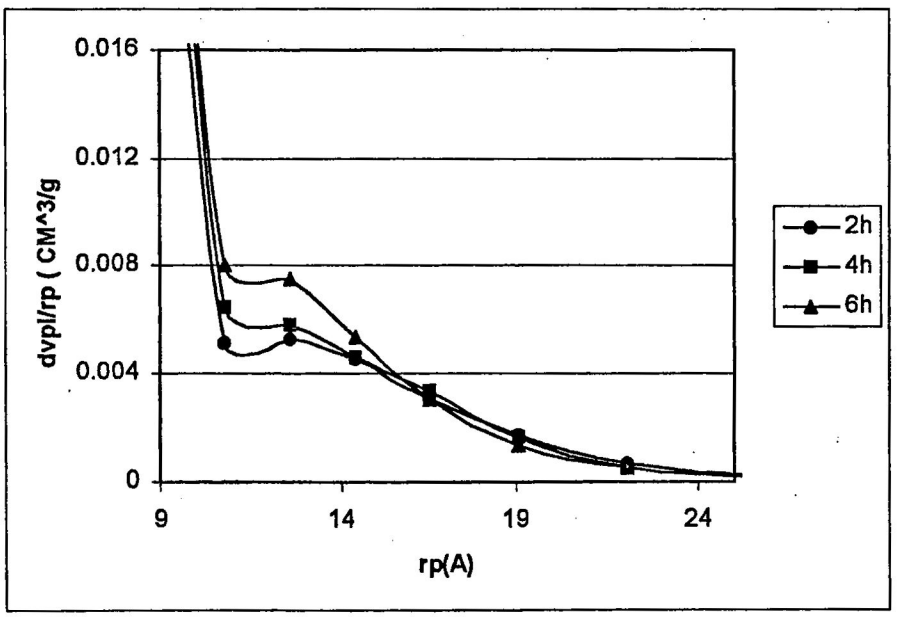

b) Pore size distribution at 2,4 and 6h mix time

Figure 19: a) Adsorption isotherm b) pore size distribution of calcined samples from various mix time at a fixed Al/p of 1.17

4.2 Effect of aluminum source

It is well known that the choice of aluminum source plays a crucial role in the synthesis and phase purity of $AlPO_4$ molecular seives.[13] Although x-ray diffraction patterns and thermal analysis indicate mesoporous type material when using aluminum hydroxide, the materials lost crystallinity due to thermal instability. One of the factors thought to affect the stability of aluminophosphates is the rate of hydrolysis and condensation of the inorganic species. It was thought that different forms of aluminum would have different rates of hydrolysis and condensation. Therefore, this was investigated further by using aluminum isopropoxide and Psuedoboehmite alumina as aluminum oxide precursors.

4.2.1 Synthesis of mesoporous aluminophosphates using aluminum isopropoxide

4.2.1.1 Effect of Al/P ratio

In order to determine the effects of varying the aluminum content, the composition of the starting mixtures was changed as follows: xAl_2O_3:P_2O_5:0.50C_{16}TMACl:1.58TMAOH:349H_2O, where x was varied from 0.58 to 2.33, at 25 °C and mix time varied from 2 to 6 hour before TMAOH addition. The x-ray diffraction patterns for a sample with Al/P ratio equal to 0.58 and 6 hour mix time are shown in Figure 20. The XRD patterns indicate a low intensity peak corresponding to an intensity of 480 counts positioned at 2θ of 2.5° suggesting a hexagonal phase. However, with an increase in synthesis Al/P ratio from 0.58 to 0.78, the hexagonal phase appeared to be highly disordered with lower intensity (150 counts). At Al/P ratio greater than 0.78

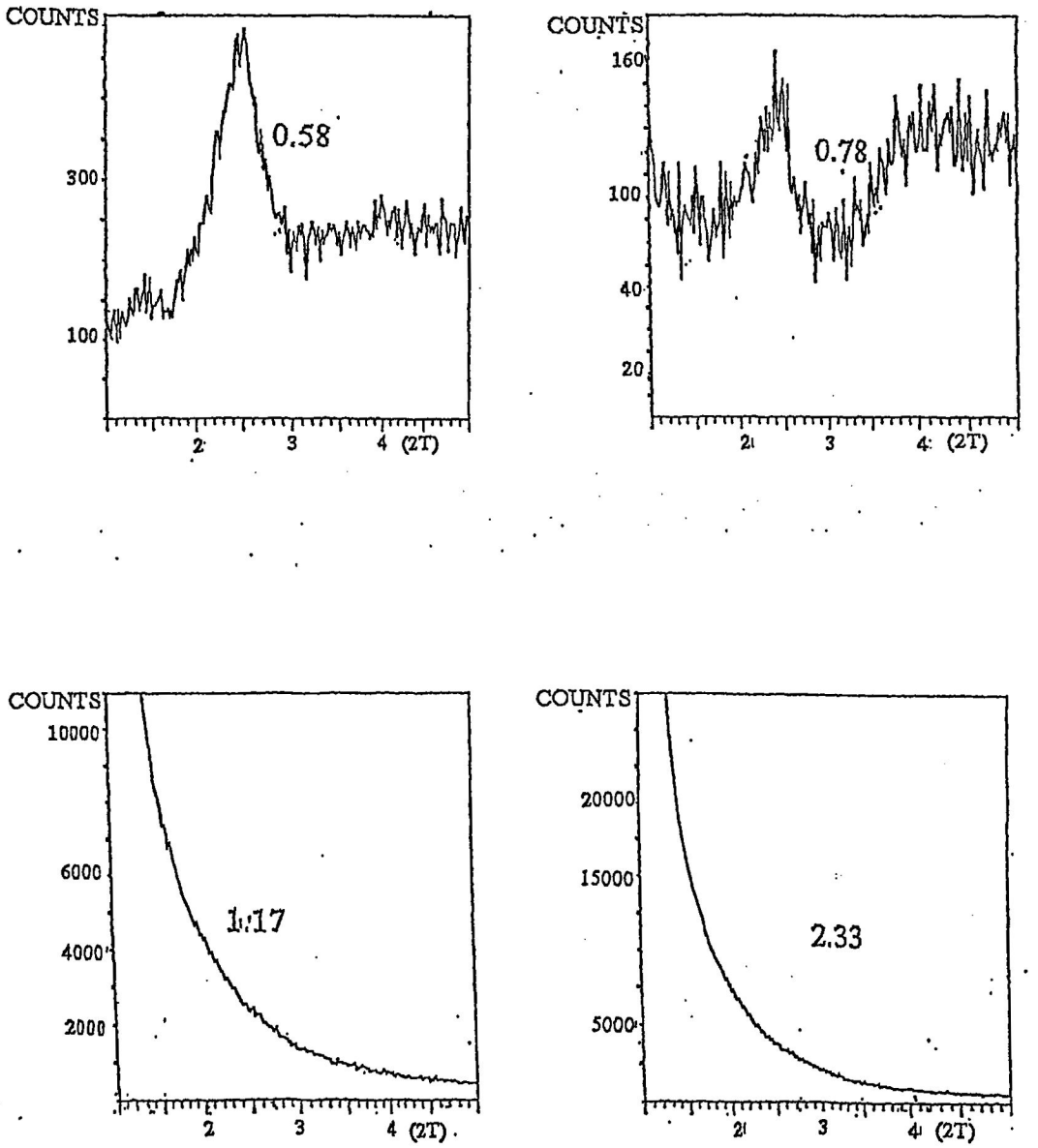

Figure 20: XRD patterns of samples synthesized at various Al/P ratios in mixture. (Al/P ratios indicated on graph).

and up to 2.33, an amorphous product was observed. XRD patterns of products calcined at 400 °C for 1 hour in nitrogen show a broad low intensity peak suggesting a highly disordered structure, due to a decrease in crystallinity. However, BET surface areas obtained at the various Al/P ratios ranged from 224 to 447 m^2g^{-1}, supporting the observation that the samples were partially stable under the calcination conditions used. Nitrogen isotherms and pore size distributions for 2 hour and 6 hour mix time are greater than 0.78 and up to 2.33, an amorphous product was observed. Nitrogen isotherms and pore size distributions for 2 hour and 6 hour mix times are shown in Figures 21 and 22. At Al/P ratios ranging from 0.58-2.33, intermediate between Type I and Type IV isotherms for 2 hour and 6 hour mixing times are observed. The isotherm at 2 hour mixing times exhibits a less steep pore filling in the relative pressure (P/Po) range of 0.14 to 0.5, characteristic of capillary condensation into uniform mesopores. The sharpness and the height of capillary condensation (pore filling) step indicated in the isotherms is a measure of the pore size uniformity.[33] The corresponding pore size distribution indicates that an increase in Al/P ratio from 0.58 to 1.17 results in an increase in pore diameter ranging from 14.4 to 19.0Å and a broader distribution. At higher Al/P ratio (2.33) however, pore diameter was 16.5Å but the distribution was broader. The departure from a sharp and clearly defined pore filling step observed are usually an indication of increase in pore size heterogeneity (i.e., widening of pore size distribution).[33] In addition, the decrease in pore volume and surface area with an increase in Al/P ratio from 0.58 to 2.33 suggests a partial collapse of the hexagonal phase during calcination resulting from the instability associated with the presence of increasing amounts of framework aluminum.[34]

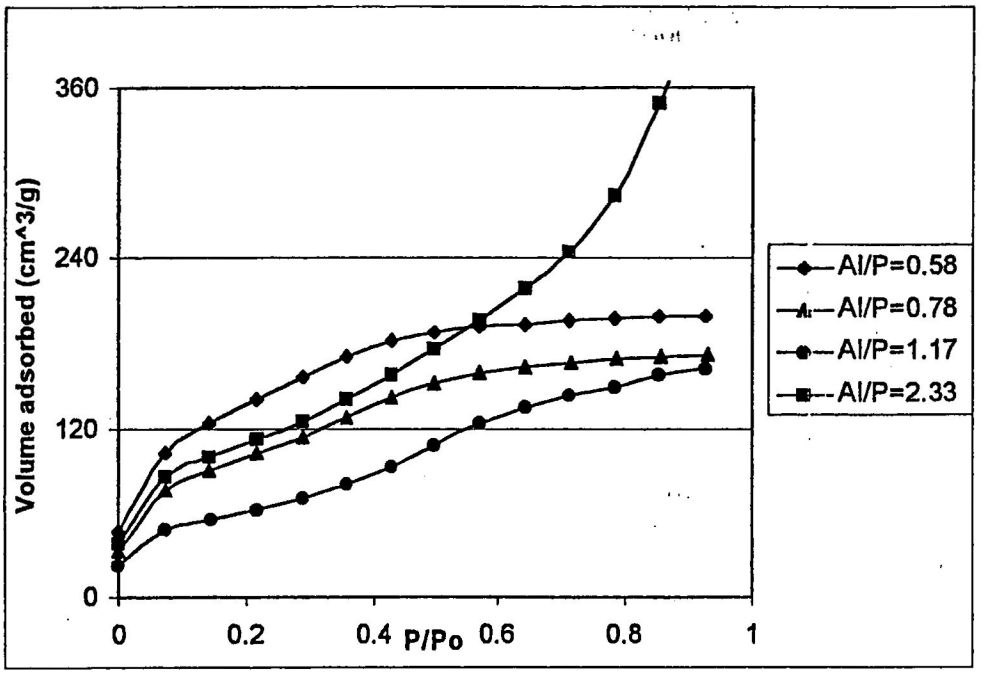

a) Adsorption isotherm

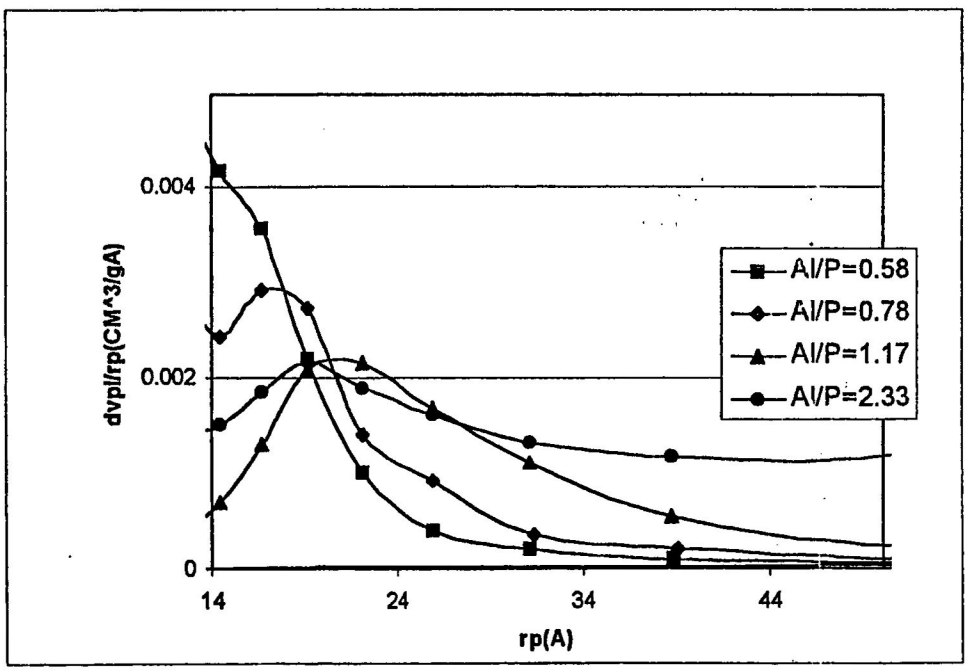

b) Pore size distribution

Figure 21: a) Adsorption isotherm and b) pore size distribution of calcined samples synthesized at various Al/P ratios (2hrs mixing before TMAOH addition)

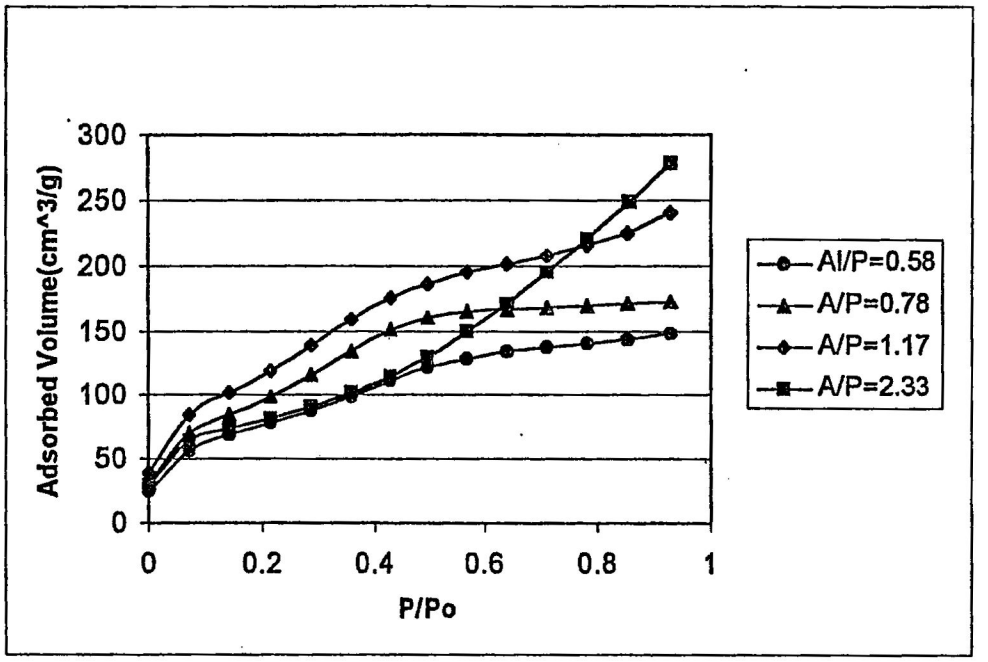

a) Adsorption isotherm

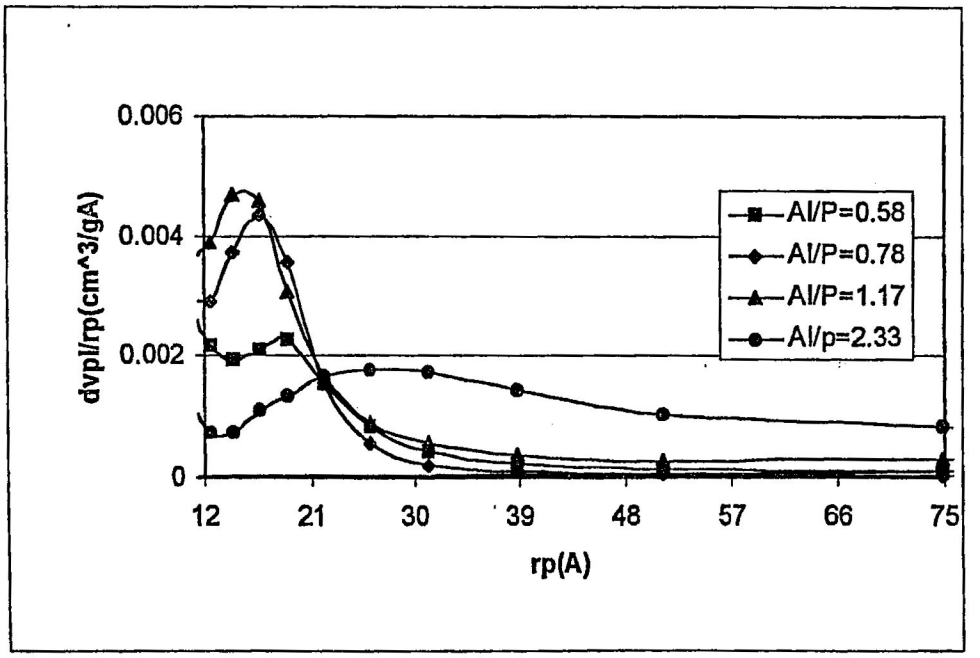

b) Pore size distribution

Figure 22: a) Adsorption isotherm and b) pore size distribution of calcined samples Synthesized at various Al/P ratios (6hrs mixing before TMAOH addition)

At 6 hour mixing time, the nitrogen isotherms indicate an increase in pore volume as the Al/P ratio increases from 0.58 to 1.17. This increase in pore volume may be due to a prolonged mixing time, which gives the inorganic species ample time to hydrolyze and condense. The corresponding pore sizes ranging from 14.4 to 19.0Å exhibit a narrow pore size distribution at Al/P ratios ranging from 0.58 to 1.17. However, at an Al/P ratio of 2.33, a broad distribution with a pore diameter of 25.9Å is obtained.

4.2.1.2 Effect of TMAOH concentration

When using aluminum hydroxide it was noted that, when aluminum hydroxide was used, no mesostructured products formed under the TMAOH free condition. One of the roles of TMAOH is to act as a basic source to adjust the pH values of the starting mixtures. TMAOH also affects the solubility of the Al sources and or aluminophosphate species in the starting mixtures.[33] Thus, it is of significance to investigate if TMAOH plays a similar role in the synthesis using aluminum isopropoxide, as in the aluminum hydroxide synthesis. The molar compositions of the starting mixtures with Al/P ratios of 0.59 and 1.17 were changed as follows:

0.59 Al_2O_3:P_2O_5:0.50 C_{16}TACl:x TMAOH:350.0 H_2O, where x =0.44-2.24

1.17Al_2O_3:P_2O_5:0.50 C_{16}TACl:x TMAOH:350.0 H_2O, where x =0.32-3.06.

For sample with Al/P ratio equal to 0.59, and TMA /P_2O_5 equal to 0.44 (pH 4.1) synthesized at the x-ray diffraction pattern (Figure 23) of an amorphous product was obtained. At TMA/P_2O_5 equal to 0.52 (pH 7.09) a lamellar phase was obtained. With an increase in TMA/P_2O_5 from 1.08 to 2.24 (pH 10.81 and 11.15), however, a

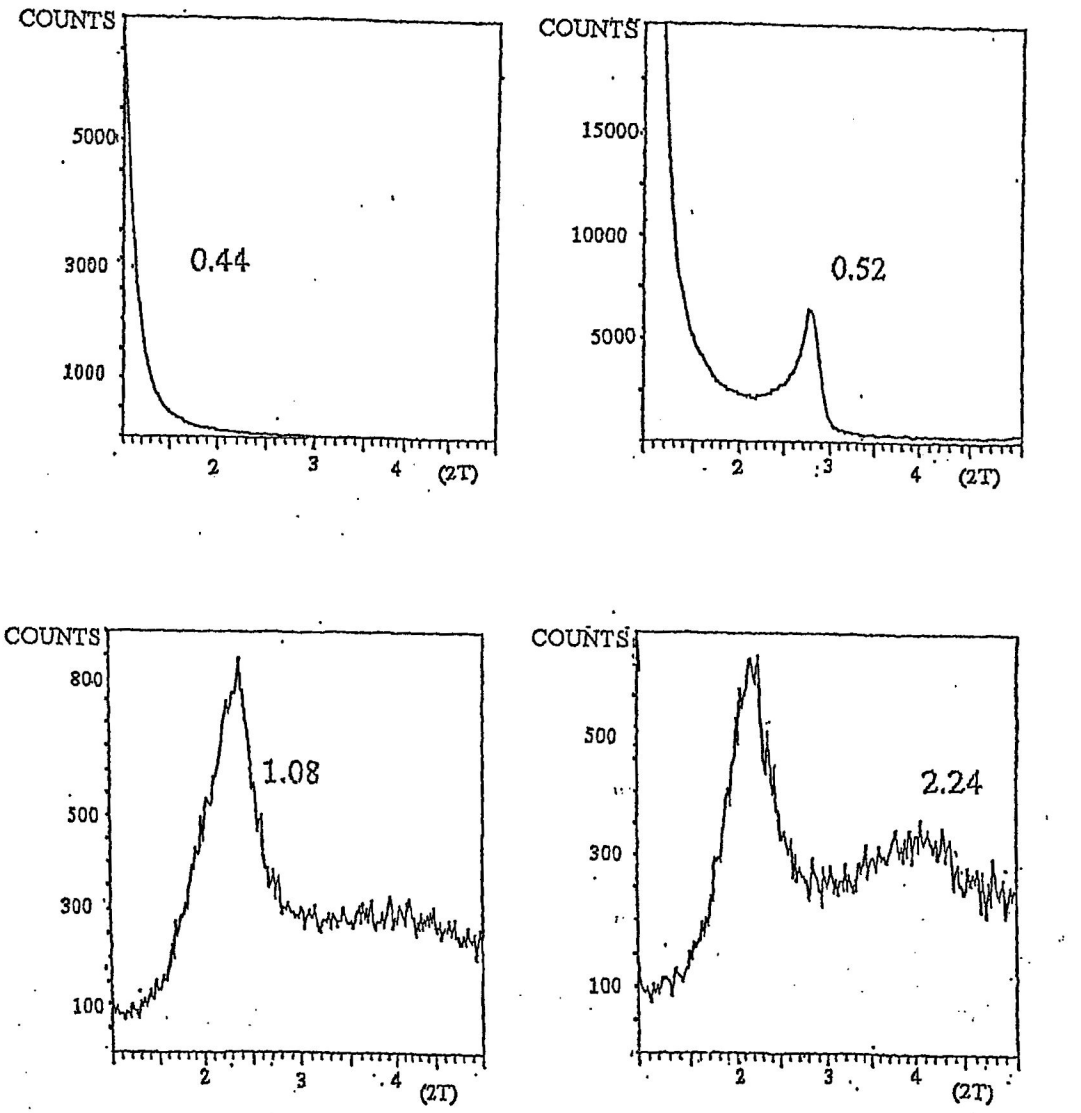

Figure 23: XRD patterns of products obtained from synthesis mixtures of various TMA/P_2O_5 ratios and fixed Al/P of 0.59 (synthesis conducted at 25°C). (TMA/P_2O_5 ratio as indicated on graph)

hexagonal phase was observed. At higher Al/P ratio (1.17) (Figure 24) an amorphous phase was obtained at TMA / P_2O_5 ranging from 0 to 0.32 (pH 4.13 to 7.00) and a hexagonal phase with low crystallinity was observed at TMA/P_2O_5equal to 0.32 (pH 9.66). An increase in TMA / P_2O_5 to 3.06 (pH 11.27) resulted in a broad, highly disordered hexagonal phase. A lamellar phase was not obtained at this ratio.

4.2.1.3 Effect of surfactant concentration

Synthesis mixtures with Al/P ratios of 0.58 and 1.16 and varying amounts of C_{16}TACl were prepared with the following molar compositions:

0.58 Al_2O_3:P_2O_5:x C_{16}TACl:3.44 TMAOH:349.0 H_2O, where x=0.24-0.74

1.16Al_2O_3:P_2O5:x C_{16}TACl:1.80 TMAOH:347.0 H_2O, where x =0.24-0.74.

X-ray diffraction patterns (Figure 25) of products synthesized at 25 °C and an Al/P ratio of 0.58 show that an increase in CTACl/P_2O_5 ratio from 0.24 to 0.32 gave a hexagonal phase with improved crystallinity. Similar trends were observed at 110 °C synthesis temperature at CTACl/P_2O_5 equal to 0.74, however a less ordered hexagonal phase was observed. In Figure 26, a synthesis using the higher Al/P ratio (1.16) conducted at 25°C resulted in amorphous product for CTACl/P_2O_5 ranging between 0.24 and 0.74. Similar trends were observed at 110 °C synthesis ranging between 0.24 and up to 0.74. At CTACl/P_2O_5 equal to 0.74 however, a lamellar phase was obtained.

Both Al/P ratios indicated that high surfactant content and elevated temperature resulted in a lamellar phase, while lower surfactant and lower temperature favors a hexagonal phase.

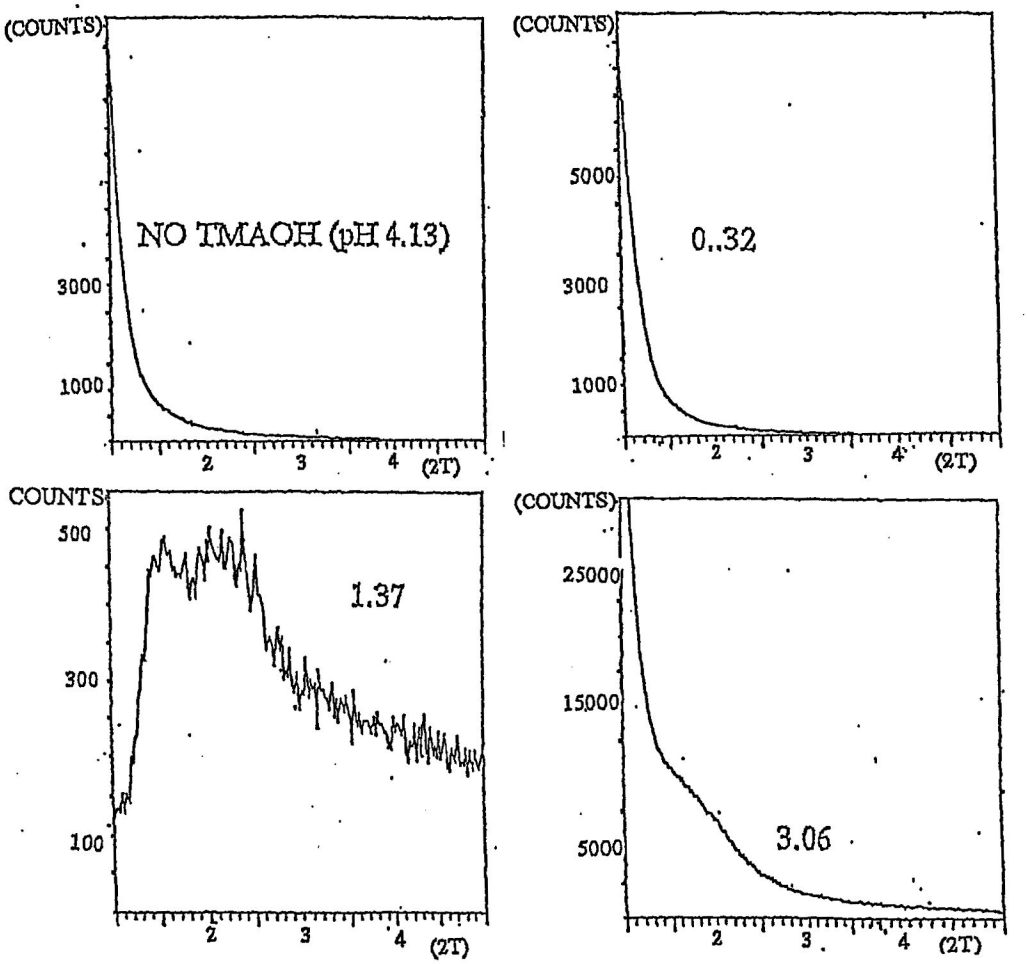

Figure 24: XRD patterns of products obtained from synthesis mixtures of various TMA/P_2O_5 ratios and fixed Al/P of 1.17 (synthesis conducted at 25°C). (TMA/P_2O_5 ratio as indicated on graph)

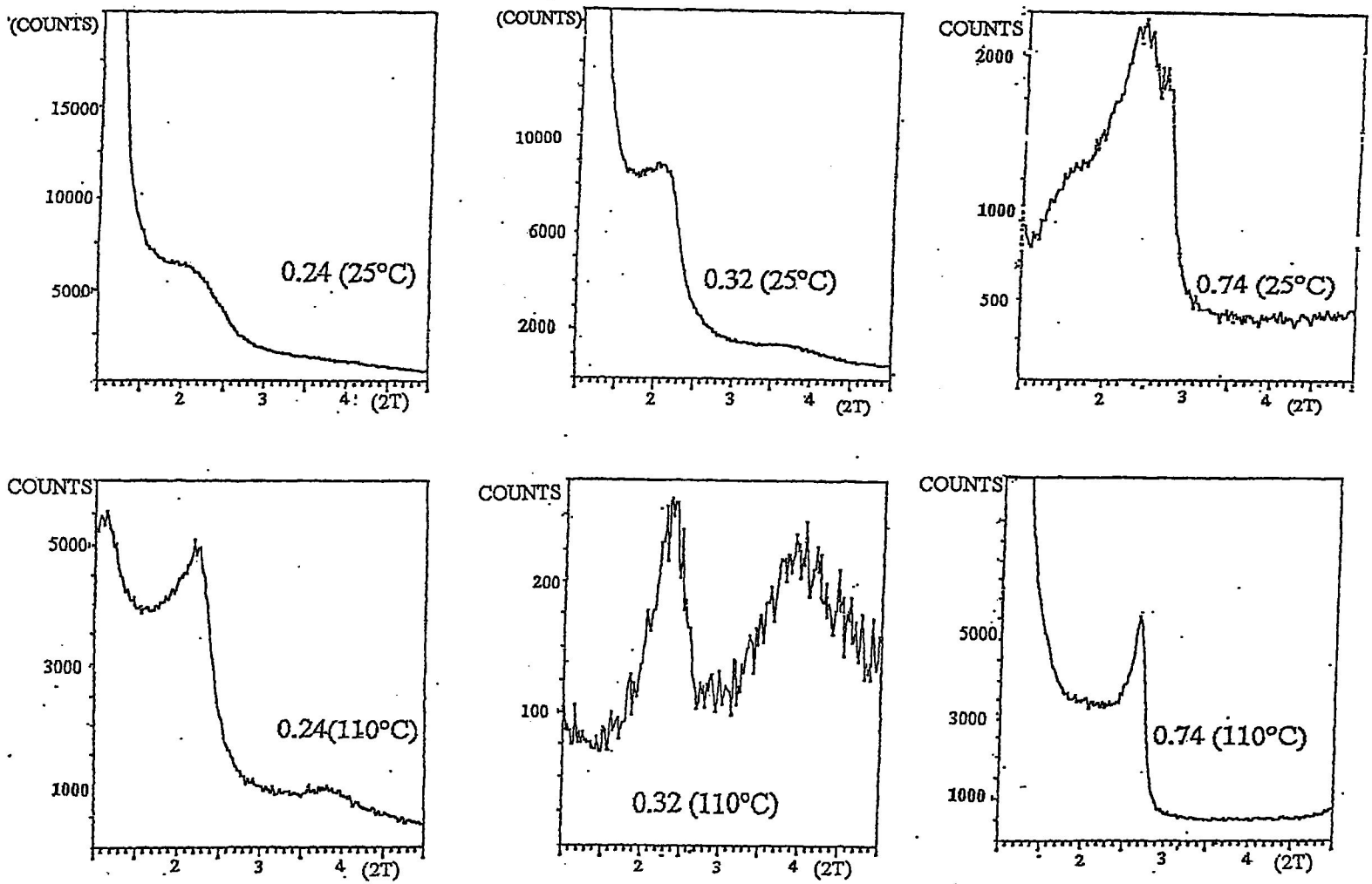

Figure 25: XRD patterns of products obtained from synthesis mixtures of various CTACl/P_2O_5 ratio and fixed Al/P of 0.58 (synthesis conducted at 25°C and 110°C)

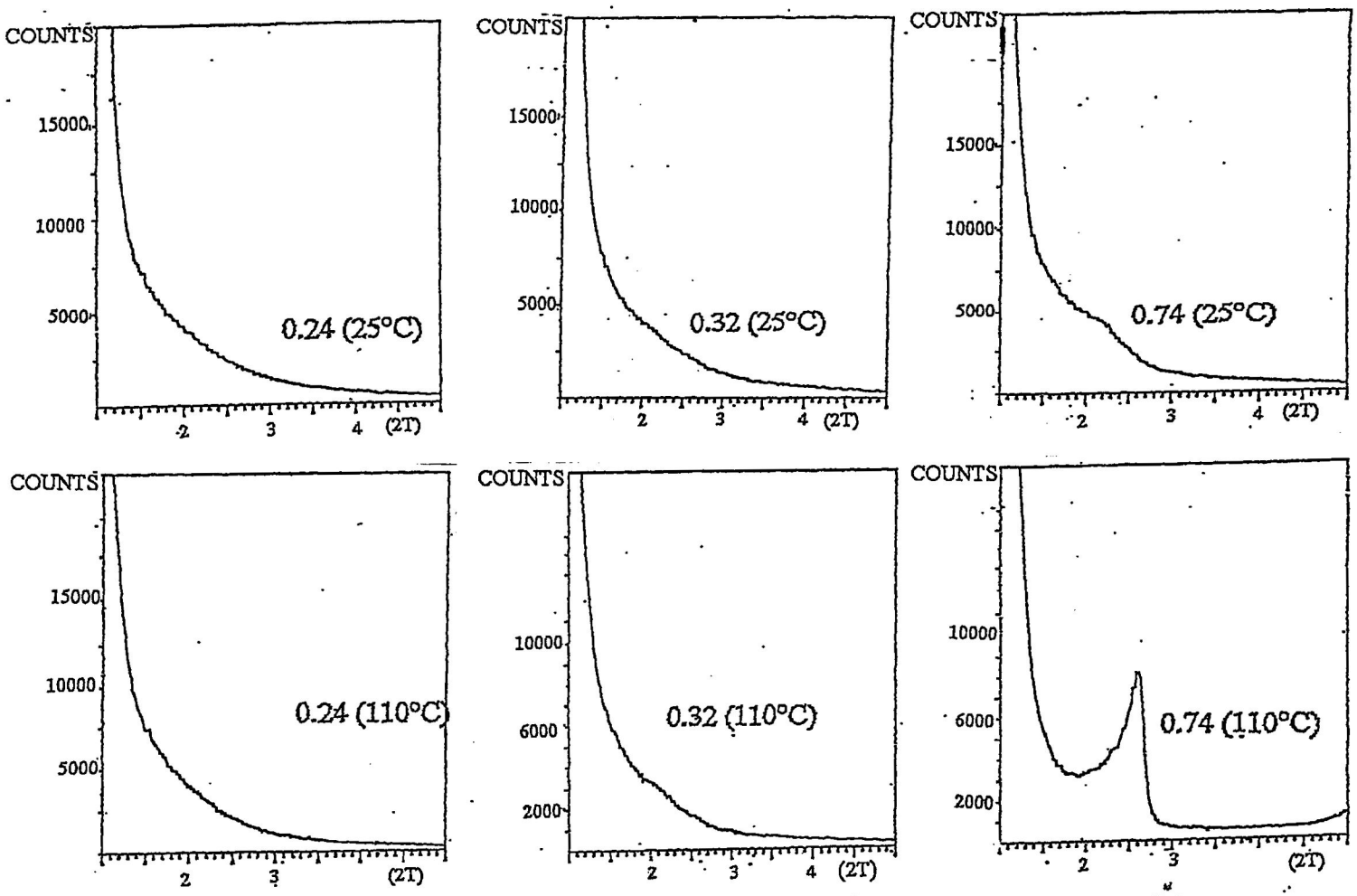

Figure 26: XRD patterns of products obtained from synthesis mixtures of various CTACl/P_2O_5 ratio and fixed Al/P of 1.16 (synthesis conducted at 25°C and 110°C)

4.2.1.4 Effect of water concentration

Using Al/P ratios of 0.58 and 1.15, the following molar compositions were prepared to study the effects of water content:

0.58 Al_2O_3:P_2O_5:0.50 C_{16}TACl:2.30 TMAOH:w H_2O, where w= 86-689

1.15 Al_2O_3:P_2O_5:0.48 C_{16}TACl:1.48 TMAOH: w H_2O, where w= 85-687

For samples with Al/P ratio equal to 0.58 synthesized at 25°C, Figure 27 shows x-ray diffraction patterns obtained for H_2O/P_2O_5 ratios ranging from 86 to 689. At H_2O/P_2O_5 ratio 86 a hexagonal phase was obtained, and with an increase in H_2O/P_2O_5 ratio from 349 to 689 a hexagonal phase with low crystallinity was obtained. An increase in Al/P ratio to 1.15 (Figure 28) resulted in a hexagonal phase at H_2O/P_2O_5 ratios of 85 and 172 and a decrease in hexagonal product quality resulted at 344 H_2O/P_2O_5. At an increased H_2O/P_2O_5 ratio of 687 a highly disordered diffraction pattern is obtained. The nitrogen isotherms and pore size distributions for Al/P ratio equal to 0.58 (Figure 29) indicate an intermediate isotherm between Type I and IV. The corresponding pore size distribution was 16.5Å at a H_2O/P_2O_5 ratio of 689, while a definite pore size could not be obtained for a H_2O/P_2O_5 ratio less than 689. The nitrogen isotherms and pore size distribution (Figure 30) for Al/P ratio of 1.15 indicate a Type IV isotherm at H_2O/P_2O_5 ratios 172 and 344, while an intermediate between Type I and IV was exhibited for a H_2O/P_2O_5 ratio equal to 86. A narrow pore diameter of 14.4Å was observed for H_2O/P_2O_5 ratio equal to 86, while an increase in H_2O/P_2O_5 ratio of 344 resulted in a broad pore size distribution with a pore size of 19.0Å. Z. Khimyak *et al.*, reported that

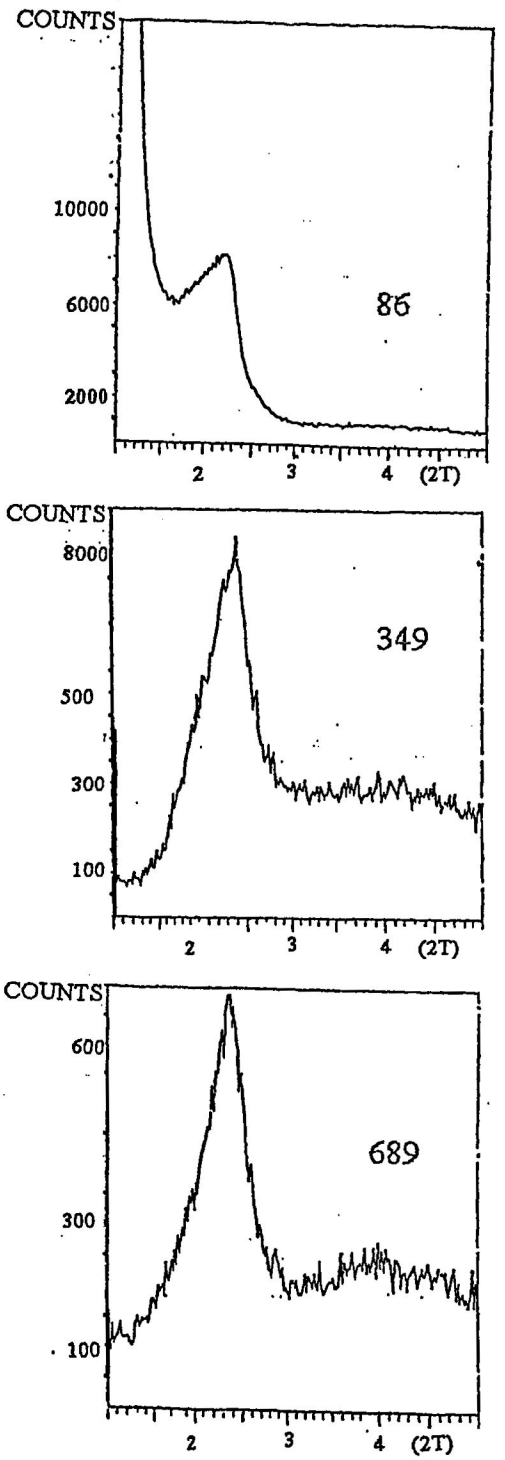

Figure 27: XRD patterns of products obtained from synthesis mixtures of various H_2O/P_2O ratio and fixed Al/P of 0.58 (synthesis conducted at 25°C) (H_2O/P_2O ratio as indicated on graph)

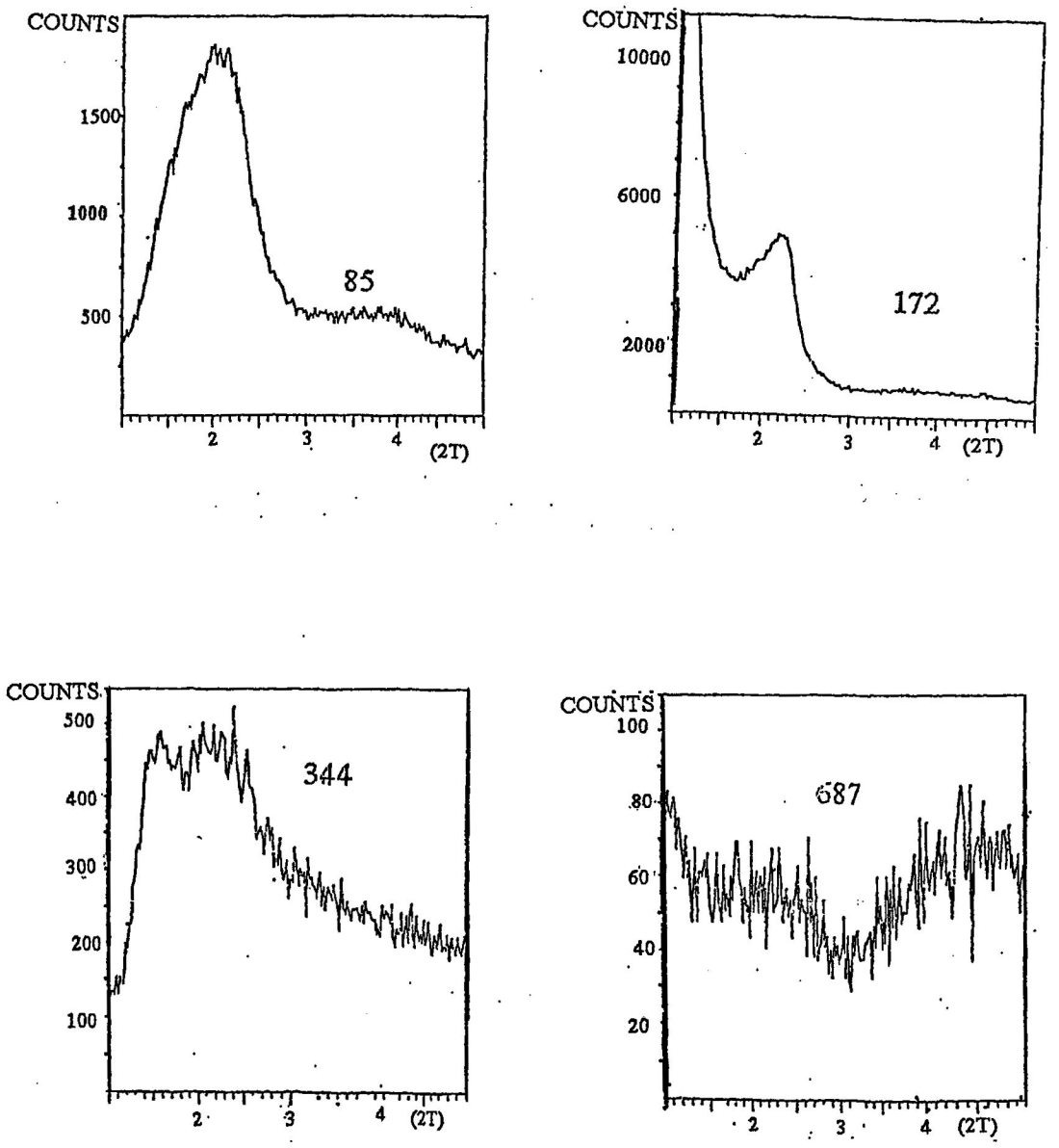

Figure 28: XRD patterns of products obtained from synthesis mixtures of various H_2O/P_2O ratio and fixed Al/P of 1.15 (synthesis conducted at 25°C) (H_2O/P_2O ratio as indicated on graph)

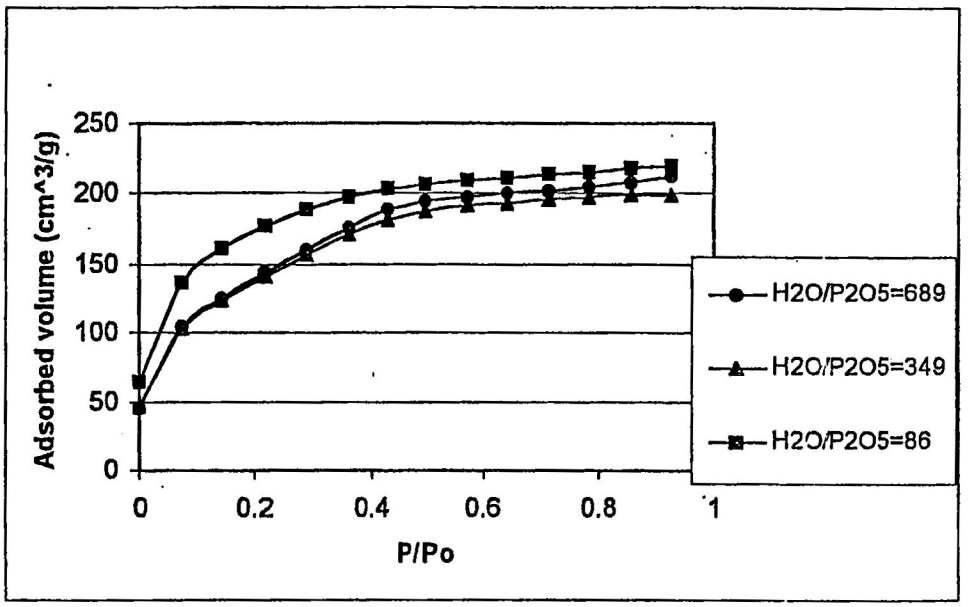

a) Adsorption isotherm

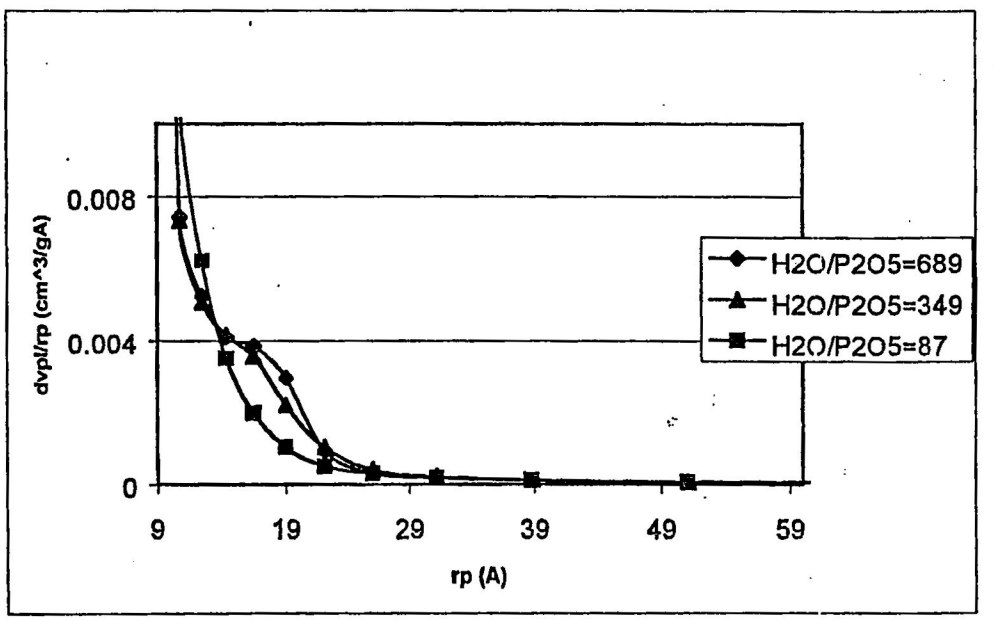

b) Pore size distribution

Figure 29: a) Adsorption isotherm and b) pore size distribution from synthesis mixtures of various H_2O/P_2O_5 ratios and fixed Al/P of 0.58 (synthesis conducted at 25°C)

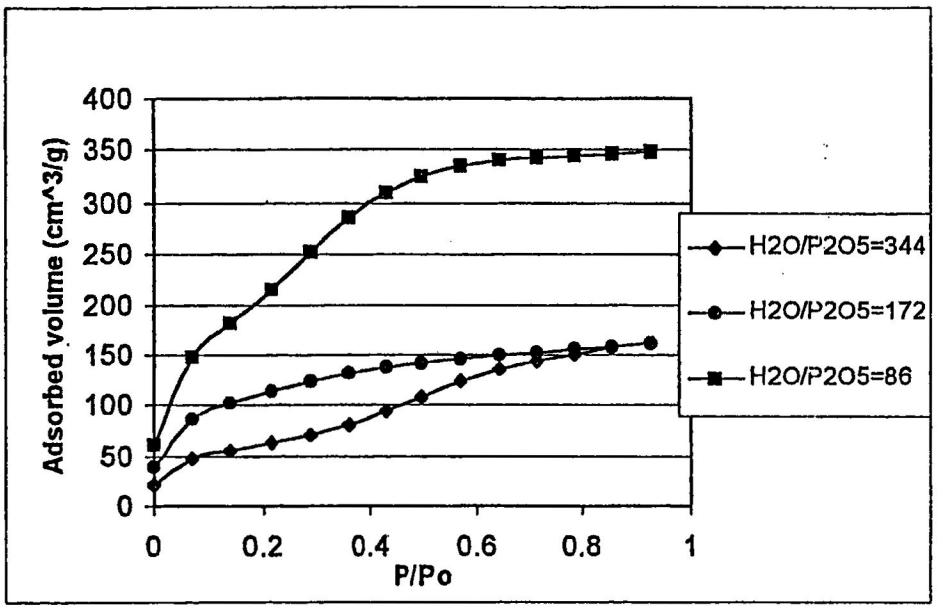

a) Adsorption isotherm

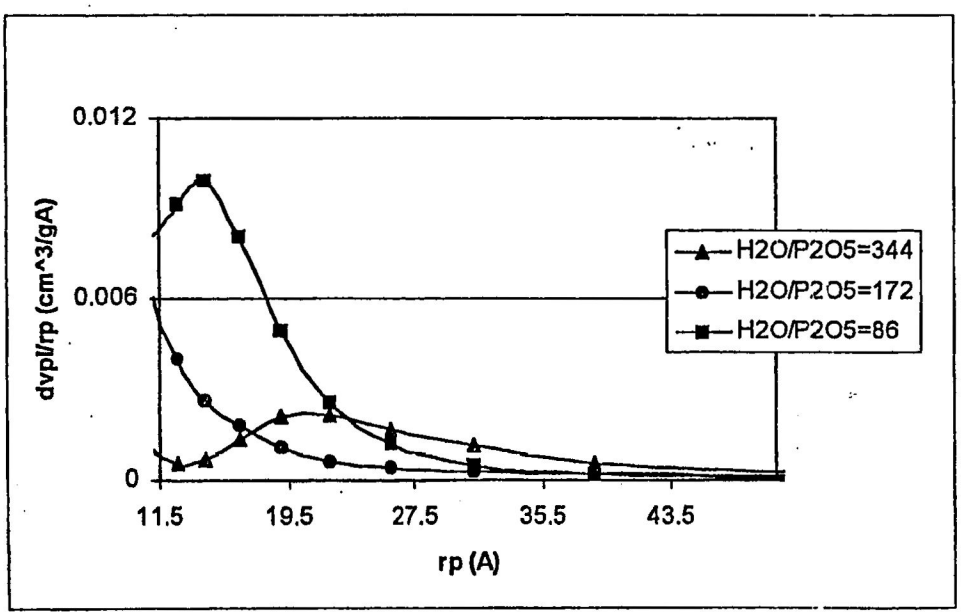

b) Pore size distribution

Figure 30: a) Adsorption isotherm and b) pore size distribution from synthesis mixtures of various H_2O/P_2O_5 ratios and fixed Al/P of 1.15 (synthesis conducted at 25°C)

synthesis with low water concentration involves a viscous mixture with no clear separation between solution and the product.[28] High water content enhances molecular transport within the reaction medium resulting in a more crystalline material. These results, however, indicate that the mixtures with high water content form materials with low crystallinity. Therefore, even the mixtures with low water content provide sufficient transport for the formation of a highly crystalline material.

4.3 Synthesis of mesoporous aluminophosphates using psuedobohemite alumina

Changing the aluminum source from aluminum hydroxide to aluminum isoropoxide was found to have a significant impact on the products obtained. This, therefore, prompted further investigation using a third source of aluminum, psuedobohemite alumina.

4.3.1 Effect of various Al/P ratios

The effect of varying the Al/P ratio was investigated using reaction mixtures of molar compositions xAl_2O_3:P_2O_5:0.50 C_{16}TACl:2.98 TMAOH:350 H_2O, where x= 0.59-2.34. For synthesis with Al/P ratio of 0.59 and 0.77 and 25 °C, the x-ray diffraction data (Figure 31) indicates a hexagonal phase with low crystallinity, as evidenced by a broad low intensity peak of 2θ at 2.1°. An increase in the synthesis Al/P ratio to 1.17 resulted in a very disordered product, while with an Al/P ratio of 2.34 an amorphous product was obtained. Comparing the psuedobohemite alumina x-ray diffraction patterns at various Al/P ratios to aluminum hydroxide indicated that products with less crystallinity, but higher surface area and pore diameter were produced using psuedobohemite alumina.

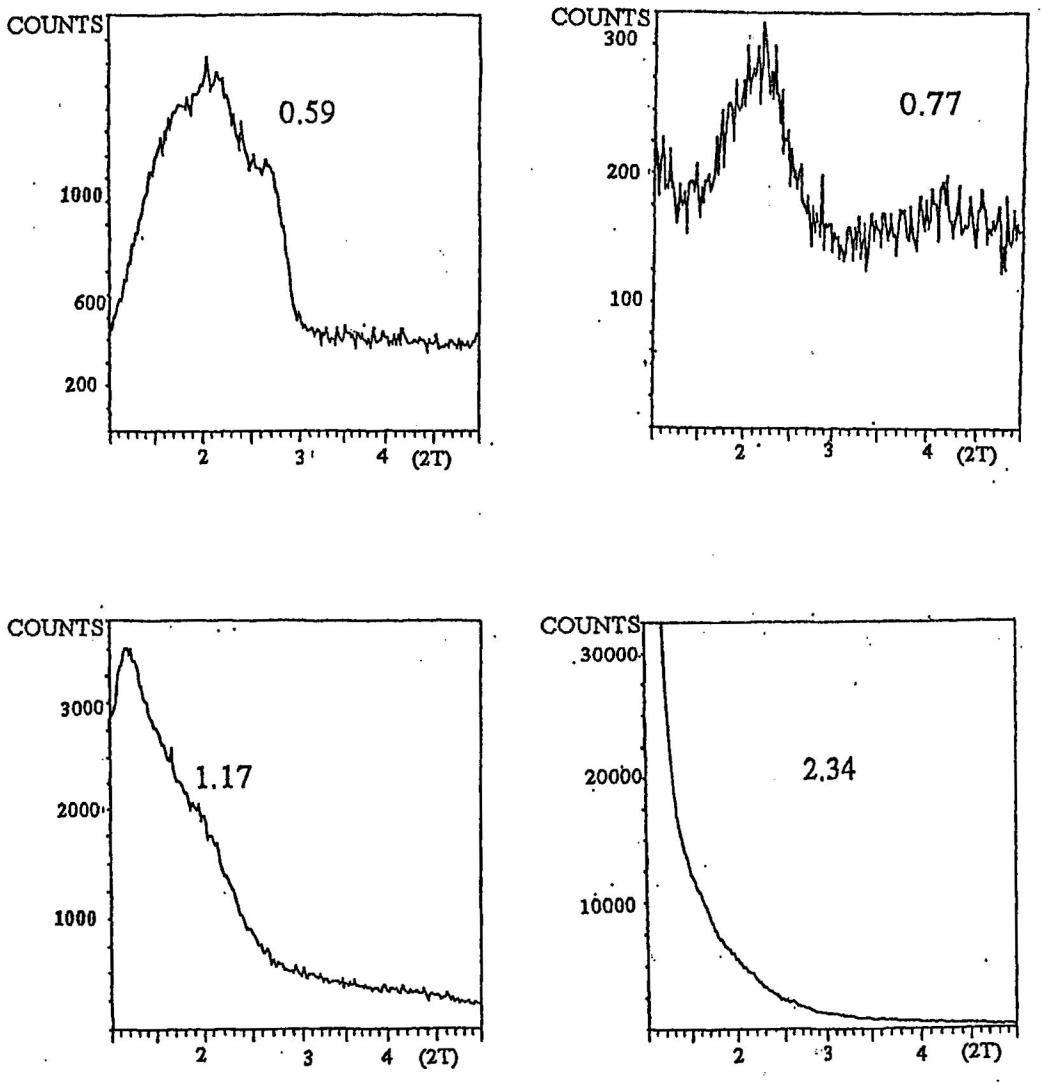

Figure 31: XRD patterns of samples synthesized at various Al/P ratios in mixture (synthesis conducted at 25°C) (Al/P ratio indicated on graph)

Calcination at 400 °C of the products from Al/P ratios 0.59 to 2.34, resulted in product loss at all Al/P ratios, except for Al/P ratio equal to 0.77, where crystallinity was partially preserved. The materials appeared to have lost their crystallinity on calcinations; however, surface area and porosimetry analysis showed that a mesoporous material of relatively high surface area was still present. With Al/P ratios of 0.59, 1.17, and 2.34, the corresponding nitrogen isotherms and pore size distribution are shown in Figures 32 a and b. A Type IV isotherm is indicated for Al/P equal to 0.59,1.17 and 2.34, while a combination of Type I and IV were observed for solids with a synthesis of Al/P ratio equal to 0.77, where an inflection (pore filing) occurred over a broad range of relative pressure. A broad distribution with a pore size of 31.2Å was exhibited for Al/P ratios 0.59 and 0.77, while a narrower distribution with a pore size of 31.2Å was obtained for Al/P ratio equal to 1.17. At Al/P ratio equal to 2.34 a narrow distribution with a pore size of 25.9Å was obtained. For a reaction temperature of 110 °C and Al/P ratio equal to 0.59, the x-ray diffraction pattern (Figure 33) shows a hexagonal phase, while with Al/P ratio greater than 0.59 and up to 2.34, amorphous products were observed. The nitrogen isotherms (Figure 34) indicate an intermediate between Types I and IV for an Al/P ratio of 0.59, while a Type IV isotherm was obtained for Al/P ratios between 0.77 and 2.34.

4.3.2 Effect of water concentration

Molar compositions containing varying amounts of water were prepared for Al/P ratios of 0.58 and 1.17 as follows:

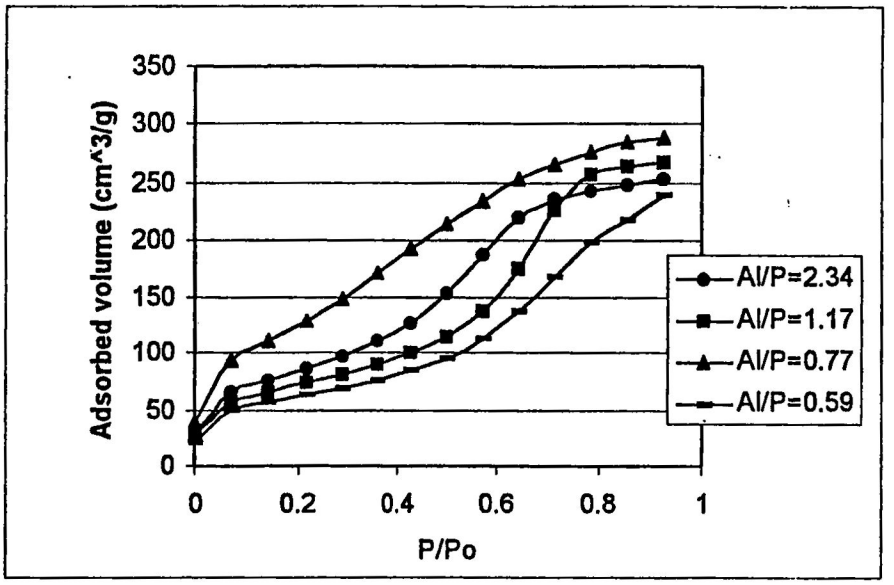

a) Adsorption isotherm

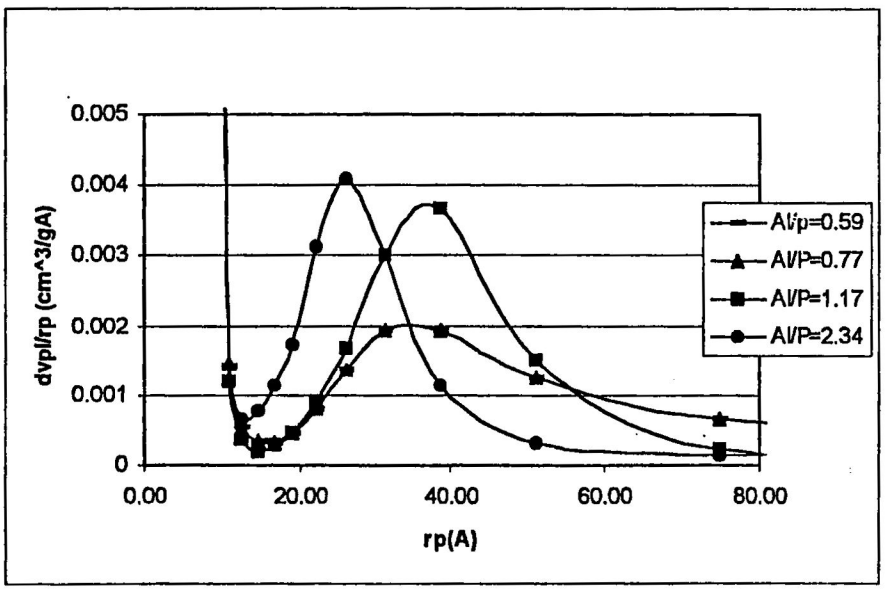

b) Pore size distribution

Figure 32: a) Adsorption isotherm and b) pore size distribution of calcined samples synthesized at various Al/P ratios in mixture (synthesis conducted at 25°C)

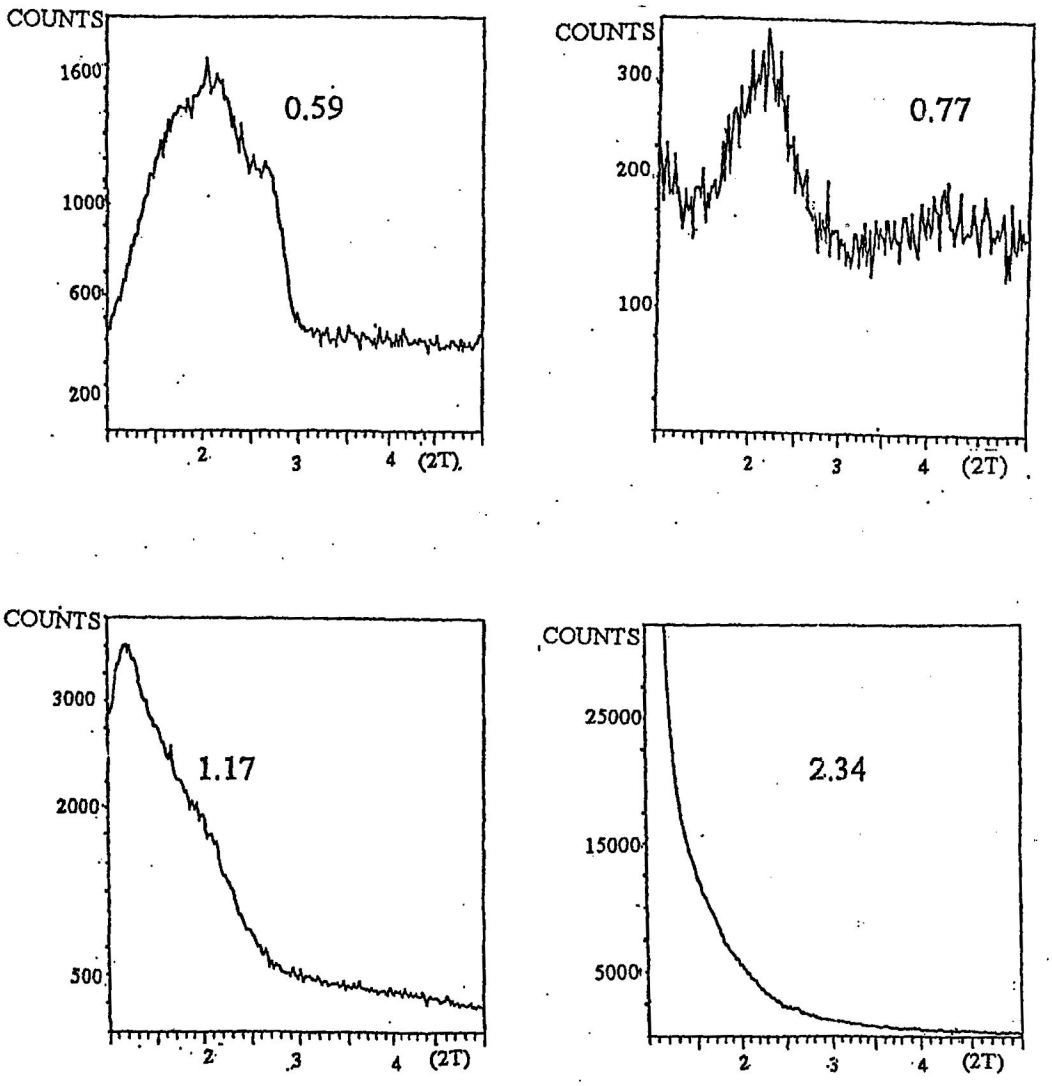

Figure 33: XRD patterns of samples synthesized at various Al/P ratios in mixture (synthesis conducted at 110°C) (Al/P ratio indicated on graph)

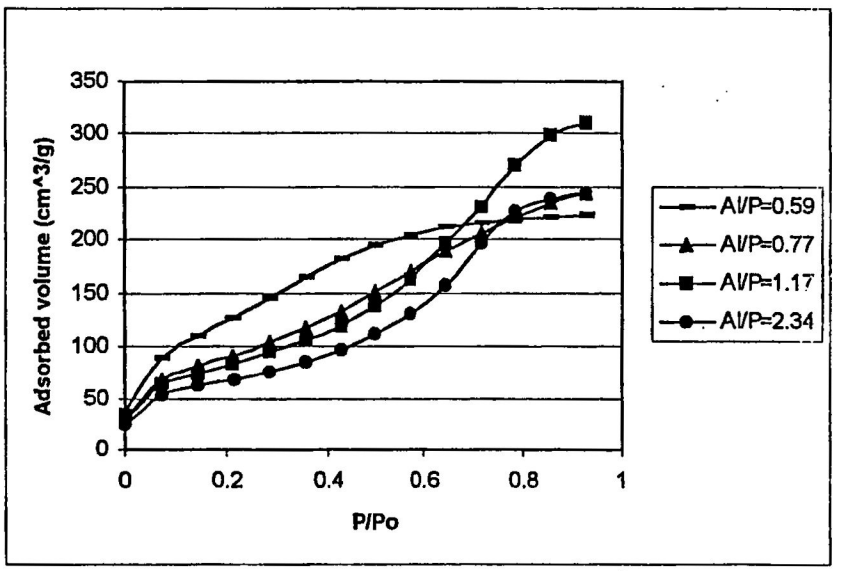

Figure 34: Adsorption isotherm of calcined samples synthesized at various Al/P ratios in mixture (synthesis conducted at 110°C)

$0.58Al_2O_3:P_2O_5:0.50\ C_{16}TACl:3.26\ TMAOH:xH_2O$, where x= 87-700

$1.17Al_2O_3:P_2O_5:0.50\ C_{16}TACl:3.22\ TMAOH:x\ H_2O$, where x= 87-700.

Previously, when using aluminum isopropoxide as the aluminum source, the water content of the synthesis mixture was observed to be an important structure directing parameter. Hence, it was instructive that water content in the psuedobohemite system be further explored. The nitrogen isotherm and pore size distribution are indicated in Figure 35 for an Al/P ratio of 1.17 at 25 °C. A Type IV isotherm was exhibited at H_2O /P_2O_5 ratios of 87.0 to 700. The pore size analysis indicates a narrow distribution with a maximum centered around 22 Å for a H_2O / P_2O_5 ratio of 700. A broad distribution was observed for H_2O / P_2O_5 ratio equal to 175 with a pore diameter of 38.8Å and for H_2O/P_2O_5 ratio equal to 87.0 with a pore size of 31.2Å. For an Al/P ratio equal to 0.58 Figure 36 a Type IV isotherm, similar to Al/P ratio 1.17, was obtained. The corresponding pore sizes at H_2O/P_2O_5 ratio equal to 172 and 700 resulted in a broad distribution with a pore size of 25 Å while at H_2O/P_2O_5 ratio equal to 87, a pore size of 22.0 Å is obtained.

For Al/P ratio equal to 1.17 synthesized at 110°C (Figure 37), a Type IV isotherm was obtained for H_2O/P_2O_5 ratios equal to 174 and 700, while an intermediate isotherm between Type I and IV was obtained at H_2O/P_2O_5 ratio equal to 175. The pore size distribution corresponding to the isotherms showed a narrow distribution with a pore size of 31.2 Å for the H_2O/P_2O_5 ratio equal to 700, while a pore diameter of 16.5 Å and 38.8Å was determined for H_2O/P_2O_5 equal to 175.0 and 87.0 respectively. Samples from synthesis at higher temperatures (110 °C) using an Al/P ratio of 0.58 (Figure 38)

show broad distribution with a pore diameter of 25Å at H_2O/P_2O_5 ratio equal to 172 and 700 while a 31.2 Å pore diameter was obtained at H_2O/P_2O_5 ratio of 87.0.

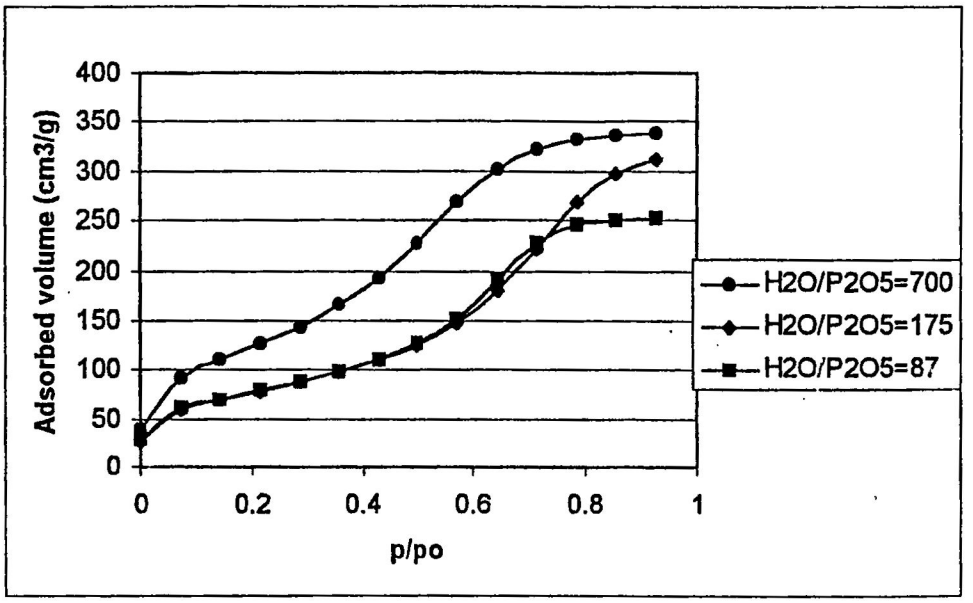

a) Adsorption isotherm

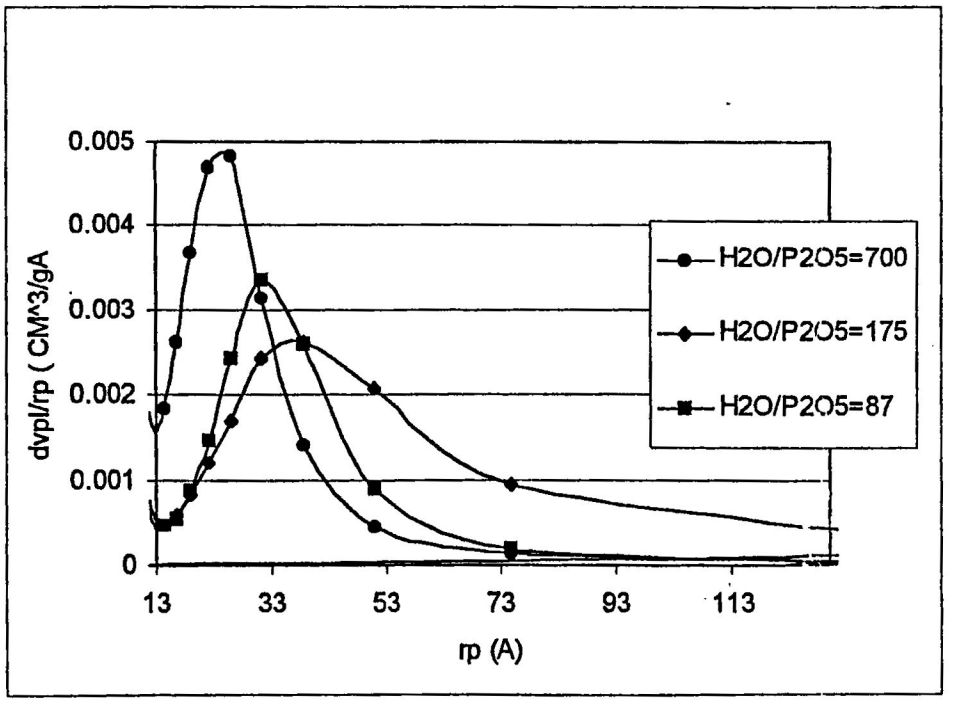

b) Pore size distribution

Figure 35: a) Adsorption isotherm and b) pore size distribution from synthesis mixtures of various H_2O/P_2O_5 ratios and fixed Al/P of 1.17 (synthesis conducted at 25°C)

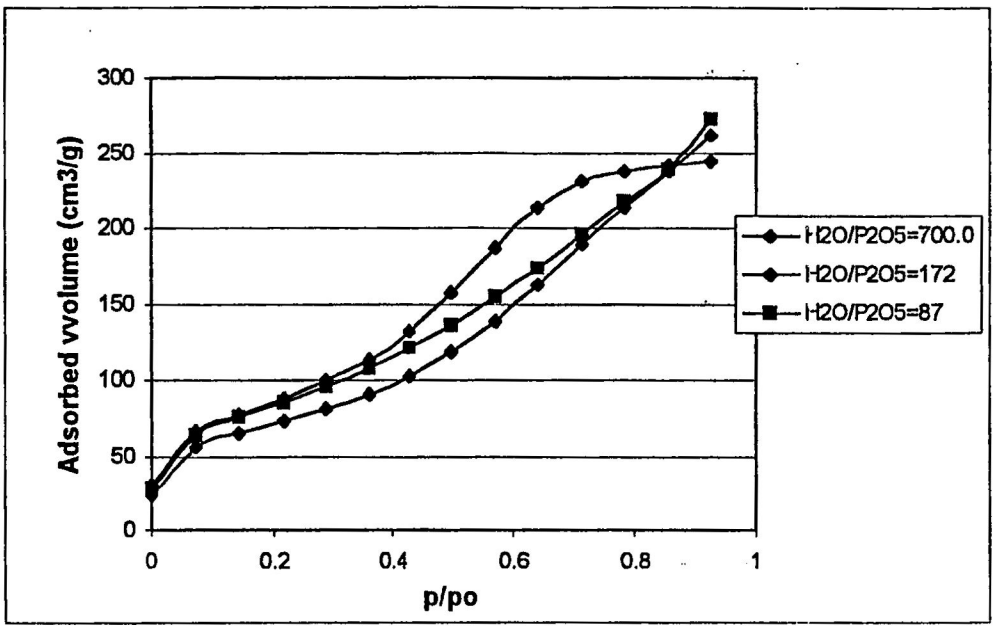

a) Adsorption isotherm

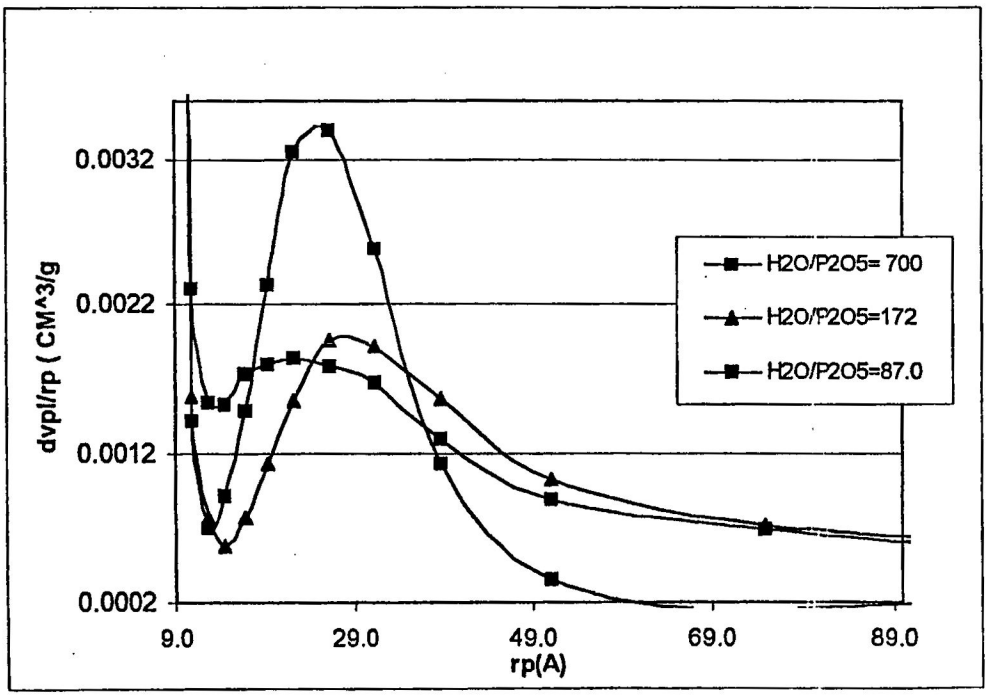

b) Pore size distribution

Figure 36: a) Adsorption isotherm and b) pore size distribution from synthesis mixtures of various H_2O/P_2O_5 ratios and fixed Al/P of 0.58 (synthesis conducted at 25°C)

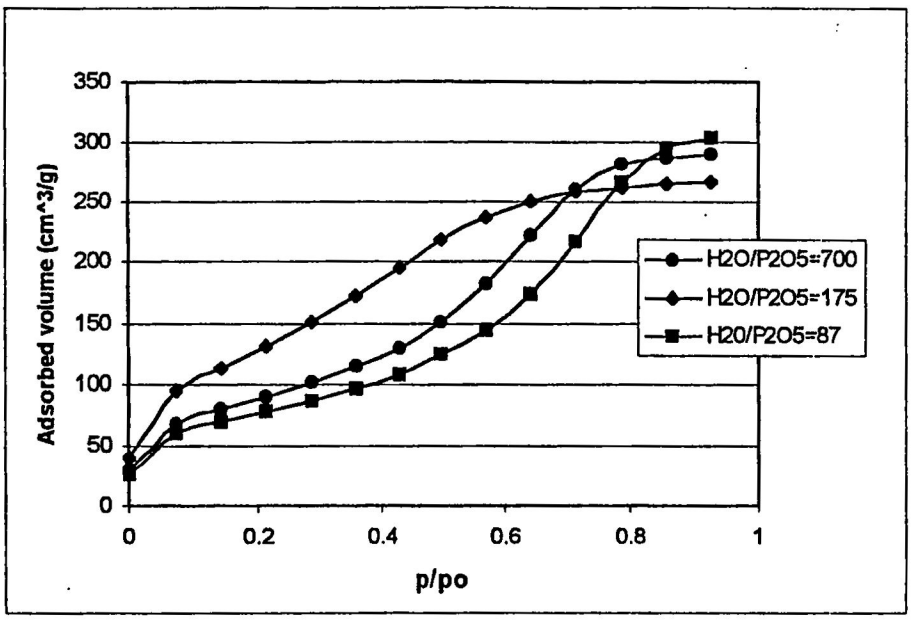

a) Adsorption isotherm

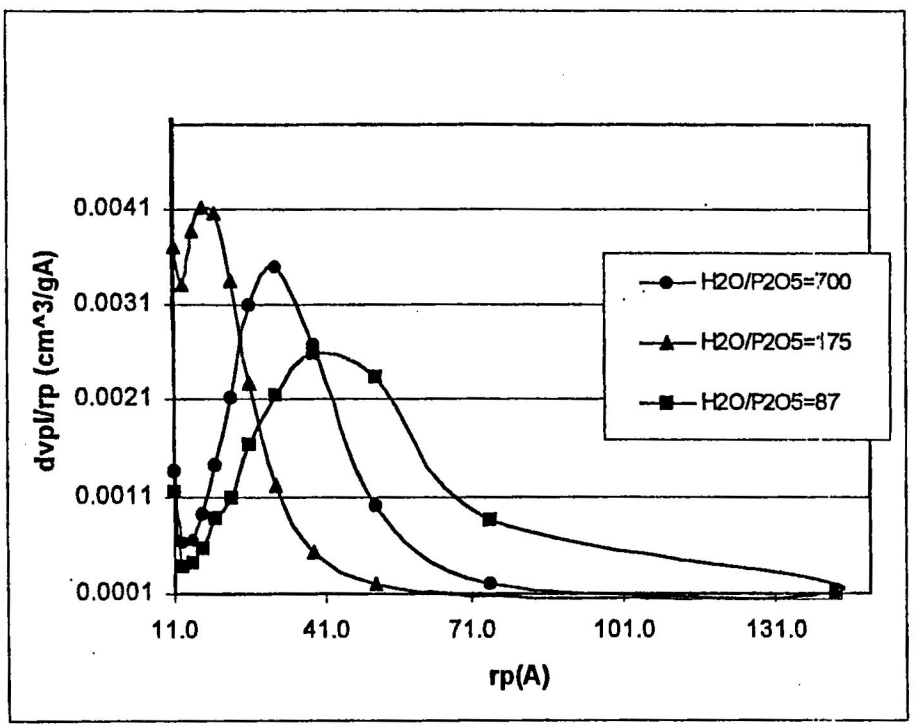

b) Pore size distribution

Figure 37: a) Adsorption isotherm and b) pore size distribution from synthesis mixtures of various H_2O/P_2O_5 ratios and fixed Al/P of 1.17 (synthesis conducted at 110°C)

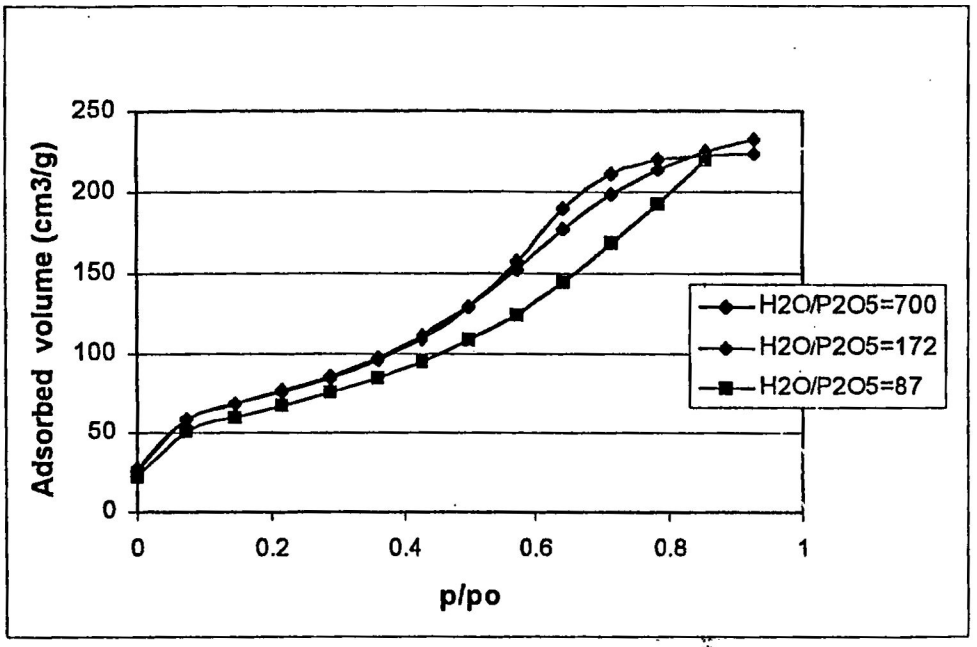

a) Adsorption isotherm

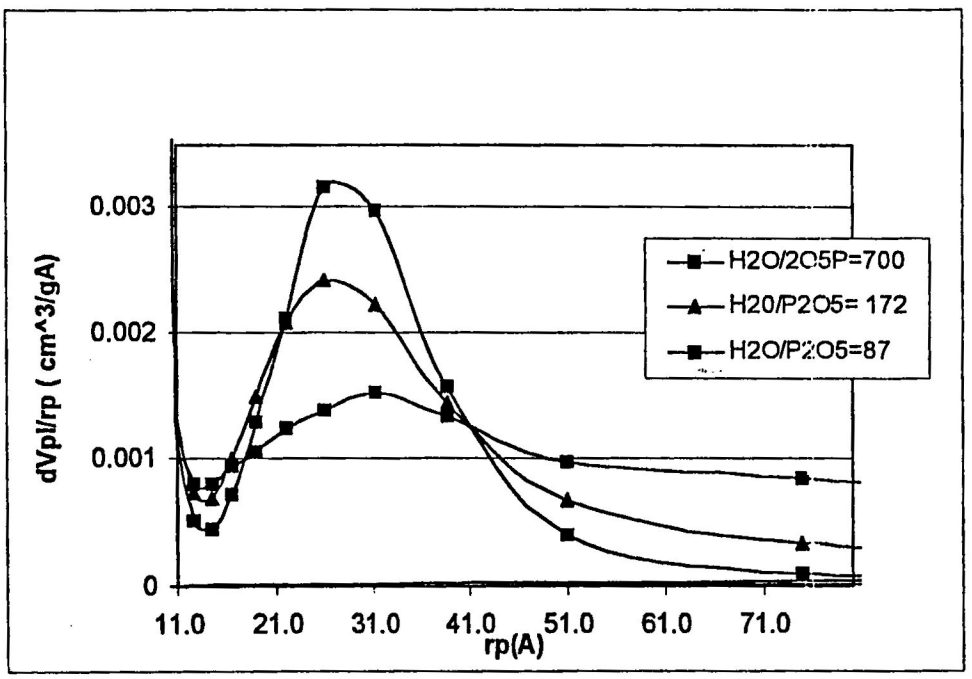

b) Pore size distribution

Figure 38: a) Adsorption isotherm and b) pore size distribution from synthesis mixtures of various H_2O/P_2O_5 ratios and fixed Al/P of 0.58 (synthesis conducted at 110°C)

CHAPTER 5

CONCLUSION AND FUTURE WORK

Mesoporous aluminophosphates were synthesized from a reactive gel via a liquid crystal templating mechanism in the presence of a cationic surfactant, CTACl. The synthesis of these materials was performed at various molar compositions. The choice of aluminum source is crucial to the type and quality of the products formed. Lamellar and hexagonal phases can be directed by altering the composition of the starting mixtures or the synthesis temperature irrespective of the three aluminum sources investigated. Low Al/P ratio, low TMAOH, high CTACl and high temperature led to a lamellar phase by facilitating condensation of inorganic precursors, while high Al/P ratio, high TMAOH, low CTACl and lower temperature led to a hexagonal phase.

However, the most well-defined products were obtained using aluminum hydroxide as the aluminum source. Synthesis in the presence of aluminum hydroxide gave a highly crystalline mesoporous type materials with Al-O-P species in predominantly tetrahedral coordination in the lamellar phase and both tetrahedral and octahedral coordination in the hexagonal phase. Upon calcination, a collapse or substantial shrinkage of the framework resulted. A micro-meso type porous material was

range of 19 Å. Synthesis with psudeobohemite alumina, however, gave a Type IV isotherm indicating mesoporosity with a pore diameter of up to 39 Å.

The lamellar and hexagonal phases obtained under various conditions indicate some porosity. However, the hydrothermal instability and lower crystallinity is a considerable drawback. Therefore, there is still a need for improvement. Further studies on the extent of hydrolysis and condensation of inorganic precursors and their impact on product stability is needed. One of the areas to look for improvement is the SBA type materials in the silicate system which have high thermal stability as well as large surface area. As indicated in our study, the choice of surfactants, among other factors, is crucial. The use of the block co-polymers for example, poly (alkylene) oxide ($EO_5PO_7EO_5$) as surfactants to synthesize the SBA type materials which help to assist in pore expansions can also be implemented in the aluminophosphate system. It is also believed that co-block polymers can increase pore wall thickness, hence their use to improve the thermal stability of aluminophosphates is of interest for further investigation.

REFRENCES

1. Petroleum Chemistry and Refining, Speight J. G., Taylor and Francis., Washington D.C., 1998.

2. Danumah C. , Zaidi S.M.J., Xu G., Voyer N., Giasson S., Kaliaguine S., Microporous and Mesoporous Materials 2000 37, p.21.

3. Breck D.W., Eversole W.G., Milton R.M., Breed T., and Thomas T.L., J. Amer.Chem.Soc., 1956 78, p.5963.

4. Flanigen E.M., Lok B. M., Patton R. L., and Wilson S. T., J. Pure and Appl. Chem., 58, No. 10, p. 1351.

5. Wilson S.T., Lok B.M., and Flanigen E.M., U.S. patent 4, 310, 440 (1982); Wilson S.T., Lok B.M., Messina C.A., Cannan T.R., and Flanigen E.M., J. Amer. Chem. Soc., 1982 104, p.1146.

6. Lok B.M., Messina C.A., Patton R.L., Gajek R.T., Cannan T.R., and Flanigen E.M., U.S. patent 4,440, 871 (1984); J. Amer. Chem. Soc., 1982 104, p.1146.

7. Reddy K.M., and Song C., J. Catalysis Letters, 1996 36, p.103.

8. Kresge C.T., Leonowicz M.E., Roth W.J., Vartuli J.C. and Beck J.S., Nature, 1992, 359, p.710.

9. Beck S., Vartuli J.C., Roth W.J., Leonowicz M.E., Kresge C.T., Schmitt K.D., Chu C.T.W., Olson D.H., Sheppard E.W., McCullen S.B., Higgins J.B., Schlenker J.L., J.Am.Chem.Soc., 1992, 114, p.10834.

10. Isabelle J. and Andre'D., J.Sol-gel Sci. and Tech., 1995,4, p.7.

11. Mackenzie J.D., J. Non-Cryst.Solids, 1982, 48, p.182.

12. Szostak R, Molecular Sieves, Principles of Synthesis and Identification, Van Nostrad Reinhold, New York City, N.Y. 1989.

13. Parsad S., Liu-Shang Bin., J. Chem. Mater., 1994, 6, p. 633.

14. Israelachvili J., Intermolecular and Surface Forces, Academic Press., London, 1991.

15. http: //www. willson.cm.utexas.edu/research/sub-files/surface phenomena/ spring 2000/ self-assembly-st.

16. Kawi S., Lai M. W., J. Chem. Commun., 1998, p.1407.

17. Sheppard E.W, Olson D.H., Schlenker J.L., Beck J.S., Helling S.D., Mccullen S.B., Leonowicz M.E., Roth W.J., Kresge C.T., Schmitt K.D., and Vartuli J.C., J. Studies in Surface Science and Catalysis, 84 p. 53.

18. Schuth F., J. Studies in Surface Science and Catalysis 135 p.1.

19. Stuky G.D., Chmelka B.F., Frederickson G.H., Huo Q., Melosh N.W., Feng J., Zhao D., Science, 1998, 279, p.120.

20. Sayari A., Moudrakovski I., and Reddy J.S., J. Chem. Mater., 1996, 8, p.2080.

21. Yue Y., Shuiln Q., Shougui L., Rongsheng L., Jiesheng C., Ruren X., Qiuming G., Faraday Transaction, 1995, 23, p.310.

22. Tiemann M. and Froba M., Chem Mater. 1998, 10, p. 3475.

23. Oliver S., Kuperman A., Coombs N., Lough A., Ozin G.A., J.S. Nature, 1995, 378, p.47.

24. Stucky G., Bu X., Feng J., Xia Y., Feng P., J. Chem. Commun., 1997, p. 949.

25. Zhao D., Luan Z., Kevan L., J. Chem. Commun., 1997, p.1009.

26. Kimura T., Sgahara Y., and Kuroda K., J. Chem. Mater., 1999, 11, p.508.

27. Cabrera S., Haskouri J.E., Guillem C., Porter A.B., Porter D.B., Mendioroz S., Marcos M.D., and Amoros P., J. Chem. Commun., 1999, p.176.

28. Khimyak Y., Klinowski Z., J. Chem. Soc., Faraday Trans., 1998, 94, p. 2241.

29. Skoog, Holler and Nieman., Principles of Instrumental Analysis, Saunders College Publishers, Florida, 1998.

30. Nuffield E.W., X-ray Diffraction Methods, John Wiley &Sons, Inc., New York City N.Y, 1996.

31. Brunauer S., Emmett P.H.; and Teller E., J. Am. Chem. Soc., 1938, 60, p.309

31. Mortlock R.F., Bell A.T., Radke C., J. Phys. Chem., 1993, 97, p.767.

33. Mokaya Robert, J. Phys. Chem. B. 2000, 104, p.8275.

34. Mokaya Robert and Jones William, J. Catalysis, 1997, 172, p. 211.